Şeyda Gölcük

M.S. Thesis of Chemistry

June - 2011

SYNTHESIS AND CHARACTERIZATION OF PROTON CONDUCTING MEMBRANES VIA PHOTOINDUCED GRAFTING

by

Şeyda GÖLCÜK

June 2011

SYNTHESIS AND CHARACTERIZATION OF PROTON CONDUCTING MEMBRANES VIA PHOTOINDUCED GRAFTING

by

Şeyda GÖLCÜK

A thesis submitted to

the Graduate Institute of Science and Engineering

of

Fatih University

in partial fulfillment of the requirements for the degree of

Master of Science

in

Chemistry

June 2011
Istanbul, Turkey

APPROVAL PAGE

I certify that this thesis satisfies all the requirements as a thesis for the degree of Master of Science.

_____

Prof. Cevdet NERGİZ
Head of Department

This is to certify that I have read this thesis and that in my opinion it is fully adequate, in scope and quality, as a thesis for the degree of Master of Science.

_____

Assist. Prof. Ali Ekrem MÜFTÜOĞLU
Supervisor

Examining Committee Members

Assist. Prof. Dr. Ali Ekrem MÜFTÜOĞLU _____

Prof. Dr. Ayhan BOZKURT _____

Assoc. Prof. Dr. Ergün GONCA _____

Assoc. Prof. Dr. Faruk YILMAZ _____

Assist. Prof. Dr. Burak ESAT _____

It is approved that this thesis has been written in compliance with the formatting rules laid down by the Graduate Institute of Sciences and Engineering.

_____

Assoc. Prof. Dr. Nurullah ARSLAN
Director

June 2011

SYNTHESIS AND CHARACTERIZATION OF PROTON CONDUCTING MEMBRANES VIA PHOTOINDUCED GRAFTING

Şeyda GÖLCÜK

M.S. Thesis – Chemistry
June 2011

Supervisor: Assist. Prof. Dr. Ali Ekrem MÜFTÜOĞLU

Co-Supervisor: Prof. Dr. Ayhan BOZKURT

ABSTRACT

Irradiation grafting is a well-established technique for the preparation of polymer electrolyte membranes for fuel cells. In this study, a novel process comprising UV-irradiation grafting of styrene onto poly(vinylidene fluoride) (PVDF), subsequent sulfonation and triazole doping has been developed for preparing anhydrous proton conducting membranes, which involves both surface and homogeneous grafting approaches. Degree of grafting of styrene on PVDF films prepared by surface grafting was investigated as a function of UV irradiation time, as varied from 0.5 h to 8 h. Anhydrous proton conducting properties of 1,2,4-triazole-functional PVDF-*g*-PSSA polymers were studied. PVDF-*g*-PSSA$(Tri)_2$ with a degree of grafting of 50.8% showed a maximum water-free proton conductivity of approximately $5x10^{-2}$ mS/cm at 150°C. For the films obtained by homogeneous grafting, the anhydrous proton conductivity of PVDF-*g*-PSSA with 22% sulfonation was measured about $1x10^{-4}$ mS/cm at 150°C. The synthesized graft copolymers were characterized by ^{1}H NMR and FT-IR spectroscopic analysis. Their thermal properties were examined by TGA and differential scanning calorimetry (DSC) measurements. With a view to use in fuel cells, ion exchange capacities, water uptakes, and hydration numbers of the prepared membranes were measured and correlated with the degree of grafting.

Keywords: PVDF, Styrene, Graft copolymers, Photoinduced polymerization, Polymer electrolyte, Proton conducting membranes.

FOTO AŞILAMA YÖNTEMİYLE PROTON İLETKEN MEMBRANLARIN SENTEZİ VE KARAKTERİZASYONU

Şeyda Gölcük

Yüksek Lisans Tezi – Kimya
Haziran 2011

Tez Danışmanı: Yrd. Doç. Dr. Ali Ekrem MÜFTÜOĞLU

Eş Danışman: Prof. Dr. Ayhan BOZKURT

ÖZ

Işınlama ile aşılama, yakıt hücrelerinde kullanılan polimer elektrolit membranların sentezlenmesinde iyi bir tekniktir. Bu çalışma ile ilk defa yüzey ve homojen UV ışınlama yöntemi kullanılarak poli(viniliden florür) (PVDF) üzerine stiren aşılanmıştır. Sonrasında sülfonlanan ve triazol ile dop edilen kopolimerlerden nemsiz proton iletken membranlar hazırlanmıştır. Yüzey aşılama yöntemiyle elde edilen PVDF filmlerindeki stiren aşılanma derecesi, 0,5 ve 8 saat arasında değişen UV aydınlatma sürelerine göre incelenmiştir. 1,2,4-triazol ile fonksiyonlanmış PVDF-*g*-PSSA polimerlerinin nemsiz proton iletken özellikleri incelenmiş ve aşılanma derecesi %50.8 olan PVDF-*g*-PSSA2Tri membranının 150°C'deki maksimum nemsiz proton iletkenliği yaklaşık $5x10^{-2}$ mS/cm olarak ölçülmüştür. Homojen aşılanmayla elde edilen filmler için ise, %22 sülfonlanmış PVDF-*g*-PSSA polimerinin 150°C'deki nemsiz proton iletkenliği yaklaşık $1x10^{-4}$ mS/cm olarak ölçülmüştür. Sentezlenen aşı kopolimerlerin yapısı ^{1}H NMR ve FT-IR analiz yöntemleriyle aydınlatılmıştır. Malzemelerin termal özellikleri termogravimetrik analiz (TGA) ve diferansiyel taramalı kalorimetre (DSC) ölçümleri ile incelenmiştir. Yakıt hücrelerinde kullanıma yönelik performans değerlendirmesi için hazırlanan membranların iyon değiştirme kapasiteleri, su tutma değerleri ve hidrasyon numaraları ölçülmüş ve aşılanma derecesi ile ilişkilendirilmiştir.

Keywords: PVDF, Stiren, Aşı kopolimerler, Foto uyarılma polimerizasyonu, Polimer elektrolit, Proton iletken membranlar.

DEDICATION

This thesis is dedicated to

my husband Kurtuluş, my son Asım Mehmet, and my daughter Meryem Elif,

for their endless love and support.

ACKNOWLEDGEMENTS

I express sincere appreciation to my supervisor Assist. Prof. Dr. Ali Ekrem MÜFTÜOĞLU for helpful discussion, his academic guidance and insight throughout the research.

I would also like to thank my co-supervisor, Prof. Dr. Ayhan BOZKURT, for his knowledge and support.

I thank Assist. Prof. Dr. Celal ÖZPINAR for his grateful encouragement and help.

I thank Prof. Dr. Naz Mohammed AGH ATABAY and Dr. Tezcan PARALI for opening their lab and research facilities for my use.

I thank my colleagues, Fatime EREN and Deniz SİNİRLİOĞLU, for their grateful help and giving me valuable advices on experimental work.

I also thank Sevim Ü. ÇELİK, Ayşe ASLAN, and Hamide AYDIN, for their help and technical support in the laboratory.

There are countless people to thank within the Chemistry Department. I would like to give special thanks and appreciation to my friends Emine TEMİZEL, Esra AYAN, Hilal DOĞAN, and to all colleagues and friends who made my stay at the university a memorable and valuable experience.

I would like to thank to Fatih University for kindly providing financial support and scholarship throughout this research.

Of course this would not be complete without thanking my family, starting with my parents who instilled in me a belief that I could achieve anything I set my heart and mind to. I have cherished every day throughout my graduate experience because of my children, who provide me with the motivation to persevere. And finally, I must thank my soul mate and loving husband more than anyone, for believing in me, for having infinite patience with me, and for providing the biggest mirror of all.

TABLE OF CONTENTS

ABSTRACT iii
ÖZ iv
DEDICATION v
ACKNOWLEDGMENT vi
TABLE OF CONTENTS viii
LIST OF TABLES xi
LIST OF FIGURES xii
LIST OF SYMBOLS AND ABBREVIATIONS xvi
CHAPTER 1 INTRODUCTION 1
CHAPTER 2 3
2.1 PHOTOPOLYMERIZATION 3
2.1.1 Photonitiation 4
2.2 PHOTOINDUCED SYNTHESIS OF GRAFT COPOLYMERS 6
2.2.1 Homogeneous photografting 8
2.2.1.1 Free Radical Systems 8
2.2.2 Surface photografting 12
2.2.2.1. Surface Photografting Method 13
2.2.3 Miscellaneous Applied Surface Grafts 15
CHAPTER 3 19
3.1 FUEL CELLS 19
3.1.1 Proton Exchange Membrane Fuel Cell (PEMFC) 20
3.2 POLYMER ELECTROLYTE MEMBRANES 22
3.2.1 Classification of Proton Exchange Membranes Materials 22
3.2.2 Hydrates Proton Conducting Membranes 23
3.2.2.1 Nafion and Perfluorinated Polymer Membranes 23
3.2.2.2 Sulfonated Hydrocarbon Polymer Membranes 25
3.2.3 Anhydrous Proton Conductive Membranes 26

3.3 PROTON CONDUCTION MECHANISMS IN PEMs 28
CHAPTER 4 EXPERIMENTAL 30
4.1 UV-INDUCED SURFACE PHOTOGRAFTING OF STYRENE ONTO PVDF FILMS 30
4.1.1 Materials 30
4.1.2 Preparation of PVDF Membranes 30
4.1.3 UV Photografting of Styrene onto PVDF Films 31
4.1.4 Sulfonation 31
4.1.5 Doping of PVDF-*g*-PSSA Films with Triazole 32
4.2 UV-INDUCED HOMOGENEOUS PHOTOGRAFTING OF STYRENE ONTO PVDF 32
4.2.1 Materials 32
4.2.2 UV Photografting of Styrene onto PVDF 33
4.2.3 Sulfonation 33
4.2.4 Doping of PVDF-g-PSSA with Triazole 33
4.3 CHARACTERIZATIONS 34
4.3.1 FT-IR and 1H-NMR Analysis 34
4.3.2 Thermal analysis 34
4.3.3 Degree of Grafting (DG) 35
4.3.4 Ion exchange capacity 35
4.3.5 Water uptake and Hydration Number 35
4.3.6 Proton Conducting Measurement 36
4.3.6.1 AC Conductivity Measurements 36
4.3.6.2 DC Conductivity Measurements 37
CHAPTER 4 RESULTS AND DISCUSSION 38
5.1 UV-INDUCED PHOTOGRAFTING OF STYRENE ONTO PVDF FILMS 38
5.1.1 Analysis of the Grafted PVDF Membranes 40
5.1.1.1 Degree of Grafting (DG) 40
5.1.1.2 ^{1}H NMR analysis 41
5.1.1.3 FT-IR analysis 42
5.1.1.4 Thermogravimetric Analysis (TGA) 44
5.1.1.5 DSC Analysis 45
5.1.2 Analysis of PVDF-g-PSSA / Proton Conducting Membranes 46
5.1.2.1 FT-IR analysis 46

5.1.2.2 The IEC Analysis 47
5.1.2.3 The Water Uptake and Hydration Number 49
5.1.2.4 Thermogravimetric Analysis (TGA) 51
5.1.3 Analysis of Triazole doped PVDF-g-PSSA.....52
5.1.3.1 FT-IR analysis 53
5.1.4 Proton conductivity.....53
5.1.4.1 The Effect of Humidity on Conductivity.....54
5.1.4.2 Anhydrous Proton Conductivity.....54
5.2 UV-INDUCED HOMOGENEOUS PHOTOGRAFTING OF STYRENE ONTO PVDF.....57
5.2.1 Analysis of the Grafted PVDF Membranes.....58
5.2.1.1 1H NMR Result.....58
5.2.1.2 FT-IR Studies 59
5.2.1.3 Thermogravimetric Analysis (TGA) 60
5.2.1.4 DSC Analysis 61
5.2.2 Analysis of PVDF-g-PSSA / Proton Conducting Membranes 62
5.2.2.1 FT-IR analysis 62
5.2.2.2 The IEC Analysis 64
5.2.2.3 The Water Uptake.....64
5.2.2.4 Thermogravimetric Analysis (TGA) 64
5.2.2.5 DSC Analysis 65
5.2.2.6 Proton conductivity 67
CHAPTER 6 CONCLUSIONS 69
REFERENCES 71

LIST OF TABLES

TABLE

2.1 Modification of Polymer Membranes via Photografting Method 17
3.1 Summary of major differences of the fuel cell types 20
4.1 Preparation of triazole doped PVDF-*g*-PSSA 32
4.2 Preparation of triazole doped PVDF-*g*-PSSA 34
5.1 Samples, and their grafting time, degree of grafting, Tg and Tm values 40
5.2 Sulfonation, T_m, IEC, water uptake, and hydration number of PVDF-*g*-PSSA membranes.....50
5.3 Maximum anhydrous proton conductivities of the polymer membranes with triazole dopant at 150°C 54
5.4 Synthesis conditions and results of PVDF-*g*-PS graft copolymers 58
5.5 Degree sulfonation, Tg, Tm, IEC, water uptake, and conductivity of PVDF-*g*-PSSA.....63

LIST OF FIGURES

FIGURE

2.1 General steps for photoinitiated free radical polymerization....4
2.2 Norrish Type I and Type II photoinitiators....4
2.3 α-Cleavage type photoinitiation....5
2.4 Hydrogen abstraction type photoinitiation....6
2.5 Synthesis of graft copolymers via photoinduced grafting onto method....7
2.6 Synthesis of graft copolymers via photoinduced grafting through method....8
2.7 Homogeneous synthesis of graft copolymers by α-cleavage type photoinitiation....9
2.8 Photoscission and self- initiation mechanism of poly(phenyl vinyl ketone) in presence of various monomers (Müftüoğlu, et al., 2010)....9
2.9 Homogeneous synthesis of graft copolymers by hydrogen abstraction type photoinitiation....10
2.10 Photoinduced synthesis of block-graft copolymers using polymeric hydrogen donor and benzophenone....10
2.11 Synthesis of graft copolymer by one component type II macrophotoinitiator....11
2.12 Photograft polymerization of vinyl monomers by photoiniferter mechanism....12
2.13 Schematic representation of photoinduced living graft polymerization....13
2.14 Schematic representation of photoinduced living graft polymerization....14
2.15 Preparation of proton conducting membranes via photografting methods (Müftüoğlu, et al., 2010)....16
3.1 Schematic illustration of an individual PEM Fuel Cell....21
3.2 Classification of proton exchange membranes based on materials (perfluorinated, partially fluorinated and non-fluorinated) and preparation method (acid-base blends and others)....22
3.3 Chemical structures of commercial perfluorinated polymer electrolyte membranes....23

3.4 Gierke's Model 24
3.5 Schmidt-Rohr's Model 25
3.6 Grotthuss mechanism (Crofts, 1996) 28
3.7 Vehicular mechanism (Kreuer et al., 1982 29
4.1 Molecular structures of a) PVDF, b) Styrene, c) Benzophenone, and d)1H-1,2,4-triazole 30
5.1 Process for synthesis of PVDF-g-PSSA proton conducting membranes by UV surface photografting 38
5.2 Degree of grafting versus UV photografting of styrene on PVDF 41
5.3 ^{1}H NMR spectra of PVDF base film and Memb 4 41
5.4 FT-IR spectra of base PVDF and PVDF-g-PS membranes with different degree of grafting (Memb 0: 2.4%, Memb 1: 6.9% and Memb 2: 18.4%) 42
5.5 FT-IR spectra of base PVDF and PVDF-g-PS membranes with different degree of grafting (Memb 4: 50.8%, Memb 6: 68% and Memb 8: 109.1%) 43
5.6 TGA data of PVDF and graft membranes 45
5.7 DSC traces of Memb 8, Memb 6 and Memb 4 recorded under inert atmosphere at a heating rate of 10 °C/min 45
5.8 The close-up view of the DSC traces of Memb 8, Memb 6 and Memb 4. 46
5.9 FT-IR spectra of base PVDF, styrene grafted PVDF (Memb 8) and proton conducting PVDF-g-PSSA membrane (Memb 8/SA) 47
5.10 Behavior of the ion exchange capacity versus the degree of grafting for proton conducting membranes 48
5.11 WU of the proton conducting membranes versus degree grafting 49
5.12 Hydration number of the proton conducting membranes versus degree grafting 50
5.13 TGA data of PVDF, PVDF-g-PS (Memb 6) and PVDF-g-PSSA (sulfonated Memb 6) membranes were recorded under N_2 atmosphere at a heating rate of 10°C/min 51
5.14 TGA data of proton conducting membranes were recorded under N_2 atmosphere at a heating rate of 10°C/min 52

5.15 The FT-IR spectra of triazole doped proton conducting membranes.....53
5.16 AC conductivity versus Frequency (Hz) for Memb 4/SA-Tri at various temperatures 55
5.17 AC conductivity versus Frequency (Hz) for Memb 4/SA-2Tri at various temperatures 56
5.18 DC conductivities of Memb 4/SA-Tri, Memb 4/SA-2Tri, Memb 6/SA-Tri, and Memb 6/SA-2Tri as a function of reciprocal temperature 56
5.19 Process for synthesis of PVDF-g-PSSA proton conducting membranes by UV homogeneous photografting method 57
5.20 ^{1}H NMR spectra of pure PVDF and PVDF-g-PS graft copolymers obtained with 0.5 h and 4 h UV irradiation.....58
5.21 Typical FTIR spectra of pure PVDF and PVDF-g-PS graft copolymers obtained with 0.5 h and 4 h UV irradiation.....59
5.22 TGA data of pure PVDF and 0.5h UV and 4h UV graft copolymers PVDF-g-PS were recorded under N_2 atmosphere at a heating rate of 10°C/min 60
5.23 DSC traces of pure PVDF and PVDF-g-PS graft copolymers obtained with 0.5 h and 4 h UV irradiation were recorded under inert atmosphere at a heating rate of 10 °C/min 61
5.24 The close-up view of the DSC traces of pure PVDF and PVDF-*g*-PS graft copolymers 62
5.25 FT-IR spectra of base PVDF, styrene grafted PVDF and proton conducting PVDF-g-PSSA membrane.....63
5.26 TGA data of PVDF, PVDF-*g*-PS and PVDF-*g*-PSSA were recorded under N_2 atmosphere at a heating rate of 10°C/min 65
5.27 DSC traces of pure PVDF and PVDF-*g*-PS graft copolymers obtained with 0.5 h and 4 h UV irradiation were recorded under inert atmosphere at a heating rate of 10 °C/min 66
5.28 The close-up view of the DSC traces of pure PVDF, PVDF-*g*-PS and PVDF-*g*-PSSA graft copolymers 66
5.29 AC conductivity versus Frequency (Hz) for PVDF-*g*-PSSA at various

temperatures 67
5.30 DC conductivities of PVDF-*g*-PSSA as a function of reciprocal temperature 68

LIST OF SYMBOLS AND ABBREVATIONS

4VP	4-vinylpyridine
AA	Acrylic acid
AAm	Acrylamide
AC	[(2-acryloyloxy)ethyl]trimethyl ammoniumchloride
AFC	Alkaline Fuel Cell
AMPS	2-acrylamido-2-methyl-1-propanesulfonic acid
BAM3G ®	Ballard Advanced Material Membrane
BE	*n*-butyl vinyl ether
BEE	Benzoin ethyl ether
BP	Benzophenone
DEAAm	*N*,*N*-diethylacrylamide
DMAAm	*N*,*N*-dimethylacrylamide
DMAEMA	2-dimethylaminoethyl methacrylate
DT	Dithiocarbamate
GMA	Glycidyl methacrylate
HBP	4-hydroxybenzophenone
HEA	2-hydroxyethyl acrylate
HEMA	2-hydroxyethyl methacrylate
ITX	2-isopropylthioxanthone
MAA	Methacrylic acid
MAn	Maleic anhydride
MBS-PBI	Methyl methacrylate butadiene styrene-polybenzimidazole
MCFC	Molten Carbonate Fuel Cell
MEA	Membrane Electrode Assembly
MMA	Methyl methacrylate
NaSS	Sodium *p*-styrene sulfonate
NIPAAm	*N*-isopropylacrylamide
NPI	Naphthalenic polyimide

NVP	*N*-vinylpyrrolidone
PAFC	Phosphoric Acid Fuel Cell
PEGMA	Poly(ethylene glycol) methacrylate
PEM	Proton Exchange Membrane
PEMFC	Proton Exchange Membrane Fuel Cell
PEO	Poly(ethylene oxide)
PFCA	Perfluorinated carboxylic acids
PFSA	Perfluorosulfonic acid
PFSI	Perfluorosufonimide ionomers
PTFE	Poly(tetraflouroethylene)
PTFE-g-TFS	Poly(tetrafluoroethylene)-*graf-t*rifluorostyrene sulfonate
PTri	1H-1,2,4-triazole
PVDF	Poly(vinylidene fluoride)
PVDF-g-PSSA	Poly(vinylidene fluoride)-*graft*-polystyrene sufonic acid
QDMAEMA	Quaternary 2-dimethylaminoethyl methacrylate
SOFC	Solid Oxide Fuel Cell
SPE	*N*,*N*-dimethyl-*N*-(2-methacryloyloxyethyl-*N*-(3-sulfopropyl) ammonium betaine
SPEEK	Sulfonated poly (ether ether ketone)
SPEEK/PEI	Sulfonated poly (ether ether ketone)/polyethyleneimine
SPPBP	Sulfonated poly(4-phenoxybenzoyl-1,4-phenylene)
SPSU/PEI	Sulfonated polysulfone/ polyethyleneimine
VOC	Volatile Organic Compound
VTF	Vogel-Tammann-Fulcher

CHAPTER 1

INTRODUCTION

Graft copolymers are well-defined copolymers, which have already demonstrated relevant properties and hence have been used in many applications (such as emulsifiers for plastics, hot melt, adhesives, ions exchange membranes, impact resistance additives). It is well-known that heterogeneous (i.e., two phases or more) graft copolymers tend to show the properties of both (or more) polymeric backbone and the oligomeric or polymeric grafts rather than averaging the properties of both homopolymers (Sauguet, 2006). Among these copolymers, fluoropolymers, such as poly(vinylidene fluoride) (PVDF), constitute one of the most important families of engineering polymers. They are well known for their physical and chemical resistance.

PVDF based proton-conducting membranes are one of the most important components for a polymer electrolyte fuel cell (PEFC), serving as a separator to prevent mixing of the reactant gases and as an electrolyte for transporting protons from the anode to the cathode. PVDF is a partially fluorinated polymer with excellent thermal, mechanical and chemical stability along with lower cost compared to perfluorinated membrane such as the Nafion series from DuPont, which is the most common polymer electrolyte membranes used in fuel cells applications (Motupally et al,. 2000). Thus, there has been a great deal of research activity on the development of novel proton conducting membranes to substitute the perfluorinated ones (Holdcroft et al., 2000, 2003).

Proton conducting PVDF graft membranes have been conventionally prepared by Atom Transfer Radical Polymerization (ATRP) (Kim, 2007; Sauguet, 2006; Chen, 2007) or using high energy beam methods, e.g. X-ray or gamma radiation, or ozone pre-treatment methods (Holmberg, 2004; Shen, 2006; Nasef, 2006). Briefly, ATRP is

among the most widely used methods of controlled radical polymerization. ATRP is a means of forming carbon-carbon bond through transition metal catalyst. One drawback of the classical ATRP method is the use of large amounts of the CuX / ligand catalyst complex required (Kim, 2007; Sauguet, 2006). Another simple and less expensive method used in radical polymerization is photopolymerization. This method is defined as the reaction of monomers or macromers to produce polymeric structures by light-induced initiation and subsequent polymerization. The general concept of photopolymerization is to conjugate and solidify the fluid reactants into a desired stable structure using *X*-ray, gamma or UV irradiation. High energy radiations (*X*-ray or gamma) may cause degradation of the base film and hence lower mechanical properties of membranes. However UV is a low-energy radiation by which significant degradation of the base film can be greatly avoided (Asano, 2007).

In this thesis, PVDF-*g*-PS graft copolymers were synthesized via UV-induced photografting of styrene onto PVDF. To date, PVDF-*g*-PSSA graft copolymers have never been synthesized by UV photopolymerization method. The degree of grafting was examined as a function of UV irradiation time. PVDF-*g*-PS graft copolymers were then sulfonated for preparing proton-conducting membranes. The synthesized graft copolymers were characterized by H-NMR and FTIR spectroscopic analysis. Their thermal properties were examined by thermogravimetry analysis (TGA) and differential scanning calorimetry (DSC) measurements. Several characteristics of PVDF graft copolymer membranes, e.g. ion exchange capacity, water uptake, hydration number were also reported. Their proton conductivity properties were analyzed and discussed in detail.

CHAPTER 2

2.1 PHOTOPOLYMERIZATION

Photopolymerization is a process in which either visible or UV light is used to generate initiating species to form polymers from reactive monomers. Absorption of incident light by one or several components of the polymerization mixture is the crucial prerequisite. First photopolymerization reported by Blyth and Hoffman more than 150 years ago was the polymerization of styrene under sunlight (Mishra, 2009).

Many factors (e.g., irradiation source, wavelength screening, distance of source from reaction cell, catalyst, photosensitizer, temperature, solvent, presence of oxygen, etc.) affect UV induced polymerization. The photopolymerizations induced by UV irradiation exhibit some advantages, e.g., fast reaction rate, low cost of processing, simple equipment, and easy industrialization. The distribution of grafted chains is limited to a shallow region near the surface. Photopolymerization thus offers the unique ability to tune and manipulate surface properties without damaging the bulk material (Deng, 2009). The pioneering work on photografting polymerization initiated by UV light was published in the 1950s by Oster and Shibata (Oster, 1950)

UV polymerization has received great interests in research and industrial applications for the last several decades, because of the rapid polymerization and high productivity rates. Industrial UV polymerization includes green chemistry reactions, namely, 100 % reactive materials and without VOC, and low energy consumption. Light-induced free radical polymerization is of enormous commercial use. Curing of coatings on wood, metal and paper, adhesives, printing inks and photoresists are based on photoinitiated radical vinyl polymerization techniques (Allen, 2010). On the other hand, a few studies related to polymer electrolyte membranes obtained via UV induced polymerization methods have been reported so far.

2.1.1 Photoinitiation

UV light is extensively used to carry out surface graft polymerization, often in the presence of a photoinitiator or photosensitizer. Photoinitiation process includes several steps as shown in Figure 2.1 (Mishra, 2009).

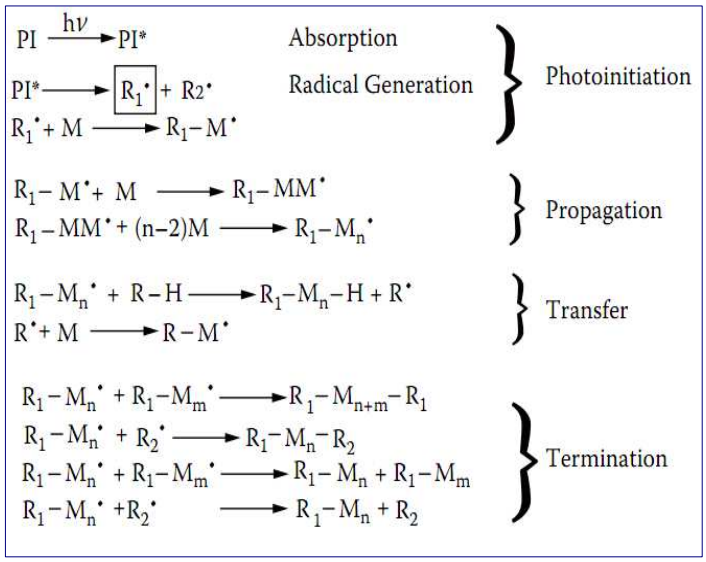

Figure 2.1 General steps for photoinitiated free radical polymerization (Mishra, 2009)

Photoinitiation: Absorption of light (UV) by a photosensitive compound. Homolytic bond rupture leads to the formation of a radical that reacts with one monomer unit. Propagation: Repeated addition of monomer units to the chain radical produces the polymer backbone. Chain transfer: Termination of growing chains by hydrogen abstraction from various species (e.g., from solvent) and concomitant production of a new radical capable of initiating another chain reaction. Termination: Chain radicals are consumed by disproportionation or recombination reactions.

Two types of photoinitiation are known so-called “Norrish type-I” and “Norrish type-II” as shown in Figure 2.2.

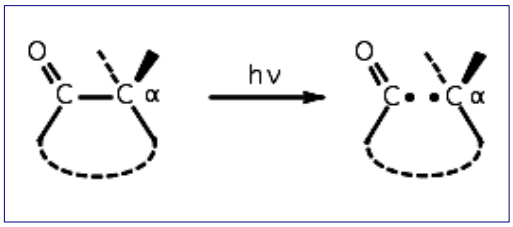

A) Norrish Type I Photoinitiators

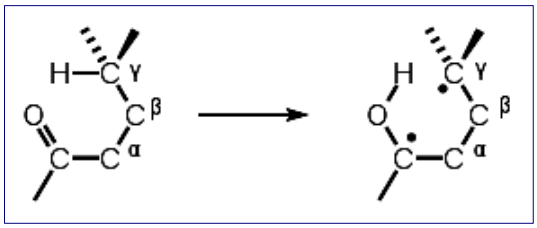

B) Norrish Type II Photoinitiators

Figure 2.2 Norrish Type I and Type II photoinitiators

In Norrish Type-I, two initiating radicals are generated by α-cleavage when the initiator is exposed to UV-light. Unimolecular initiators undergo a homolytic bond cleavage upon absorption of light. Benzoin derivatives are used for this purpose (Figure 2.3). Such chromophores attached to the polymer trunk, in-chain or side-chain will afford block and graft copolymers, respectively. Here, homopolymer formation is an intrinsic outcome of this kind of initiation, which originates from the low molar mass initiator fragment. These free radical species are able to initiate the polymerization and crosslinking reactions of vinyl monomers (Allen, 2010).

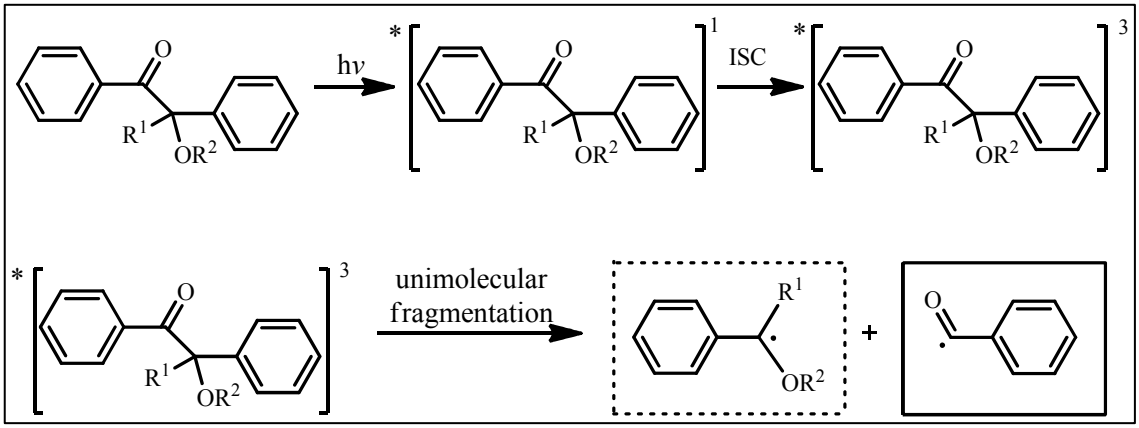

Figure 2.3 α-Cleavage type photoinitiation (Muftuoglu, *et al.*, 2010)

In Norrish Type-II, excitation energy of certain compounds (sensitizer) is lower than the bond dissociation energy so they do not initiate the polymerization. Instead, a coinitiator should be present in the medium as the source of initiating radicals. The chromophore, so called sensitizer, absorbs UV radiation and is excited to a triplet state. This stage is accompanied by abstraction of labile hydrogen from the coinitiator to form two radical species (Figure 2.4). The radical formed on the sensitizer is usually unreactive and does not take part in initiation. This way, homopolymer formation can be prevented. The most common sensitizers are aromatic ketones such as benzophenones with maximum absorbance at 254 nm. Others include thioxanthones and dyes, having absorbances in UV-visible region. Type II initiating systems have two distinct pathways: (1) Hydrogen abstraction from a suitable hydrogen donor, and (2) Photoinduced electron transfer reactions and subsequent fragmentation (see Figure 2.4) (Allen, 2010).

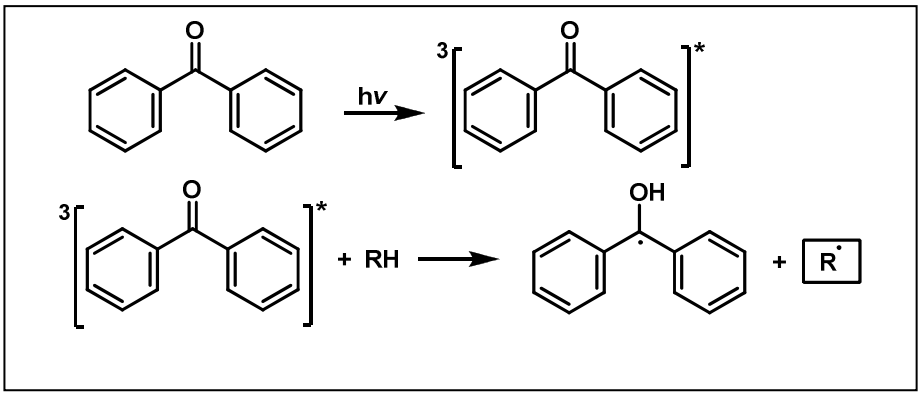

Figure 2.4 Hydrogen abstraction type photoinitiation (Muftuoglu, et al., 2010).

The most common sensitizers are aromatic ketones such as benzophenones with maximum absorbance at 254 nm. Others include thioxanthones and dyes, having absorbances in UV-visible region. It is noteworthy that aliphatic ketones, such as butanone, pentan-2-one, pentan-3-one, and heptan-3-one have been found to be potential sensitizers for photografting when they were in suitable ketone/water/alcohol mixed solvents (Wang, 2004). Another interesting case is the self-initiation of some acrylic and styrenic monomers upon UV irradiation. Since this process is quite slow, a photoinitiator is normally required. Recent findings on the self-initiation of maleic anhydride (Deng, 2001), styrene (Wang, 2004) and a number of acrylic monomers (Deng, 2001) have demonstrated that photopolymerization and photografting could possibly be achieved without using photoinitiators or sensitizers.

2.2 PHOTOINDUCED SYNTHESIS OF GRAFT COPOLYMERS

Covalent attachment of polymer chains with different chemical natures onto a substrate, so-called grafting, has emerged as an elegant technique in achieving targeted physical and mechanical properties. Graft chains can be positioned either along a polymer backbone resulting new macromolecular structures or along surfaces in 2-D, in which case, providing the desired physical properties on the surfaces and interphases without altering the properties of the bulk.

In principle, one can get access to graft structures by the following well-known strategies: (1) “grafting from” (2) “grafting onto” (3) “grafting through”. In the first one,

graft chains are grown out of a polymer backbone. Here, the backbone acts as a side-functional macro-initiator in the polymerization of a certain monomer. In the second method, preformed polymer chains carrying antagonist groups at one ends are chemically linked to the backbone. The last one involves copolymerizing macromonomers. That is, the backbone is synthesized through the polymerizable moieties attached to termini of polymeric chains, simultaneously yielding the graft copolymer (Muftuoglu, et al., 2010).

Part of grafting strategies can be used in association with photoinduced grafting methods. No work related to photoinduced "grafting onto" technique, has been reported which seems almost impossible to achieve. "Grafting Onto" is best defined as the attachment of end-functional polymeric chains, namely telechelics, onto specific sites on polymer backbones or surfaces via a chemical reaction (Figure 2.5).

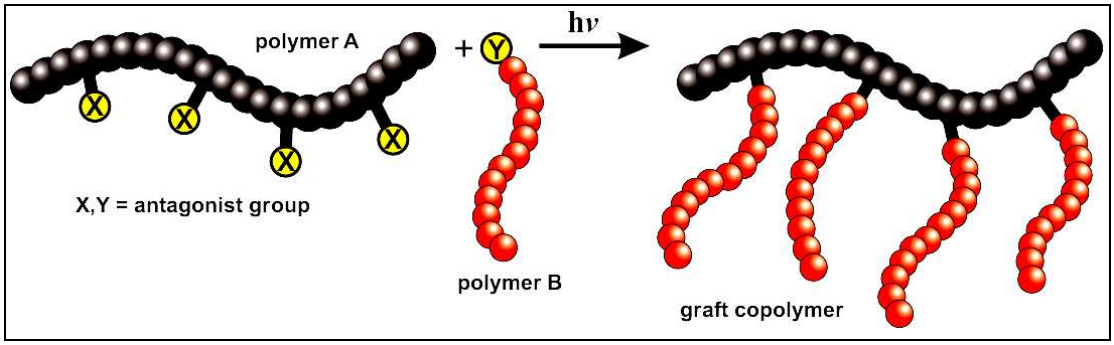

Figure 2.5 Synthesis of graft copolymers via photoinduced grafting onto method. (Muftuoglu, et al., 2010).

"Grafting through" is a common way of preparing synthetic graft copolymers through polymerization of macromonomers, where the mode of initiation is simply of low practical value (Figure 2.6). Thermally initiated controlled polymerizations are more complementary in "grafting through" strategy than photoinitiated ones. Although a few studies have been reported by several authors (Allen, 2010, Capek, 2000, and Degirmenci, 2004).

As previously stated, "grafting from" methodology consists of polymerization of monomers initiated from active sites distributed along a polymer backbone or a surface. Photoinitiated polymerizations can well be adapted to this approach. Both type-I and

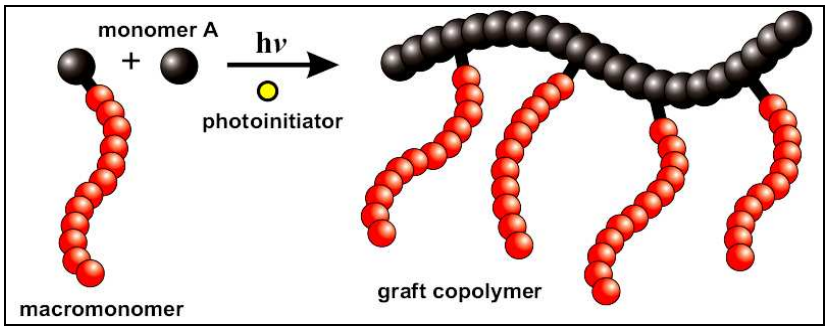

Figure 2.6 Synthesis of graft copolymers via photoinduced grafting through method. (Muftuoglu, et al., 2010).

type-II initiations can be used effectively. Most of the reported studies are based on this technique (Muftuoglu, et al., 2010).

2.2.1 Homogeneous photografting

When the polymeric substance to be grafted should be dissolved in a solution, every chain in the polymer contains the graft chains after grafting reaction. Then the substrate is said to be homogeneously grafted. However, this is not the case in surface grafting, wherein the graft chains are merely held on substrate surfaces. A modification at the surface molecules usually have been intended as to retain the properties in the bulk. Depending on the extent of penetration of the solvent through the substrate surface, the depth of grafting can be adjusted (Muftuoglu, et al., 2010). Surface grafting in thin films or porous membranes sometimes results in homogeneously grafted layers.

2.2.1.1 Free Radical Systems

a) α-Cleavage Initiation

Initiation can be achieved by the radicals generated upon photolysis of type-I initiator moieties at a specific wavelength, as depicted in Figure 2.7. In this case, homopolymer formation is also expected due to the presence of low molar-mass radicals.

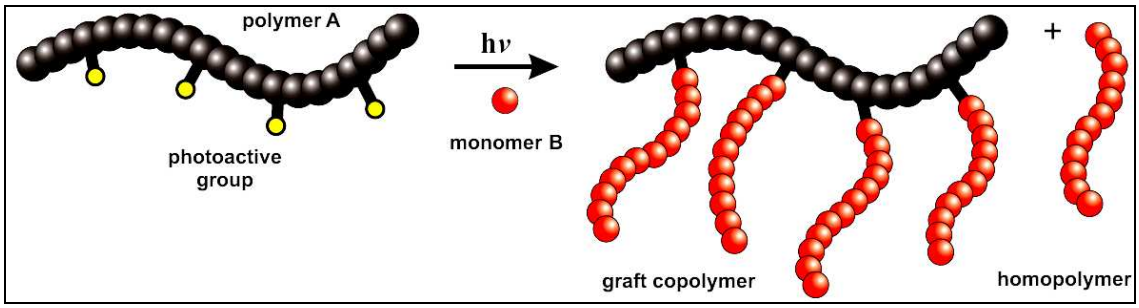

Figure 2.7 Homogeneous synthesis of graft copolymers by α-cleavage type photoinitiation (Muftuoglu, et al., 2010).

In the early work of Norrish (Guillet, 1955), it has been demonstrated that, upon irradiation poly(methyl vinyl ketone) in conjunction with acrylonitrile, vinyl acetate or methyl methacrylate in dioxane solution, it went through α-cleavage and yielded graft- and homo- polymers of the corresponding monomers according to the mechanism outlined in Figure 2.8.

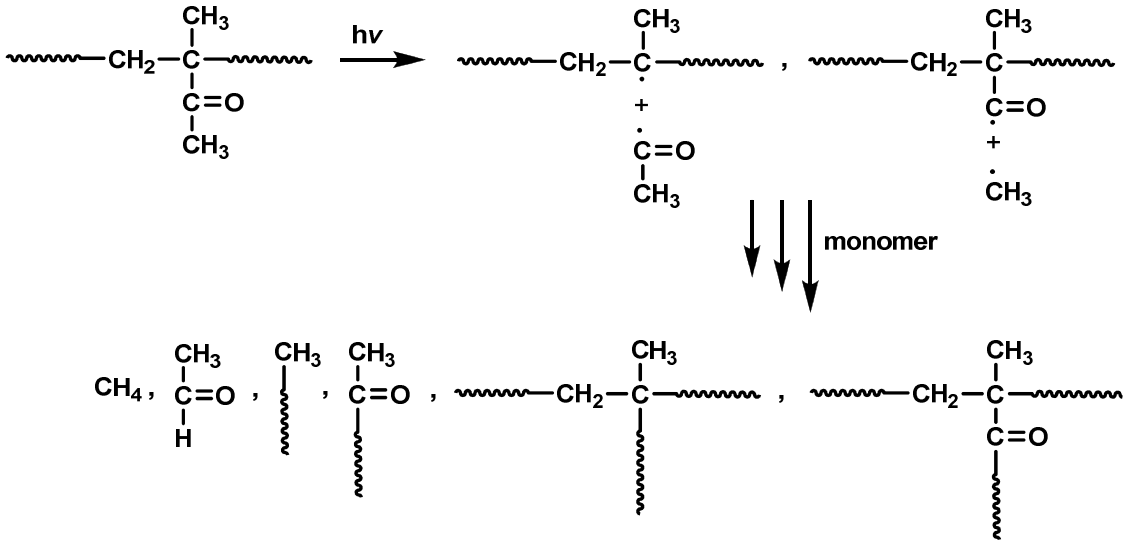

Figure 2.8 Photoscission and self- initiation mechanism of poly(methyl vinyl ketone) in presence of various monomers (Muftuoglu, et al., 2010).

b) Hydrogen Abstraction Initiation

Use is made of type-II initiation if the precursor polymer is open to H-abstraction from the side chain by an excited photosensitizer (Figure 2.9). For instance, tertiary amines are capable of donating hydrogen radicals when irradiated by a UV source in the presence of benzophenone. The ketyl radical formed from benzophenone is unreactive

towards initiating new chains, thereby, homopolymer formation is avoided. This is a profitable feature of this kind of initiation.

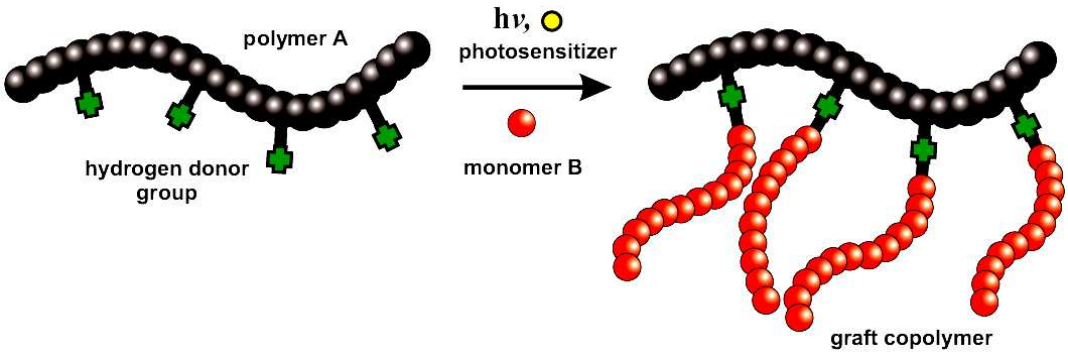

Figure 2.9 Homogeneous synthesis of graft copolymers by hydrogen abstraction type photoinitiation (Muftuoglu, et al., 2010).

Muftuoglu *et al*. (Muftuoglu, 2004) described the preparation of methyl methacrylate brushes on a poly(*N*,*N*-dimethyl-4-vinylphenethylamine-*block*-styrene) copolymer backbone (Figure 2.10).

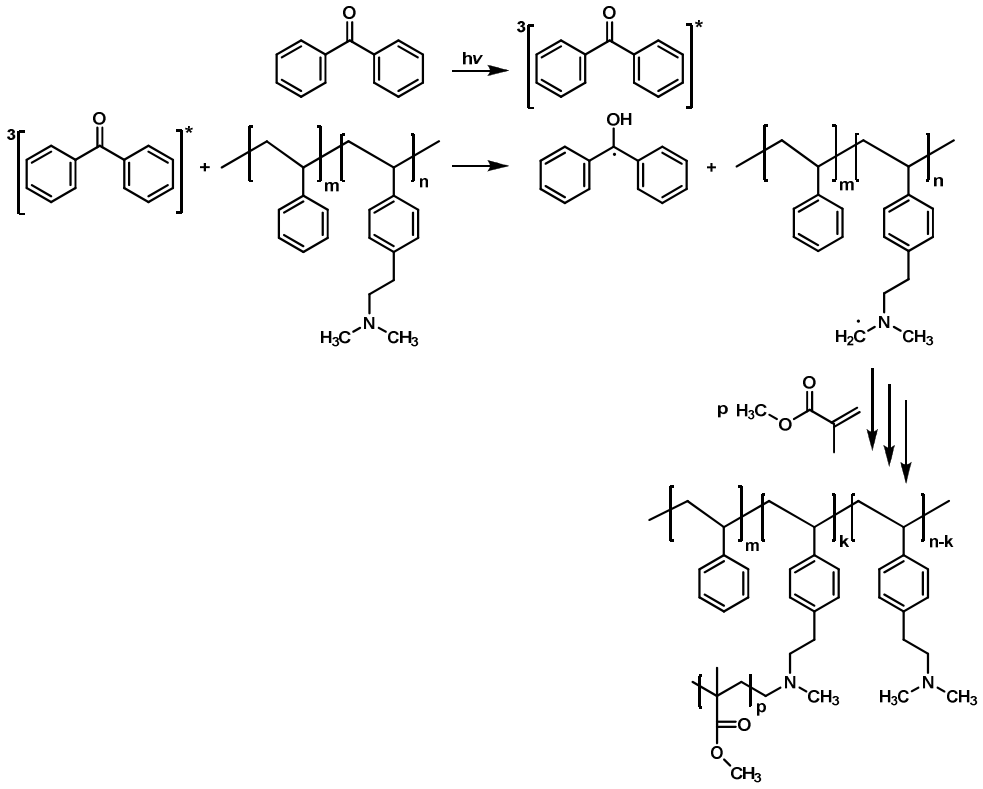

Figure 2.10 Photoinduced synthesis of block-graft copolymers using polymeric hydrogen donor and benzophenone.

The precursor diblock copolymer was synthesized through living anionic polymerization, in which one of the blocks held single *N*,*N*-dimethyl amino moiety in each repeating unit. Upon exposure to UV-light in the presence of benzophenone, carbon centered radicals generated via H-abstraction from *N*,*N*-dimethyl amino groups by the triplet benzophenone initiated the polymerization, the block-graft copolymer eventually being formed.

It is also possible to anchor the sensitizer one way or the other to the trunk polymer. Actually, macrophotoinitiators are frequently used in curing applications and present such advantages as non-yellowing, low-odor, low contaminant release, etc., in processing over the low molecular analogues. Additional advantages originate, in the case of photografting (Mateo, 1993), from their macromolecular orientation giving rise to intramolecular reactions that would generate more free radicals and promote grafting while the termination rate of active species is reduced by the low mobility as well as caging of the chains (Figure 2.11).

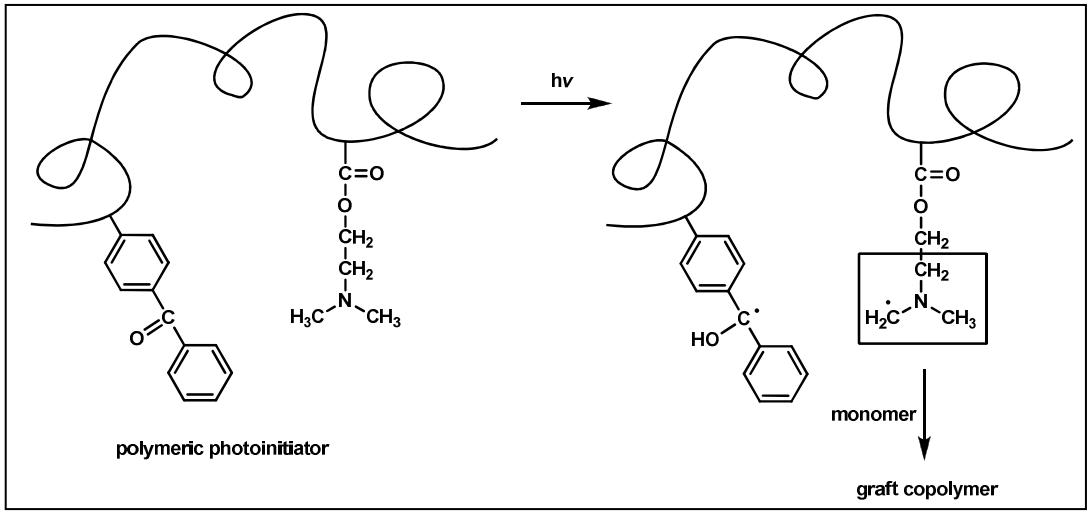

Figure 2.11 Synthesis of graft copolymer by one component type II macrophotoinitiator

c) Photoiniferter

This technique, developed by Otsu *et. al*., employs dithiocarbamate groups as the iniferter for the controlled growth of polymer chains. An iniferter is a species acting as an initiator, chain transfer agent, and terminator. Upon UV-irradiation, a pair of radicals is formed through bond rupture, the mechanism of which is shown in Figure 2.12. The alkyl radical initiates polymerization while the dithiocarbamate radical with much less

reactivity takes part in the reversible activation and deactivation of the propagating chain end. As long as irradiation is continued, the equilibrium between active and dormant chains prevails and addition of a number of monomers is allowed each time the chain is active in a quasi-living manner. Depending on the location of dithiocarbamate groups in the backbone, block and graft copolymers have been prepared.

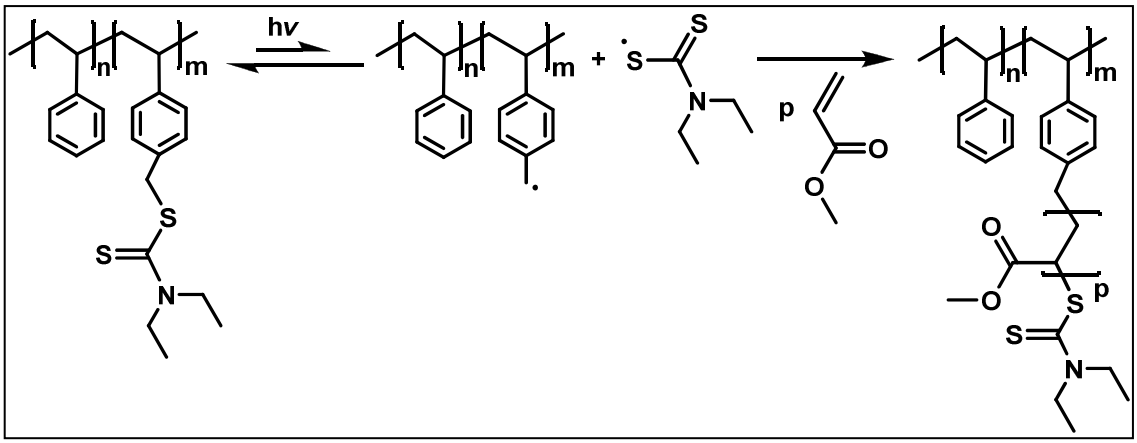

Figure 2.12 Photograft polymerization of vinyl monomers by photoiniferter mechanism (Muftuoglu, et al., 2010).

2.2.2 Surface photografting

In this process, a polymer surface is chemically modified by grafting or by the generation of active sites that can lead to the initiation of a graft polymerization. Most of the known procedures for surface grafting are based on “grafting from” technique. The surfaces to be grafted include a wide range of commodity polymers with different forms such as films, membranes, sheets, fibers, foams, granules, besides inorganic surfaces such as gold, silicon, etc. surface grafting are based on “grafting from” technique (Muftuoglu, et al., 2010). Both Norrish Type-I and Norrish Type-II initiations may be used effectively. Compared with Norrish Type I photoinitiators, Norrish Type II photoinitiators are more frequently used, because the latter results in higher grafting efficiency, while the former leads to higher polymerization yield and higher polymerization rate, but lower grafting efficiency (Deng, 2009). Among the existing Norrish type II photoinitiators, probably the most widely selected have been benzophenone (BP) and its derivatives, shown to effectively initiate or co-initiate a number of radical-induced surface photografting polymerizations (Deng, 2000). In this

thesis, surface grafting method is used to obtain PVDF based proton conducting membranes.

2.2.2.1 Surface Photografting Method

a) Mutual Irradiation Technique

Mutual irradiation is a direct method, at which the substrate, the photoinitiator and the monomer are simultaneously exposed to UV irradiation. This technique is unable to eliminate the homopolymer formation, since a great many radicals caused by irradiation of the monomer will be present in the medium. Only a limited number of works have been reported concerning surface grafting via UV irradiation without utilizing any photoinitiators or sensitizers. Because, in most cases, the radicals generated on the surface are inadequate to afford graft chains with quantitative yields, the addition of a photosensitizer is essential. In the work of Uchida, *et.al*., using the mutual (simultaneous) irradiation method in the absence of a photosensitizer, polyacrylamide has been grafted onto the surface of a poly(ethylene terephthalate) (PET) film so as to enhance the low water wettability of PET (Uchida *et al*., 1989). Polyethylene (PE) is surface modified via attachment of hydrophilic polymer chains in an attempt to improve wettability, adhesion, lubrication, biocompatibility, etc (Uyama *et al*., 1998 and Kato *et al*., 2003). In a typical work, methacrylic acid (MAA), and acrylic acid (AA) have been photochemically grafted on high density polyethylene films using benzophenone as a sensitizer and a variety of solvents (Wang *et al*., 2004).

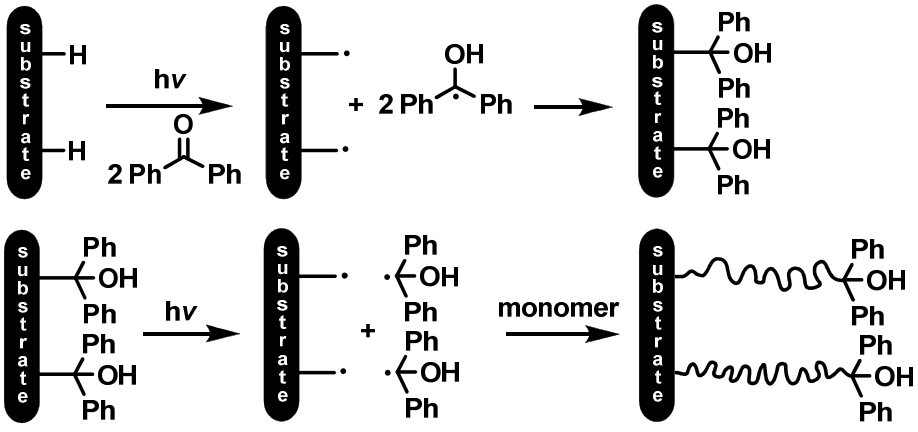

Figure 2.13 Schematic representation of photoinduced living graft polymerization (Muftuoglu, et al., 2010).

Bowman and coworkers have developed a novel sequential UV-induced living graft polymerization method consisting of two steps (Ma *et al*., 2000). In the first step, a surface initiator has been prepared from polymeric substrate and benzophenone upon UV irradiation in the absence of monomer. That is, the semipinacol radicals produced by hydrogen abstraction from the surface polymer recombine with the surface radicals. In the second step, monomer introduced to the polymerization vessel has been polymerized through a living mechanism mediated by the surface bound semipinacol radicals (Figure 2.13).

b) Pre-irradiation Technique

In pre-irradiation technique, the substrate is preirradiated in the presence of air or in an inert atmosphere, followed by addition of the monomer in bulk, in solution or in vapor phase. Oxidation of the surface radicals in air generates surface bound peroxide groups, which are subsequently heated or UV-irradiated to generate peroxy radicals. In the other case, the radicals formed at the surface of the substrate in an inert atmosphere or in vacuum survive for a certain period and the introduction of the monomer in the second step affords graft copolymer (Figure 2.1). The advantage of this method is that the homopolymer formation is prevented (Figure 2.14A). However, some homopolymer chains may still be formed from hydroxyl radicals as seen in Figure 2.14B.

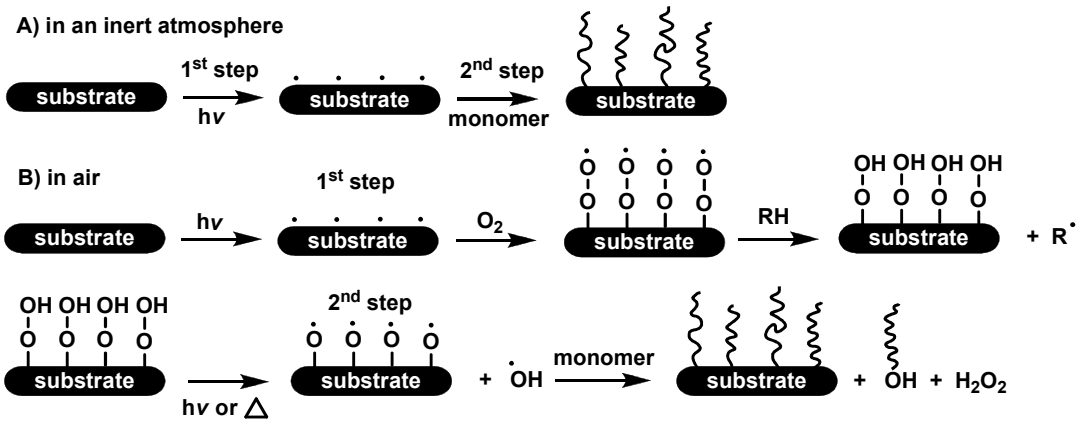

Figure 2.14 Schematic representation of photoinduced living graft polymerization (Muftuoglu, et al., 2010).

On the other hand, peroxy radicals may initiate oxidative degradation, possibly leading to flaking of the polymer substrate. In any case, specific stabilizers have proved to be successful in partly inhibiting degradation (Muftuoglu, et al., 2010).

c) Vapor Phase Photografting

Being pretreated with benzophenone, the substrate, in contact with vaporized monomer, is exposed to UV-light to achieve grafting (Ranby, 1998, Allmer *et al*., 1988 and Ranby, 1992). Coating benzophenone onto surfaces may be performed by casting the benzophenone solution onto the surface followed by drying (Ogiwara *et al.*, 1981). Another way is to expose the substrate to benzophenone vapor in conjunction with vaporized monomer in a solvent-free atmosphere (Wirsen *et al.*, 2005) The advantages of vapor phase grafting include efficient use of monomer, less homopolymer formation, and easy isolation of the grafted substrate from the polymerization medium. Sometimes, the to-be-grafted surface is dipped in an acetone solution containing around 0.5 wt % poly(vinyl acetate) besides sensitizer (Amornsakchai *et al.*, 1998 and Kubota *et al.*, 1990) The main role of poly(vinyl acetate) addition is to provide homogeneous distribution of the sensitizer on the sample surface.

d) Immersion Photografting

As the name implies, the surface to be grafted is immersed in a solution containing sensitizer and monomer or alternatively solutions of each sequentially. The examples given thus far also fall into this category, regardless of the number of steps grafting has been conducted.

2.2.3 Miscellaneous Applied Surface Grafts

a) Membranes

Photografting is a fashionable method in the modification of polymer membranes (Ulbricht, 2006). Polymeric membranes play an important role in various membrane separation processes, namely, gas separation, reverse osmosis, pervaporation, ultrafiltration, nanofiltration, microfiltration as well as in applications such as

biomaterials, catalysis, proton conductivity, etc. Desirable mechanical and separation features can be imparted to hydrocarbon polymer membranes by grafting certain monomers, considering whether they operate in aqueous or non-aqueous conditions.

A novel route to the preparation of proton-conducting membranes has been proposed by Chen et. al. (Chen *et al*., 2006). The method consists of UV-induced photografting of styrene into polytetrafluoroethylene (PTFE) films and subsequent sulfonation (Figure 2.15).

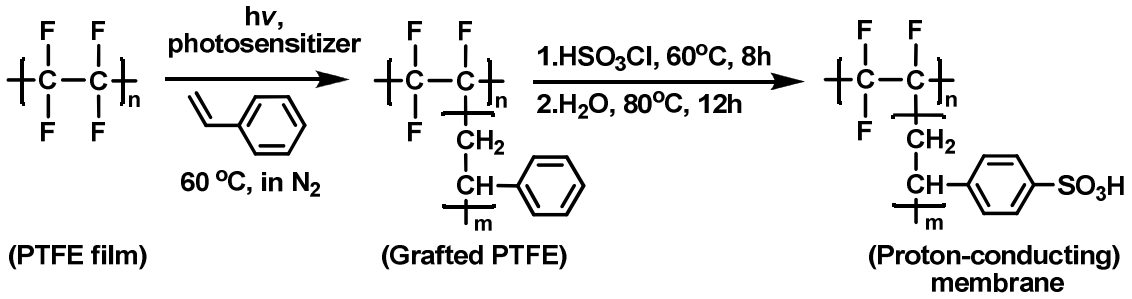

Figure 2.15 Preparation of proton conducting membranes by photografting methods (Muftuoglu, et al., 2010).

It was found that graft chains penetrated through the films and only 7 % grafting improved proton conductivity providing better mechanical properties, which resemble those of Nafion membrane. A follow-up paper (Asano *et al*., 2007) includes SEM images of the surface and cross-section morphologies indicating that completely sulfonated graft chains were effectively constructed to form the network for proton transport. Same authors (Chen *et al*., 2006) compared the efficiencies of modified poly(tetrafluoroethylene-co-ethyle) films, obtained by vapor- and liquid-phase photografting of styrene, in fuel cell applications. They have found proton conductivities as high as 0.065 and 0.087 S/cm for vapor- and liquid-phase grafts, respectively.

A process comprising photografting poly(acrylic acid) onto polysulfone ultrafiltration membranes has been studied (Bequet *et al*., 2000). The effect of graft parameters such as irradiation time, wavelengths, and monomer concentration on the membrane performance has been examined. Use of *N*,*N'*-methylene bisacrylamide as a crosslinking agent has resulted in a more stabilized grafting, in which no photoinitiator

and no reactant purification is needed. The water softening measurements of the membranes were obtained in dead-end mode and at a 95% recovery. The results demonstrated the feasibility of photografting in the preparation of nanofiltration membranes.

Recently, Ulbricht and coworkers (Susanto et al., 2007) have reported the preparation of low-fouling ultrafiltration membranes by simultaneous photograft copolymerization of hydrophilic poly(ethylene glycol) methacrylate onto a polyethersulfone membrane. A broad characterization using flux measurement and sieving curve analysis, FTIR-ATR spectroscopy, contact angle and zeta potential measurement has been carried out. Membrane performance was assessed utilizing model solutions of sugarcane juice polysaccharides and the protein BSA. All modified membranes showed more resistance to fouling and higher rejection than unmodified ones. Surface functionalization was best achieved with relatively high monomer concentrations (40 g/L) and moderate irradiation periods (1.5–3 min). Some other examples from literature are presented in Table 2.1(Muftuoglu, et al., 2010).

Table 2.1 Modification of Polymer Membranes via Photografting Method

Membrane	Monomers	PI	Ref.
Poly(ethylene terephthalate) (PET)	NIPAAm	BP	Geismann, 2007; Yang, 2003
	4VP	BP	Yang, 2005
	AA	BP	Yang, 2005; Zhang, 2006.
	NIPAAm	-	Curti, 2005
Poly(tetrafluoro ethylene) (PTFE)	St	XT	Chen, 2006; Asano, 2007
	HEMA	BP	Yamada, 2006
	HEA	BP	Yamada, 2006
	DMAEMA	-	Yamada, 2001; Yamada, 1996
	MMA	-	Yamada, 1996
Polysulfone (PS)	NaSS	HBP	Akbari, 2007
	NaSS	-	Akbari, 2006; Akbari, 2002
	AC	-	Akbari, 2006
	AA	-	Bequet, 2000; Shim, 1999
Polyethersulfone (PES)	PEGMA	-	Susanto, 2007
	SPE	-	Susanto, 2007
	AMPS	BP	Hilal, 2003
	qDMAEMA	BP	Hilal, 2003
Polypropylene (PP)	AA	BP	Ma, 2001
	NVP and MAn	BP	Xing, 2005
	NVP and BE	BP	Xing, 2003
	AMPS	BP	Piletsky, 2000
	PEGMA	BP	Ma, 2001
	DMAEMA	BP	Yamada, 2003
	MAA	BP	Yamada, 2003
Polyethylene (PE)	GMA	BP	Yamada, 2006
	GMA	XT	Irwan, 2004
	DMAEMA	BP	Yamada, 2003
	NIPAAm	XT	Peng, 2001
	MAA	XT	Peng, 2001

	AA	BP	Costamagna, 2006
Low-density polyethylene (LDPE)	St	BP	Zhang, 2006
	MMA	BP	Zhang, 2006
	AAm	BP	Zhang, 2006
	St and MAn	BP	Deng, 2005
	NIPAAm	XT	Irwan, 2003, Kubota,1994
	MAA	BP	Yamada, 2003
	AA	BP	Zhang, 2006, Yamada, 2003
	AA	ITX	Zhang, 2006
	DMAEMA	BP	Yamada, 2003
Poly (vinylidene fluoride) (PVDF)	AA	BP	Ma, 2001
	PEGMA	BP	Ma, 2001
	DMAEMA	BP	Ma, 2001
Polyacrylonitrile (PAN)	AA	DT	Wang, 1997
	qDMAEMA	-	Kobayashi, 1991
	NaSS	-	Kobayashi, 1991, Kobayashi, 1992
Polyurethane (PU)	AAm	-	Guan, 2000
	HEE	-	Guan, 2000
	MAA	-	Guan, 2000
Polyamide (PA)	DEAAm	BP	Wu, 2006
Polystyrene (PSt)	NIPAAm	-	Curti, 2005
Poly(vinyl chloride) (PVC)	AA	BP	Costamagna, 2006
Poly-L-lactide (PLLA)	HEMA	-	Ma, 2001
	MAA	-	Ma, 2001
	AAm	-	Ma, 2001
Polypropylene-g-poly(acrylic acid) (PP-g-PAA)	NIPAAm	-	Yang, 2004
Styrene–butadiene–styrene rubber (SBS)	DMAEMA	-	Yang, 1999
	4VP	BEE	Yang, 1997
Poly(tetrafluoroethylene-co-ethylene) (PETFE)	St	XT	Chen, 2006

CHAPTER 3

3.1 FUEL CELLS

The principle of the fuel cell was first discovered by William Grove in 1893. After years NASA demonstrated some potential applications in providing power and drinking water in space flights. As a result of this, industry started to recognize potential commercial applications of fuel cell driven by technical, economic, and social forces such as high performance reliability, durability, characteristics, and environmental feasibility. Fuel cell is similar to a battery. It uses an electrochemical process to directly convert chemical energy to electricity and water. Unlike a battery, a fuel cell does not require recharging nor does it run down as long as fuel and air are provided. (Lin, 2000)

Fuel cells may be classified based on the used criteria to different methods which typically depend on the different parameters related to operating conditions and fuel cell structure. Fuel cell systems have different variables such as type of the electrolyte used in fuel cell, type of the exchanged ion through the electrolyte, type of the reactants (e.g. primary fuels and oxidants), operating temperature and pressure, direct and indirect usage of the primary fuels in fuel cell system, And finally the primary and regenerative systems. It is common that fuel cells are generally classified and nominated based on the nature of used electrolyte in the fuel cell. Therefore, based on this classification, fuel cells include the following different types: (1) alkaline fuel cells (AFC) with the alkaline solution electrolyte (such as potassium hydroxide KOH), (2) phosphoric acid fuel cells (PAFC) with acidic solution electrolyte (such as phosphoric acid), (3) solid proton exchange membrane (PEMFC) which are known to polymer electrolyte membrane fuel cells and their electrolyte consist of the proton exchange membrane, (4) molten carbonate fuel cells (MCFC) with molten carbonate salt electrolyte, (5) solid oxide fuel cells (SOFC) with ceramic ion conducting electrolyte in solid oxide form. (

Xianguo, 2006) Table 3.1 summarizes the typical characteristics of these various fuel cell systems. Fuel cells can be used as highly efficient and non-polluting power sources.

Table 3.1 Summary of major differences of the fuel cell types (Lin, 2000).

Fuel Cell	Electrolyte	Temprature (^{o}C)	Electrochemical reaction	Applications
Alkaline (AFC)	Potassium Hydroxide	90-100	A:H_2+2OH^-→2H_2O+2e^- C:1/2O_2+ H_2O+2e^-→2OH^-	Military Space Flight
Phosphoric Acid (PAFC)	Phosphoric Acid	175-200	A:H_2→2H^++2e^- C:1/2O_2+ 2H^++2e^-→ H_2O	Electric Utility Transportation
Molten Carbonate (MCFC)	Lithium, Sodium and/or Potassium Carbonate	600-800	A:H_2+CO_3^{2-}→H_2O+CO_2+2e^- C:1/2O_2+ CO_2+2e^-→ CO_3^{2-}	Electric Utility
Solid Oxide (SOFC)	Zirconium Oxide doped byYttrium	600-1000	A:H_2+O^{2-}→H_2O+2e^- C:1/2O_2+2e^-→O^{2-}	Electric Utility
Proton Exchange Membrane (PEM)	Solid Organic Polymer (poly-perflourosulfonic acid)	60-100	A:H_2→2H^++2e^- C:1/2O_2+2H^++2e^-→H_2O	Electric Utility Portable Power Transportation

A: Anode, C: Cathode

3.1.1 Proton Exchange Membrane Fuel Cell (PEMFC)

The proton exchange membrane fuel cell, also called the solid polymer fuel cell, uses a polymer to conduct mobile ions (H+) through the system. This low temperature fuel cell boasts a rapid start time as well as a compact unit design, no specific orientation requirements, and no corrosive fluid hazards, all of which make it ideal for use in vehicles and portable devices. The operating conditions vary with purpose; however PEM fuel cells generally operate at temperatures ranging from 85 to 105°C and at ambient pressure or higher (Larminie, 2003).

The main functioning unit of a PEM fuel cell is the membrane electrode assembly or MEA. The MEA is comprised of a very thin membrane, a polymer electrolyte which serves to facilitate proton transport from the anode to the cathode, sandwiched between a two electrodes. The electrodes are carbon – supported catalyst fixed to porous carbon cloth or paper. This assembly of anodic diffusion layer, catalyst layer, membrane, catalyst layer, cathodic diffusion layer is perfectly aligned and hot pressed until it is one inseparable unit. (Larminie, 2003).

Within a PEM fuel cell, the primary reactions taking place are that the hydrogen gas enters through the field flow plates of the anode and diffuses through the carbon cloth or paper. It reacts with the platinum catalyst, losing two electrons which are conducted by the carbon out to the external circuit as the remaining protons are transported through the membrane. Meanwhile, air enters the cathode side of the assembly. The oxygen molecule is broken and the ions react with the protons from the membrane and electrons arriving through the external circuit to make water. The overall system of a PEM fuel cell is shown in Figure 3.1.

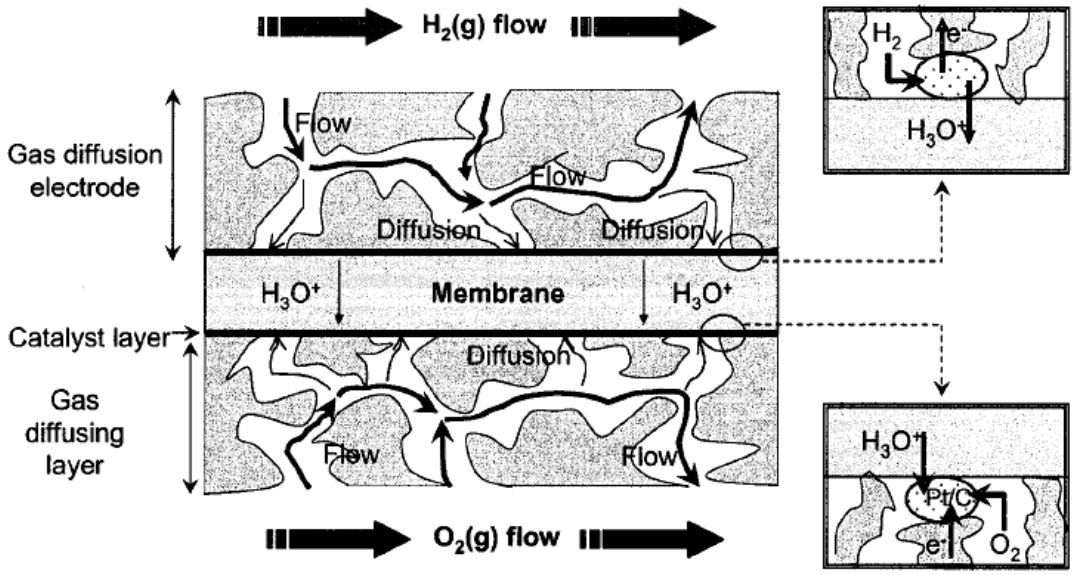

Anode: $H_2(g) \rightarrow 2H^+ + 2e^-$

Cathode: $1/2O_2(g) + 2H^+ + 2e^- \rightarrow H_2O(l)$

Net Reaction: $H_2(g) + 1/2O_2(g) \rightarrow H_2O(l)$

Figure 3.1 Schematic illustration of an individual PEM Feul Cell (Siu, 2000)

The PEMFC is an attractive power source for vehicles and portable electronic devices due to its high power density and relatively low operating temperature. Other advantages of PEMFCs over other types of fuel cells are their nonvolatile electrolytes and efficient energy conversion. To achieve high performance in fuel cell applications, the polymer electrolyte as membrane must possess the following desirable properties: high proton conductivity to support high currents with minimal resistive losses, zero electron conductivity, adequate mechanical strength and stability, chemical and

electrochemical stability under operating conditions, moisture control in stack extremely low permeability to fuel or oxidant, low production cost and the capability for easy fabrication.

3.2 POLYMER ELECTROLYTE MEMBRANES

3.2.1 Classification of Proton Exchange Membranes

The polymer electrolyte membrane materials, used in synthesis, can be classified into three immense groups: perflourinated ionomers (or partially perflourinated), non-flourinated hydrocarbons (including aliphatic or aromatic structures), and acid–base complexes (Smitha et al., 2005). The classification of membranes is shown in Figure 3.2

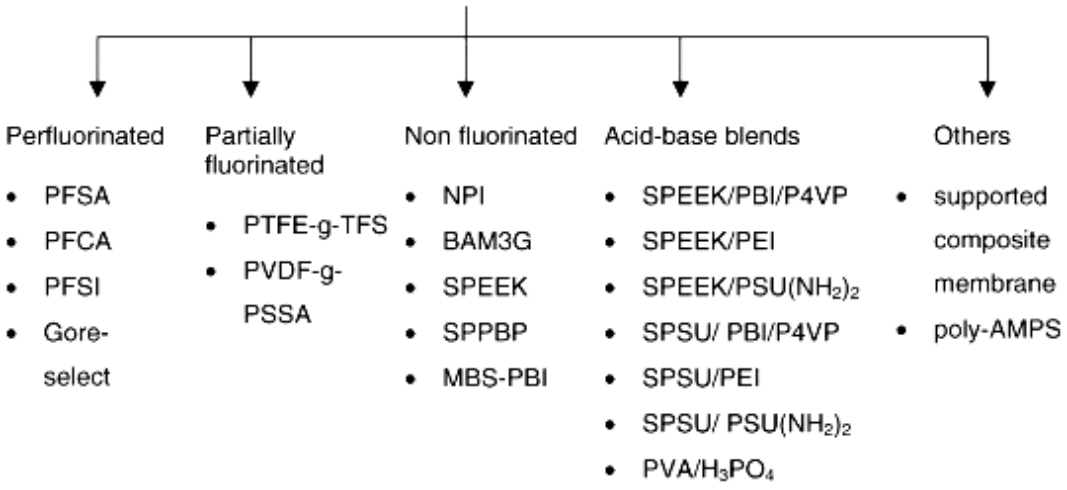

Figure 3.2 Classification of proton exchange membranes based on materials (perfluorinated, partially fluorinated and non-fluorinated) and preparation method (acid-base blends and others).

3.2.2 Hydrous Proton Conducting Membranes

3.2.2.1 Nafion and Perfluorinated Polymer Membranes

Polyelectrolyte membranes (PEMs) are generally based on hydrated sulfonated polymers. Among these, perfluorosulfonic acid membranes, such as Nafion®, have drawn much interest because of their chemical and electrochemical stability. Nafion

was first developed in the late 1960s by DuPont (structure shown in Figure 3.3). It has a structure of copolymer from fluoro 3,6-dioxo 4,6-octane sulfonic acid with polytetra-fluorethylene (PTFE) that Teflon backbone of this structure gives the hydrophobic nature for membrane and hydrophilic sulfonic acid groups (HSO_3-) have been grafted chemically into backbone by the free radical initiated copolymerization (Rikukawa et al., 2000). These ionic groups have caused the absorption of the large amount of water by polymer and therefore, lead to hydration of polymer. Thus, the factors affecting the performance of the suitable proton exchange membrane are the level of hydration and thickness of the membrane which is playing an important role in deciding their suitability for application in fuel cell. (Appleby et al., 1989)

There are three common types of Nafion, 112, 115, and 117. The designation 117 refers to a film having 1100 equivalent weight (EW), the number of grams of dry Nafion per mole of sulfonic acid groups when the material is in the acid form, and a thickness of 0.007 in (Martwiset, 2009).

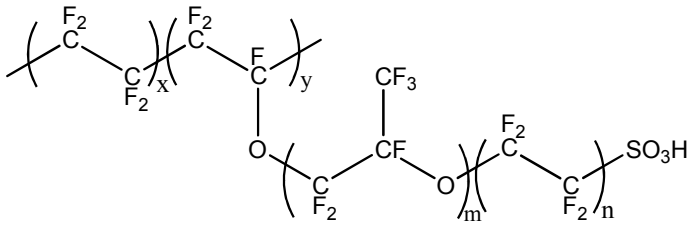

Nafion®: m≥1, n = 2, x = 5-13.5, y = 1000
Aciplex® : m = 0-3, n = 2-5, x = 1.5-14
Flemion® : m = 0 or 1, n = 1-5
Dow Membrane: m = 0, n = 2, x = 3.6-10, y = 1000

Figure 3.3 Chemical structures of commercial perfluorinated polymer electrolyte membranes.

Similar polymers are produced by Asahi Glass (Flemion®), Asahi Chemical (Aciplex-S®) and Dow Chemical Company. Among the four major types, the DuPont product is considered to be superior because of its high proton conductivity, good chemical stability and mechanical strength (Motupally et al,. 2000). Figure 3.3 shows the chemical structures of Nafion® and other famous perfluorinated electrolyte membranes.

The proton transport of hydrated Nafion is dominated by a vehicular mechanism, where protons diffuse through the material. Because of the random structure and the organization of the crystalline and ionic domains, the morphology of Nafion is not well defined. A number of studies using small-angle X-ray scattering (SAXS), wide-angle X-ray diffraction (WAXD), (Hsu et al., 1981, Gierke et al., 1983, Fujimura et al., 1981) small-angle neutron scattering (SANS) (Roche et al., 1981) and atomic force microscopy (AFM) have been conducted to develop an understanding of the morphology of Nafion. Gierke et al. proposed a model based on SAXS observations hypothesizing that clusters of sulfonate groups are organized as inverted micelles, connected by 1-nm-diameter channels (Figure 3.4) (Gierke et al., 1982).

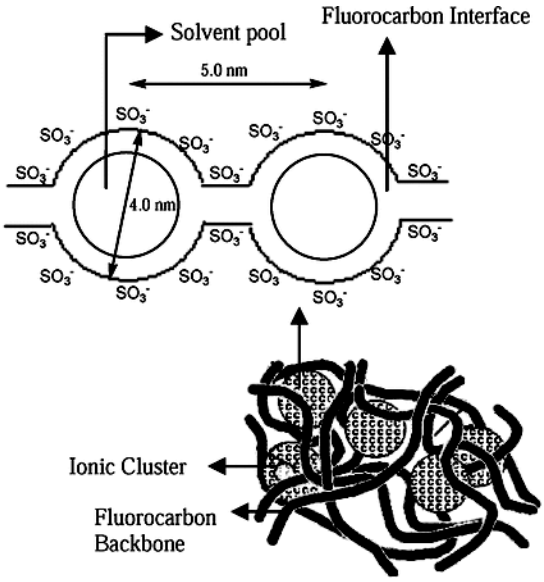

Figure 3.4 Gierke's Model

Although this model is the most popular, the presence of elongated structures was reported from the SAXS studies by a number of other groups (Londono et al., 2001, Van der Heijden et al., 2004). Recently, Schmidt-Rohr and Chen (Schmidt-Rohr et al., 2008) proposed a new structure of the Nafion ionomer shown in Figure 3.5. Using a new calculation method on previously reported SAXS data, they suggested that hydrated Nafion consists of long parallel water channels in cylindrical inverted

micelles. The water channels are packed randomly, surrounded by the ionic side groups with the polymer backbones on the outside.

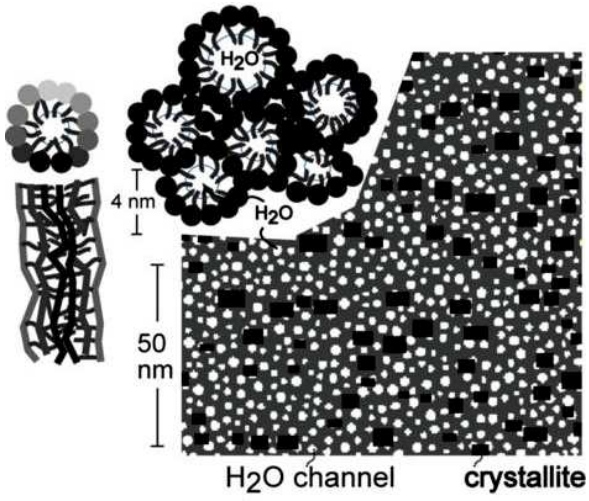

Figure 3.5 Schmidt-Rohr's Model

All these morphological studies support claims that the positive attributes of Nafion® as a fuel cell membrane with respect to its high proton conductivity and mechanical integrity are related to its extensive nano-scale phase separation (Yang et al., 2005 and Mauritz et al., 2004).

3.2.2.2 Sulfonated Hydrocarbon Polymer Membranes

Despite these positive attributes Nafion-based PEMs do have critical drawbacks that limit their use: They are limited to fuel cells that operate below 80 °C, tendency to dehydration, difficult to synthesize and process, expensive to produce and suffer from high methanol permeability (which is relevant for the DMFC mode) (Hickner, 2004). These shortcomings have generated development of new membrane materials. Sulfonated styrene-ethylene-butylene-styrene (SEBS) membrane from Dais Analytic and BAM® from Ballard Advanced Materials Corporation are two commercially available styrene-based polymers. The main disadvantage of SEBS is the poor oxidative stability due to its aliphatic character (Hodgdon, 1968). Polystyrene-graft-poly(styrene sulfonic acid), (Holdcroft et al., 2002) poly(ethylene-co-tetrafluoroethylene)-graft-poly(styrene sulfonic acid) (Holdcroft et al., 2000,2003) and poly(vinylidene fluoride)-graft-poly(styrene sulfonic acid) (PVDF-g-PSSA) (Flint et al., 1997) are graft

copolymers containing ionic grafts bound to hydrophobic backbones. Poly(arylene ether) materials such as poly(arylene ether ether ketone) (PEEK), poly(arylene ether sulfone), and their derivatives have been widely studied due to their availability and oxidative and hydrolytic stabilities. The naphthalenic polyimides are more stable than the phthalic polyimides, which undergo hydrolysis, in a fuel cell environment (Savadogo, 1998). Other high performance polymeric backbones that have been investigated include poly(phenylquinoxaline), (Kopitzke et al., 1998) poly(2,6-dimethyl-1,4-phenylene oxide), (Kruczek, 1998) poly(4-phenoxybenzoyl-1,4-phenylene), (Kobayashi et al., 1998) poly(phthalazinone ether ketone), (Gao et al., 2003) polyphosphazene (Wycisk et al., 1996 and Guo et al., 1999) sulfonated polysiloxanes (Gautier-Luneau et al., 1992), and (partially) fluorinated polyolefins (Gubler et al., 2004).

3.2.3 Anhydrous Proton Conductive Membranes

Proton exchange membrane (PEM) fuel cells have gained prominence after they become applicable to various technological areas particularly on portable power generating systems. In general, polymer based proton conducting materials can be categorized according to the temperature range in which they exhibit high proton conductivity. The first class of materials that can be utilized in the temperature range 25-100°C because their conductivity depends on water content. Within this family of polymers, hydrated perfluorosulfonic acid membranes such as Nafion®, well-established low temperature materials since 1960. These materials are typically phase separated into hydrophilic/hydrophobic domains and conductivity occurs via transport of dissociated protons by the dynamics of water (Kreuer et al., 1993). These hydrated systems have been used as the polymer electrolytes in hydrogen/oxygen polymer electrolyte fuel cells (PEMFCs) due to excellent chemical and mechanical stability as well as high proton conductivity (Rikukawa and Sanui, 2000, Motupally et al., 2000, Costamagna and Srinivasan, 2001). However, there are several limitations in perfluorosulfonic acid membranes, which retard spread industrial application. One of the main hurdles for the widespread utilization of PEMFC power sources is the need for better performing and more cost effective membranes. (Steele et al., 2001 and Rusanov et al., 2002) Most current research efforts have focused on systems relying on water as the media for proton transport. This limits the operating temperature to ~100 °C. (Hickner et al., 2004,

Rikukawa et al., 2000, Rusanov et al., 2002) However, there are many advantages in developing PEMFC's capable of operating at temperatures close to 200 °C. Operating at such temperatures increases the efficiency of the fuel cell by increasing the kinetics of the redox reaction, and by improving the tolerance of the system for CO, which is present in hydrogen fuel refined from hydrocarbons. Running the cell at high temperatures will also reduce the overall cost by decreasing the platinum loading required in the electrodes, as well as simplify the overall heat management of the device (Lecolley et al., 2003).

Several alternative PEMFC systems were produced to overcome the drawbacks of perfluorosulfonic acid based materials. The first method was doping of polymers with H3PO4 to obtain conductivity by proton transport mechanism that occurs through phosphate ions ($H_4PO_4^+$, H_2PO_4) (Bozkurt, 1999, Lassegues, 2001, Bouchet, 1991 and Rikukawa, 2000). The another method was doping of the polymers with aromatic heterocyclic structures such as imidazole (Yang, 2001, Kreuer, 1998 and Sevil, 2004), pyrazole (Kreuer, 1998), benzimidazole (Yamada, 2003), triazole and tetrazole (Unugur, 2008). Since these azole groups have high melting points (100–200 °C), they were successfully substituted in water and provided high proton conductivity. There is a strong demand for designing alternative membranes by chemical immobilization of protogenic solvents into polymer (Unugur, 2008).

In general, there are three different approaches toward anhydrous PEMs in terms of their chemical structure and conductivity mechanisms:

a) Polymer-acid complexes. These are based on polymer networks which contain ether, amide, amine or imino groups are doped with strong acids such as H_3PO_4 or H_2SO_4.

b) Intrinsic proton conductors based on homopolymers, copolymers, and polymer networks produced by tethering the heterocyclic proton solvent.

c) Polymer/heterocycle hybrid electrolytes. In principle, these materials consist of acidic host matrix that forms complexes with amphoteric heterocycles and conduction occurs through protonic defects. (Unugur, 2008)

3.3 PROTON CONDUCTION MECHANISMS IN PEMs

Proton conduction is fundamental for proton exchange membrane fuel cells and is usually the first characteristic considered when evaluating membranes for potential fuel cell use. Resistive loss is proportional to the ionic resistance of the membrane and high conductivity is essential for the required performance especially at high current density. At a molecular level, the proton transport in hydrated polymeric matrices is in general described on the basis of either of the two principal mechanisms: “proton hopping” or “Grotthus mechanism” and “diffusion mechanism” which water is as vehicle or “vehicular mechanism” (Murthy, 2005).

In proton hopping mechanism protons hop from one hydrolyzed ionic site (SO_3^- H_3O^+) to another across the membrane. The produced proton by oxidation of hydrogen in anode adheres to water molecule than the provisional hydronium ion is formed and one different proton from same hydronium ion hops on the other water molecule. The simple scheme of the hopping mechanism is shown in Figure 3.6.

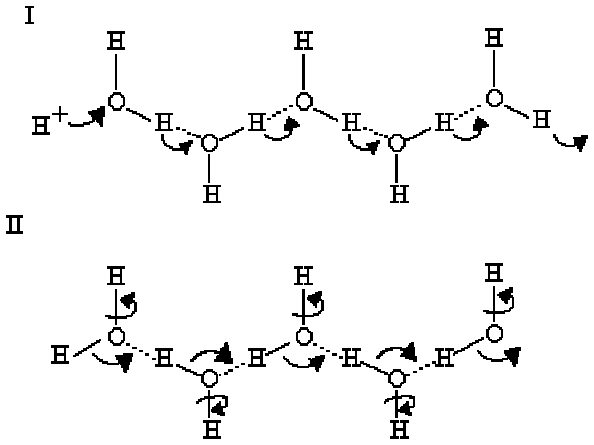

Figure 3.6 Grotthuss mechanism (Crofts, 1996)

The first process leads to a polarization of the hydrogen bond chain, i.e. to a local relative charge displacement, but not to dc conductivity. The second process causes the depolarization of the chain by reorientation of the water dipoles. The hopping mechanism has little contribution to conductivity of perflourinated sulfonic acid membranes.

The second mechanism is a vehicular mechanism proposed by Kreuer (Kreuer et al., 1982). In this mechanism hydrated proton (H_3O^+) diffuses through the aqueous

medium in response to the electrochemical difference. In vehicular mechanism, the water connected protons ($H^+(H_2O)_x$) in the result of the electroosmotic drag carry the one or more molecules of water through the membrane and itself are transferred with them. The major function of the formation of the vehicular mechanism is the existence of the free volumes within polymeric chains in proton exchange membrane which allow the transferring of the hydrated protons through the membrane (Deluca, 2004). According to this mechanism, the proton does not migrate as H^+ but as H_3O^+ or NH_4^+, bonded to a "vehicle" such as H_2O or NH_3. The "unloaded" vehicles move in the opposite direction shown in Figure 3.7.

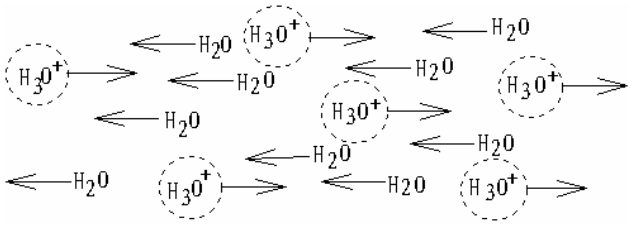

Figure 3.7 Vehicular mechanism (Kreuer et al., 1982).

The two mechanisms essentially differ from the nature of the H bonds formed between the protonated species and their environments. The Grotthuss mechanism is preferred in media which support strong hydrogen bonding, while vehicle mechanism is preferred in species with weaker hydrogen bonding.

CHAPTER 4

EXPERIMENTAL

4.1 UV-INDUCED SURFACE PHOTOGRAFTING OF STYRENE ONTO PVDF FILMS

4.1.1 Materials

Polyvinylidene fluoride (PVDF, average Mw ~534,000) was purchased from Fluka. The inhibitor in styrene (>99%, Merck) was eliminated by an alumina column and stored at -20°C. Dimethylformamide (DMF, ≥ 99.9 %), chlorosulfonic acid (≥ 97 %), *N*,*N*- dichloromethane (≥ 99%) and toluene (≥ 99 %) were purchased from Merck. Benzophenone (BP, ≥ 99 %), polyvinyl acetate (PVA, average Mw ~83,000), 1H-1,2,4-triazole (> 98%), sodium chloride and sodium hydroxide were supplied from Aldrich. They were all reagent grade and used as received. The molecular structures of the chemicals are shown in Figure 4.1.

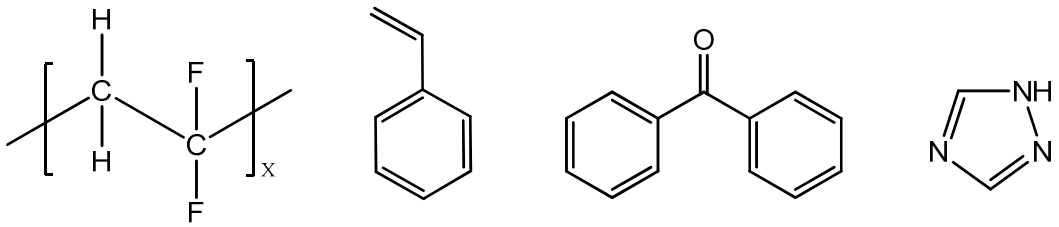

(a) **(b)** **(c)** **(d)**

Figure 4.1 Molecular structures of (a) PVDF, (b) Styrene, (c) Benzophenone, and (d) 1H-1,2,4-triazole

4.1.2 Preparation of PVDF Membranes

The membranes were prepared from 7% (w/w) PVDF polymer solutions in DMF. The solution was cast on PTFE petri dish to form thin film and dried at room

temperature for several hours before heating at 50 °C for 2 h under vacuum. Finally, the polymer was recovered as a flat-sheet membrane from the bottom of the PTFE petri dish. The thickness of the received membranes is in the range of 40–50 µm. All PVDF films were cut into 2cm × 2cm pieces and stored in vacuum at 40 °C before use.

4.1.3 UV Photografting of Styrene to the PVDF Films

The UV surface photografting of styrene onto the PVDF base film was carried out as follows. First, a 40 µm thick PVDF film was immersed in acetone solution containing 0.5 wt % benzophenone and 0.5 wt % poly(vinyl acetate) for 5-7 s at room temperature, and then it was dried under vacuum for 24 h at 40 °C before use. Then, for photografting, 1 mL of styrene, 10 mL of distilled water, and 3 mL of acetone were mixed in a quartz tube and nitrogen was bubbled through the solution for about 30 min to remove the oxygen before the irradiation. The photoinitiator-coated PVDF film was kept standing in a quartz tube containing the styrene solution and the quartz tube was placed into the photoreactor equipped with a 400W medium pressure mercury lamp (254 nm) to induce grafting. The temperature inside the UV reactor was kept at 60 °C during irradiation. The grafted film was removed and washed with toluene for several hours to remove the unreacted monomer and homopolymer. The obtained membrane was then dried in a vacuum oven at 40 °C. (Asano et al., 2007) Degree of grafting with variation of the UV exposure time was also examined. For this purpose, grafted PVDF films were prepared under the same conditions but with different irradiation times (i.e., 0.5 h, 1 h, 2 h, 4 h, 6 h, and 8 h).

4.1.4 Sulfonation

The grafted PVDF-*g*-PS films were sulfonated using a sulfonating reagent composed of lower chlorosulfonic acid concentration of 0.2 M in dichloromethane. The sulfonation was performed at 60 °C for 8 h under reflux. After sulfonation, the films were washed several times with dichloromethane to remove the excess of chlorosulfonic acid and then dried in a vacuum oven overnight. The sulfonated membranes were then hydrolyzed in distilled water at 80 °C for 12 h and the resulting membranes (PVDF-*g*-PSSA) were dried in vacuum.

4.1.5 Doping of PVDF-*g*-PSSA Films with Triazole

The reaction of PVDF-*g*-PSSA films with 1H-1,2,4-triazole (Tri) was carried out according to a procedure given in the literature (Moore et al., 1992). A stoichiometric amount of Tri and PVDF-*g*-PSSA were mixed in DMF and the resulting mixture was stirred for several hours at 60°C until getting a homogeneous milky solution. Solutions with x (= 1.0 and 2.0) moles were prepared, where x is the number of moles of triazole per mole of polymer repeating unit. The films were then cast onto PTFE plates and dried under vacuum at 50°C and stored at 40°C in vacuo. The doping procedure is summarized in Table 4.1.

Sample	Dopant	x	Sample weight	mol. Triazole	Solvent
PVDF-*g*-PSSA (4 h UV, 84 % SA)	Triazole	1	0.036 g (0.093 mmol SA)	0.006 g (0.093 mmol)	DMF
	Triazole	2	0.033 g (0.084 mmol SA)	0.012 g (0.0168 mmol)	DMF
PVDF-*g*-PSSA (6 h UV, 96 % SA)	Triazole	1	0.042 g (0.184 mmol SA)	0.013 g (0.184 mmol)	DMF
	Triazole	2	0.043 g (0.191 mmol SA)	0.026 g (0.382 mmol)	DMF

Table 4.1 Preparation of triazole doped PVDF-*g*-PSSA

4.2 UV-INDUCED HOMOGENEOUS PHOTOGRAFTING OF STYRENE ONTO PVDF

4.2.1 Materials

Polyvinylidene fluoride (PVDF, average Mw ~534,000 g/mol) was purchased from Fluka. The inhibitor in monomer styrene (>99%, Merck) was eliminated by an alumina column and stored at -20 °C. Sulfuric acid (95-97%), *N*,*N*-dimethylformamide (DMF, $\geq$ 99.9 %), dichloromethane ($\geq$ 99%) were purchased from Merck. Benzophenone (BP $\geq$ 99 %), 1H-1,2,4-triazole (>98%), acetic anhydride (Aldrich, 99.5%), sodium chloride and sodium hydroxide were supplied from Aldrich. They were all reagent grade and used as received.

4.2.2 UV Photografting of Styrene onto PVDF

The UV homogeneous photografting of styrene onto the PVDF was carried out as follows. First, 0.8 g PVDF was dissolved in 12 mL DMF in a round-bottom flask at 60 °C. For photografting, 24 mL of styrene, 0.76 g benzophenone and 60 mL of DMF were mixed in a quartz tube and PVDF solution was then added into the mixture. After preparing homogeneous solution, nitrogen was bubbled through the solution for about 30 min to remove the oxygen before the irradiation. The quartz tube was placed in a photoreactor equipped with a 400W medium pressure mercury lamp (254 nm) to induce grafting. After quartz tube was irradiated for a certain time, the resulting polymer solution was precipitated in excess methanol with stirring. The obtained suspension was filtered and the solid product was dried at 40°C under vacuum. Then, the solid polymer was put into CH_2Cl_2 at room temperature. Soluble polymers in CH_2Cl_2 (PS) and insoluble parts of the (PVDF-*g*-PS) were separated and vacuum dried at 40°C before analysis. The grafted copolymers were prepared for two different irradiation times (0.5 h and 4 h) under the same conditions.

4.2.3 Sulfonation

The sulfonation reaction was carried out in DMF solvent, following previously reported procedures (Veriss et al., 1991). Typically, in a 100 mL two-neck flask that was nitrogen-purged, equipped with condenser, 20 mL of DMF and 0.72 g of PVDF-g-PS were added, and the mixture was heated to 50°C under stirring until the copolymer completely dissolved. Acetyl sulfate solution was prepared by injecting 7.76 mL of acetic anhydride and 45 mL anhydrous CH_2Cl_2 into a three-neck nitrogen-purged flask. The solution was cooled to 0°C in an ice bath and 4 mL of 95-97% sulfuric acid was added dropwise to the solution. The resulting acetyl sulfate solution (20 mL) was transferred to the polymer solution. Sulfonation reaction was performed at 40 °C for 20 h. The resulting mixture was extracted and precipitated in water with stirring. The sulfonated polymer was filtered and dried at 30°C under vacuum.

4.2.4 Doping of PVDF-g-PSSA with Triazole

The reaction of PVDF-g-PSSA with 1H-1,2,4-triazole (Tri) was carried out according to the literature (Moore et al., 1992). Tri was added into the PVDF-g-PSSA

solution in DMF with stoichiometric ratio (1:1). The resulting mixture was stirred for several hours at 60 °C until getting a homogeneous milky solution. Then the films were cast onto PTFE plates and dried under vacuum at 50°C, and stored under vacuum at 40°C. The doping procedure is summarized in Table 4.2.

Table 4.2 Preparation of triazole doped PVDF-g-PSSA

Sample	Dopant	x	Sample mole	Triazole mole	Solvent
PVDF-g-PSSA (4 h UV, 22 % SA)	Triazole	1	0.132 g (0.057 mmol SA)	0.004 g (0.057 mmol)	DMF

4.3 CHARACTERIZATIONS

4.3.1 FT-IR and ^{1}H-NMR Analysis

The FT-IR spectra (4000-400 cm^{-1}, resolution 4 cm^{-1}) were recorded with a Bruker Alpha-P in ATR-FTIR system. ^{1}H-NMR (300 MHz) spectra was obtained on a Bruker AM 400 or an AC 200 Spectrometer with the samples dissolved in either chloroform-*d* or dimethyl sulfoxide-*d6* (DMSO-*d6*).

4.3.2 Thermal Analysis

Thermal stabilities of the all samples were examined by thermogravimetry (TG) analysis with a Perkin Elmer STA 6000. The samples (~ 10 mg) were heated from room temperature to 800°C under N_2 and O_2 atmosphere at a scanning rate of 10°C /min. The effect of dopant on thermal stability was determined using TG curves. Differential scanning calorimetry (DSC) data were obtained using Perkin Elmer JADE DSC instrument The measurements were carried out at a rate of 10°C/min under nitrogen atmosphere and heating-cooling curves were recorded at a rate of 10°C/min. The glass transition temperatures were determined from the second heating curves and the effect of dopant on glass transition temperature was studied.

4.3.3 Degree of Grafting (DG)

The graft weight of the films was determined from the increase in weight after grafting, using the following equation:

$$Degree\ \ of\ \ grafting\ \ (\%) = \frac{Wg - Wo}{Wo} \times 100 \tag{4.1}$$

where W_o and W_g are the weights of the film before and after grafting, respectively. The degree of grafting was varied by changing the irradiation time.

4.3.4 Ion Exchange Capacity

The ion exchange capacity (IEC) of the membranes was measured by the classical titration method. The membrane samples in acidic form were soaked in 1.0 mol/L NaCl solution for 24 h before measuring IEC. The protons released due to the exchange reaction with Na ions were titrated against 0.02 mol/L standardized NaOH solution, using phenolphthalein as an indicator. The IEC of membranes were calculated using the following equation:

$$IEC = \frac{(\text{vol. NaOH, ml}) \times (conc.\ \text{NaOH, M})}{(\text{dry wt. of membrane, g})} \tag{4.2}$$

4.3.5 Water Uptake and Hydration Number

The water uptake (*WU*) measurements were made according to the literature (Li, 2004, Smitha, 2006). The pre-weighed dry films (W_{dry}) of the membranes were soaked into water at 50 °C. The external liquid of the swollen membranes was wiped out and weighted (W_{wet}). The solvent uptake values were obtained using the following equation:

$$WU\ (\%) = \frac{Wwet - Wdry}{Wdry} \times 100 \tag{4.3}$$

The hydration number, that is, the number of water molecules per sulfonic acid group (nH_2O/SO_3H), of the proton-conducting membranes was calculated as:

$$Hyd.Num. = \frac{\mathrm{WU}}{1.8 \times \mathrm{IEC}} \tag{4.4}$$

4.3.6 Proton Conductivity Measurements

The proton conductivity studies of the samples were performed using a SI 1260-Schlumberger impedance spectrometer. The conductivities were measured in the frequency range 1 Hz to 1 MHz at 10°C intervals. The temperature was controlled with a Novocontrol cryosystem, which is applicable between -150°C and 400°C with a precision of 0.01°C. The hot pressed pellets of the samples with a diameter of 10 mm and thickness of about 0.2-0.3 mm were sandwiched between two gold-coated electrodes and their conductivities were measured with 10°C intervals under dry-nitrogen atmosphere.

4.3.6.1 AC Conductivity Measurements

The AC conductivities, σ_{ac} (ω) of the polymers were measured at several temperatures using impedance spectroscopy. Frequency dependent AC conductivities (σ_{ac} (ω)) were measured using Eq. 4.5;

$$\sigma'(\omega) = \sigma_{ac}(\omega) = \varepsilon''(\omega)\,\omega\,\varepsilon_o \tag{4.5}$$

where σ‘ (ω) is the real part of conductivity, ω = 2πf is the angular frequency, ε_o is the vacuum permittivity (ε_o = 8.852 x 10^{-14} F/cm), and ε“ is the imaginary part of complex dielectric permittivity (ε*).

4.3.6.2 DC Conductivity Measurements

The DC conductivity, σ_{dc} is derived from the log scale σ_{ac} versus frequency (*f*) curves by linear fitting plateau regions and extrapolating to zero frequency. If the system exhibits Arrhenius behavior, the conductivity isotherm can be fitted by Arrhenius equation (Eq. 4.6);

$$\ln \sigma = \ln \sigma_0 - E_a / kT \tag{4.6}$$

where σ_o is the pre-exponential terms, E_a is the activation energy, and k is the Boltzmann constant. If the system follows VTF behavior the curved DC conductivity isotherm can be fitted by Vogel-Tamman–Fulcher-type (VTF) equation (Eq. 4.7);

$$\log \sigma = \log \sigma_0 - E_v / [k(T - T_0)] \tag{4.7}$$

where σ_o is the conductivity at infinite temperature, E_v is the Vogel activation energy and T_o is the Vogel temperature.

CHAPTER 5

RESULTS AND DISCUSSION

5.1 UV-INDUCED SURFACE PHOTOGRAFTING OF STYRENE ONTO PVDF FILMS

PVDF-*graft*-polystyrene sulfonic acid proton conducting membranes were prepared via irradiation of the cast films coated with sensitizer, followed by sulfonation as outlined in Figure 5.1.

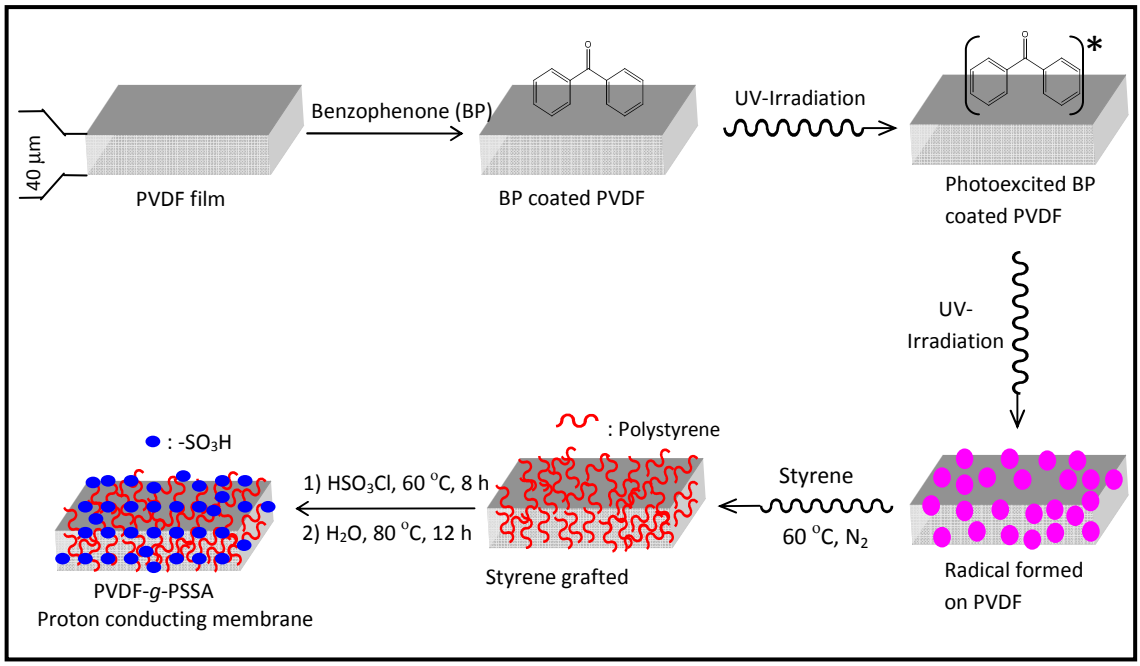

Figure 5.1 Process for synthesis of PVDF-g-PSSA proton conducting membranes by UV surface photografting method.

Styrene monomers were successfully grafted onto the PVDF films with different degrees of grafting. First, BP sensitizer was coated onto the PVDF films with the use of poly(vinyl acetate) as an adhesion agent (Kubota et al, 1990). Then, the films were immersed in the styrene solution and exposed to UV irradiation at 60°C for grafting.

During UV irradiation, the coated sensitizer was excited, and macromolecular radicals were generated on the surface of PVDF membranes by abstraction of fluorines or hydrogens (Asano, 2007). These radicals at the PVDF surfaces initiated the polymerization of styrene. Aseno *et al*., suggested that small amounts of radicals might also be generated inside the PTFE films because of the multiple reflection of UV among the crystalline particles. The grafting in this system seemed to have an interface mechanism, in which grafting started at the layers close to the surface of the film. These grafted layers, which swell in the grafting solution, allowed progressive diffusion of the monomer toward the inner regions of the film (Ivanov, 1992). The two grafting interfaces at the two sides of the PVDF film continue to move further into the film interior. Therefore, during grafting, the membrane surface area and thickness both increased, indicating that the grafting proceeded from the surface to the interior of the PVDF films. The degrees of grafting in the membranes were determined and characterized.

The grafted films were sulfonated to obtain the proton conducting membranes. Sulfonation of PVDF-*g*-PS was conducted with chlorosulfonic acid as sulfonating agent and dichloromethane as solvent. Chlorosulfonic acid is very stable, highly reactive in electrophilic substitutions of aromatic rings and convenient at the laboratory level and the solvent is very suitable and quite miscible with chlorosulfonic acid (Cremlyn, 2002). After the first step of sulfonation reaction, colorless membranes became dark brown in color. The sulfonyl chloride groups are easily hydrolyzed in hot water to form the sulfonic acid groups (Chen et al., 2006). Therefore, hydrolysis was directly carried out in distilled water at 80°C for 12 h. The resulting membranes were transparent, flexible and light brown in color when in the water-saturated state. Sulfonation degrees of sulfonated membranes were determined and characterized. The graft samples were listed in Table 5.1 as Memb 0 - Memb 8 for short, representing the six different graft copolymers of PVDF-*g*-PS with varying UV irradiation times (graft time). Some of the selected sulfonated membranes were finally doped with triazole to examine the anhydrous proton conductivity at 150°C.

Table 5.1 Samples, and their grafting time, degree of grafting, Tg and Tm values.

Sample	Graft Time (h)	D.G (%)	Tg (°C)	Tm (°C)
Memb 0	0.5	2.4	a	158
Memb 1	1	6.9	a	156
Memb 2	2	18.4	a	156
Memb 4	4	50.8	93	158
Memb 6	6	68	100	156
Memb 8	8	109.1	105	155

a: Not detected due to low degrees of grafting

5.1.1 Analysis of the Grafted PVDF Membranes

5.1.1.1 Degree of Grafting (DG)

The degree of grafting of styrene on PVDF films were investigated as a function of UV irradiation time, as varied from 0.5 h to 8 h. Table 5.1 lists the calculated degree of grafting of the corresponding PVDF-*g*-PS membranes. Figure 5.2 shows the degree of UV photografting of styrene on PVDF films as a function of grafting time (UV irradiation time). It was seen that the degree of grafting increased with the grafting time, reaching above 100 % after 8 h.

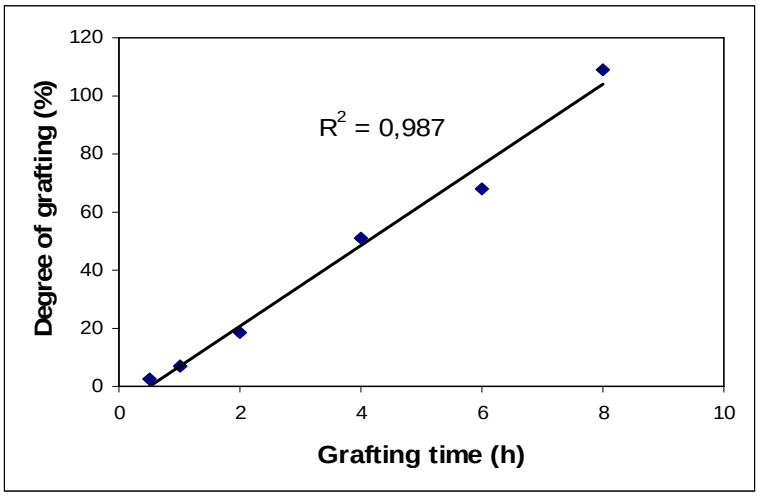

Figure 5.2 Degree of grafting versus UV photografting of styrene on PVDF films

Asano and his coworkers (Asano, 2007) reported about 10 % increase in the degree of grafting of styrene on PTFE films after 8 h. Chen et al. (Chen, 2006) also found that the degree of grafting for ETFE films reached up to 59 % after 6 h of UV irradiation.

5.1.1.2 ^{1}H NMR analysis

The successful graft copolymerization was confirmed using ^{1}H NMR spectroscopy. ^{1}H-NMR spectra for PVDF and PVDF-*g*-PS (Memb 4) were presented in Figure 5.3

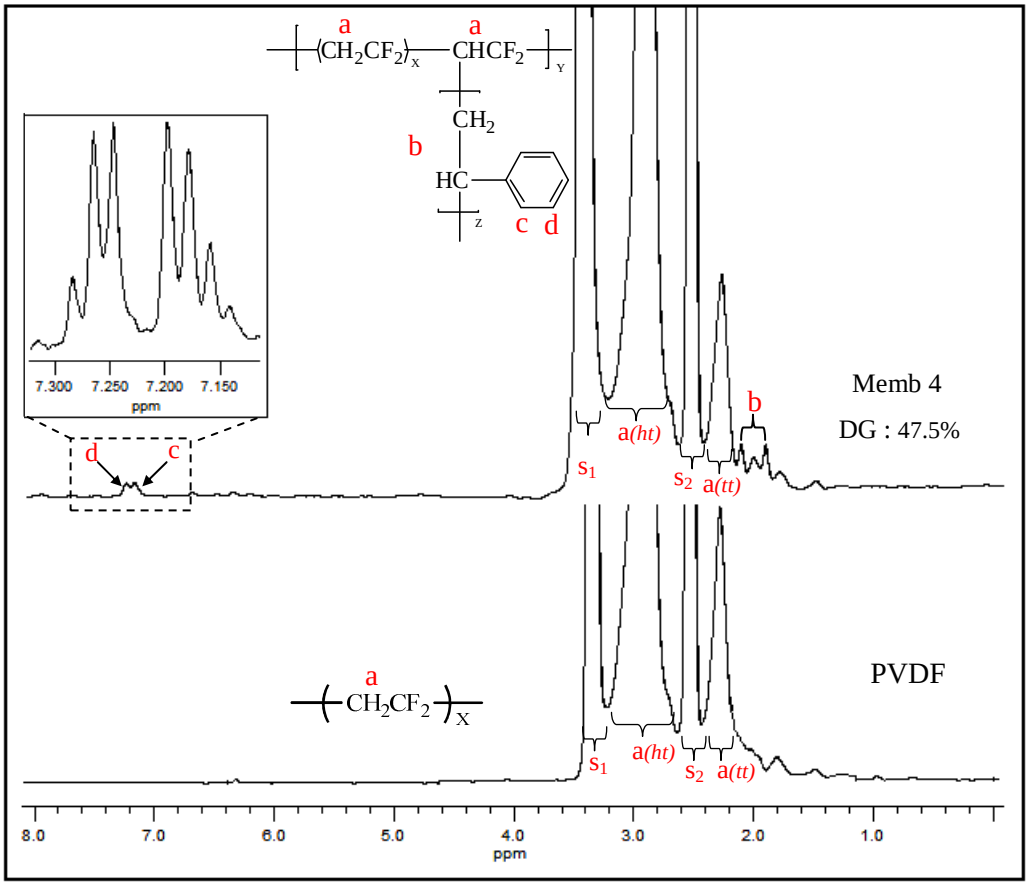

Figure 5.3 ^{1}H NMR spectra of PVDF base film and Memb 4

For both samples, the peaks of solvent (DMSO) and water appeared at 2.6 and 3.5 ppm, respectively. The ^{1}H NMR spectrum exhibited the characteristic multiplets centered at 2.9 and 2.3 ppm originating from the methylene groups in -CH_2-CF_2-C**H_2**-CF_2-CH_2-CF_2- and -CF_2-C**H_2**-C**H_2**-CF_2- sequences appearing in the normal tail-to-head and reversed tail-to-tail VDF additions (Guiot et al. 2002, Guiot et al., 2005). The spectrum of the PVDF-*g*-PS graft copolymers exhibited additional signals located in the

1.8-2.1 ppm and 7.3-7.1 ppm ranges assigned to methylene and methyne groups of polystyrene and to the aromatic protons, respectively.

5.1.1.3 FT-IR analysis

Infrared spectroscopy was employed to provide information about the chemical structure of the unmodified and modified PVDF membranes. Figures 5.4 and 5.5 show the FTIR spectra of the PVDF base film and styrene grafted PVDF films with different degree of grafting.

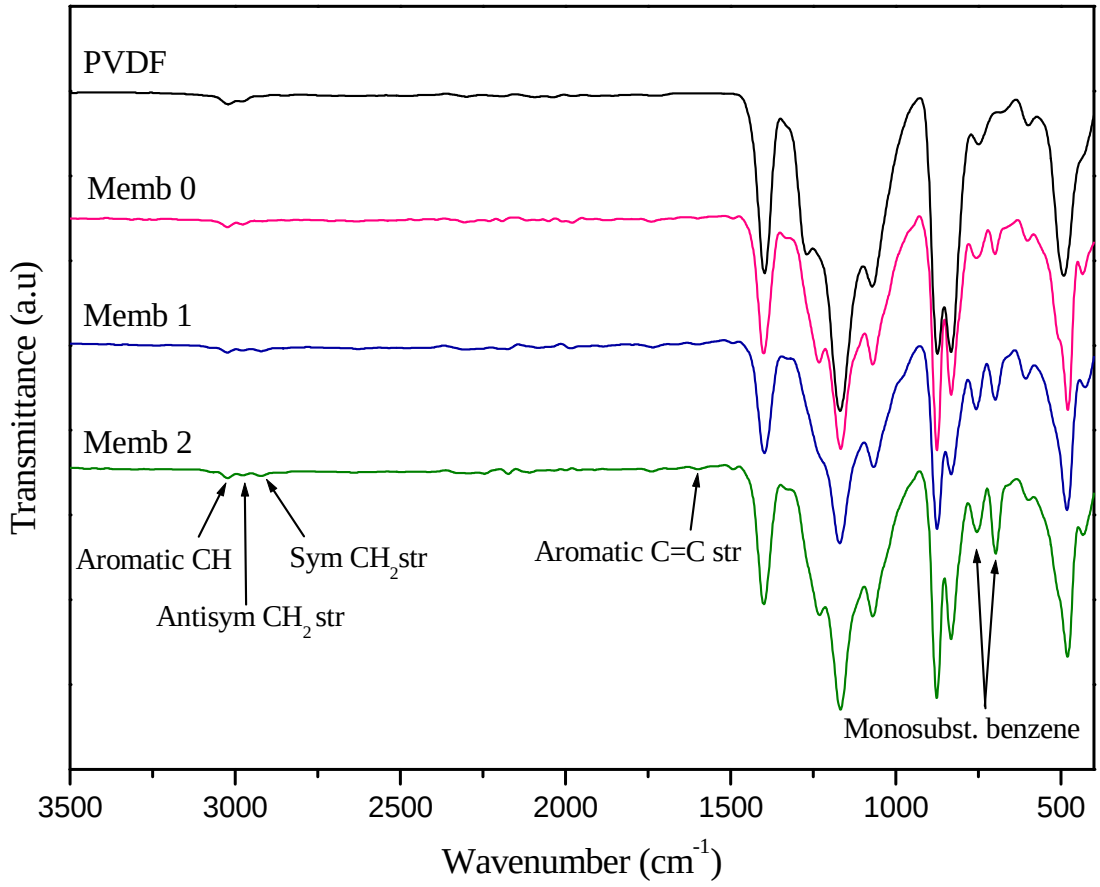

Figure 5.4 FT-IR spectra of base PVDF and PVDF-*g*-PS membranes with different degree of grafting (Memb 0: 2.4%, Memb 1: 6.9% and Memb 2: 18.4%)

The asymmetric and symmetric stretching vibrations of the CH_2 group in the PVDF base film (Figure 5.4 and 5.5) were located, respectively, at 3024cm^{-1} and 2982cm^{-1}. The strong peak appeared at 1403 cm^{-1} corresponds to CH_2 stretching vibrations. The very strong and wide peaks between 1242–1064 cm^{-1} which correspond

to the C–F stretching were characteristic peaks of the PVDF base film. For the styrene grafted PVDF membranes the presence of the benzene rings in the graft chains was confirmed by the =C–H stretching vibration at 3026 cm^{-1} and the skeletal C=C stretching vibration at 1493 and 1601 cm^{-1}.

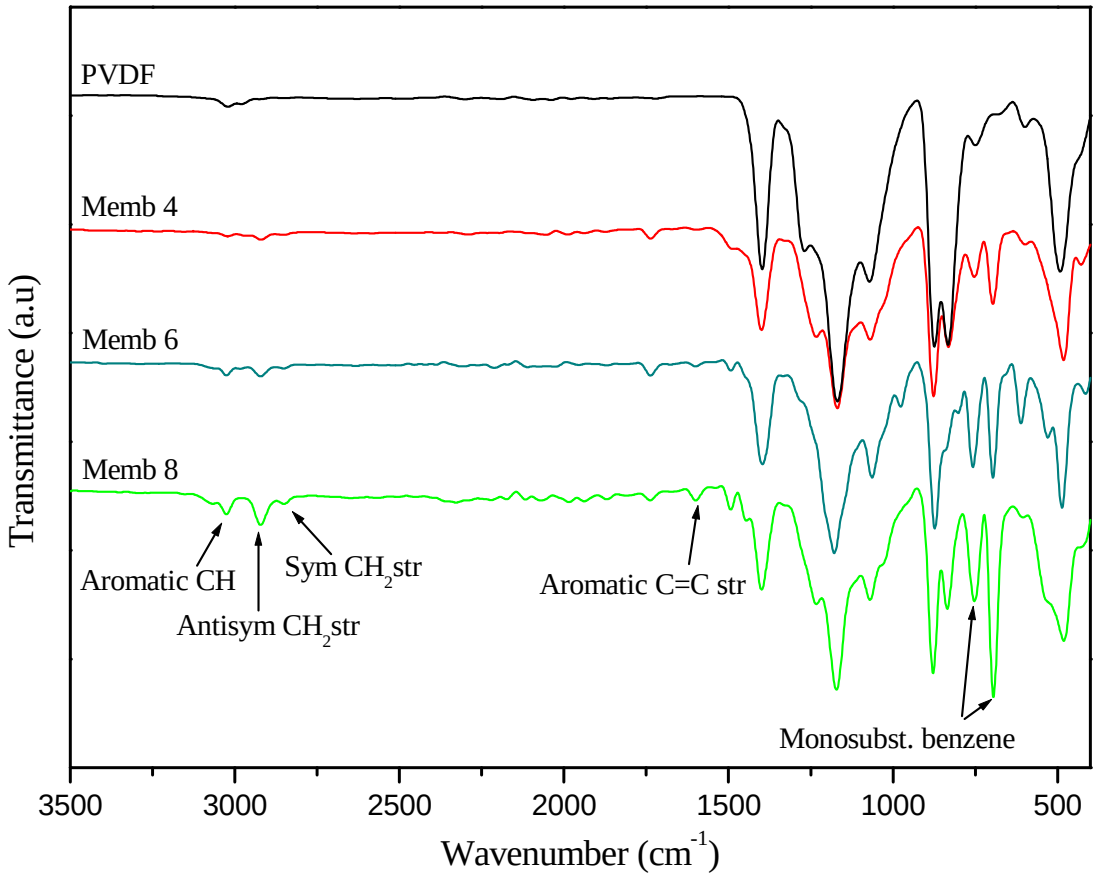

Figure 5.5 FT-IR spectra of base PVDF and PVDF-*g*-PS membranes with different degree of grafting (Memb 4: 50.8%, Memb 6: 68% and Memb 8: 109.1%)

The absorption bands at 2800–2900 cm^{-1} and 2900–3000 cm^{-1} were assigned to the symmetric and asymmetric $–CH_2$ stretching vibrations, respectively. The monosubstitution of the benzene ring was confirmed by the two bands of C–H aromatic out-of-plane deformation at 752 cm^{-1} and 695 cm^{-1}. Furthermore, the intensity of these new peaks related to the graft chains increased with the increase in the degree of grafting. These signs confirmed that the monomers were grafted onto the PVDF base films, and the variation in the intensity of the polystyrene characteristic bands reflects the difference in the degree of grafting. All the FTIR absorption peaks related to the graft chains become stronger with an increase in the degree of grafting (Kim, 2007).

5.1.1.4 Thermogravimetric Analysis (TGA)

The thermal stabilities of base PVDF and PVDF graft membranes were investigated by TGA as shown in Figure 5.6. The base PVDF showed excellent thermal stability up to 448 °C, above which it started to decompose to about 30 wt % (Kim, 2008). The TGA curves of PVDF-*g*-PS polymers with varying degrees of grafting showed a satisfactory thermal stability up to 381 °C.

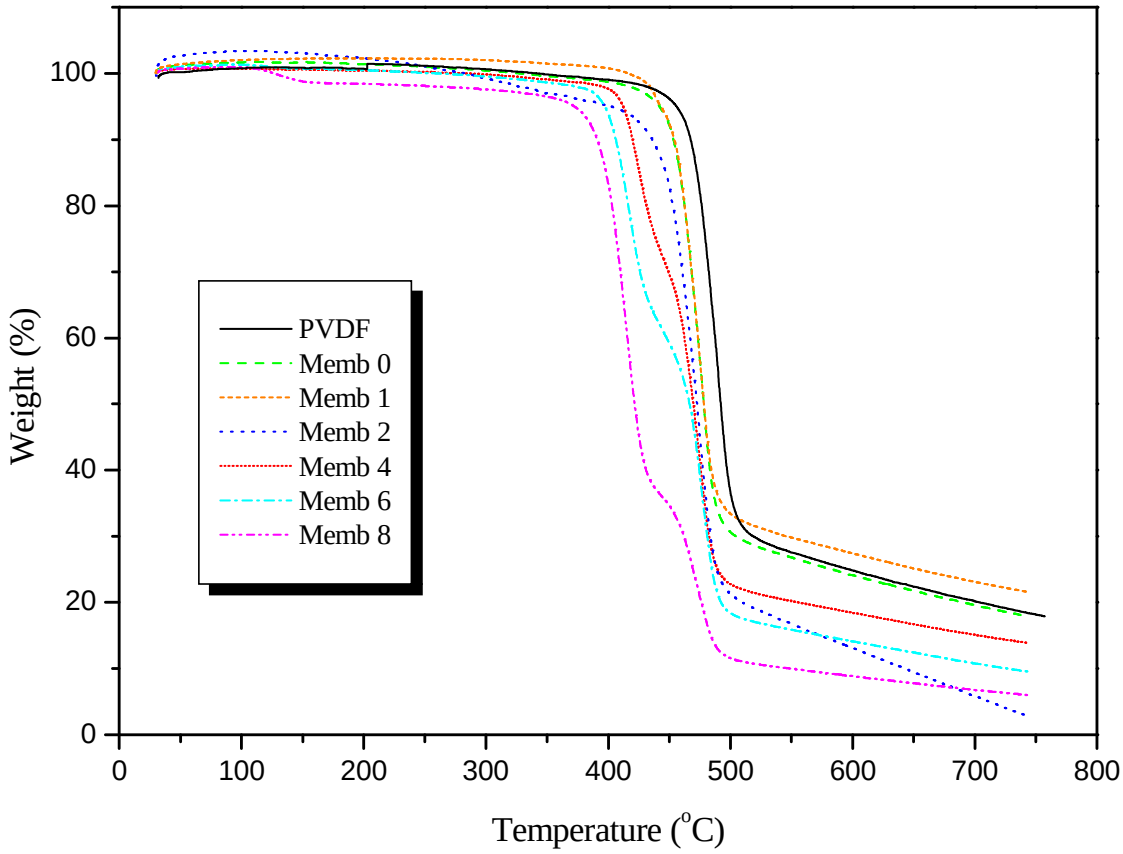

Figure 5.6 TGA data of PVDF and graft membranes

The graft polymers showed degradation patterns owing to depolymerization and decomposition of PVDF. The initial weight loss was attributed to the loss of polystyrene (depolymerization). The weight loss in the second step was due to decomposition of PVDF by random chain scissions, reported as characteristic of the PVDF backbone degradation (Sauguet, 2006 and Nasef, 2010).

The TG analysis of the graft copolymers revealed that the thermal stability decreased as the degree of grafting increased. For instance, Memb 0 (degree of grafting: 2.4%) was found to be thermally stable up to 442 °C while Memb 8 (degree of grafting: 109.1%) was found to be stable up to 381°C. This suggested that the higher the styrene amount in the graft, the lower its thermal stability (Valade, 2006).

5.1.1.5 DSC Analysis

Differential scanning calorimetry (DSC) was performed to measure the glass transition temperatures of the Memb 4, Memb 6 and Memb 8. Figure 5.7 shows the DSC curves between 54°C - 200°C for the membranes and their corresponding Tg values are listed in Table 5.1. Figure 5.8 illustrates a close-up view of the DSC curves between 90°C -145°C. Tg of pristine PS was nearly 108°C. Memb 4, Memb 6 and Memb 8 had definite glass transition temperatures at 93°C, 100°C and 105°C, respectively.

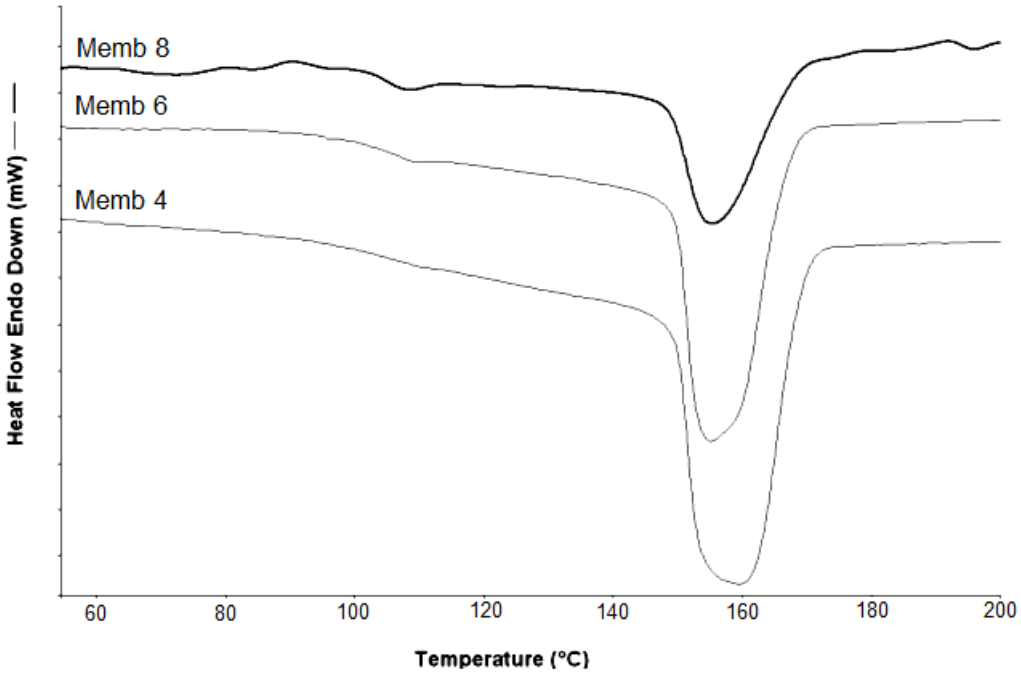

Figure 5.7 DSC traces of Memb 8, Memb 6 and Memb 4 recorded under inert atmosphere at a heating rate of 10 °C/min.

The obtained Tg values were assigned to that of poly(styrene) grafts. Some of the membranes did not show Tg values, which might be due to low degree of grafting. The DSC results demonstrated that as the quantity of grafting increased, the glass transition temperature of the samples shifted to higher temperatures. The increase in the glass transition temperatures can be attributed to the fact that the degree of grafting increased with the irradiation time.

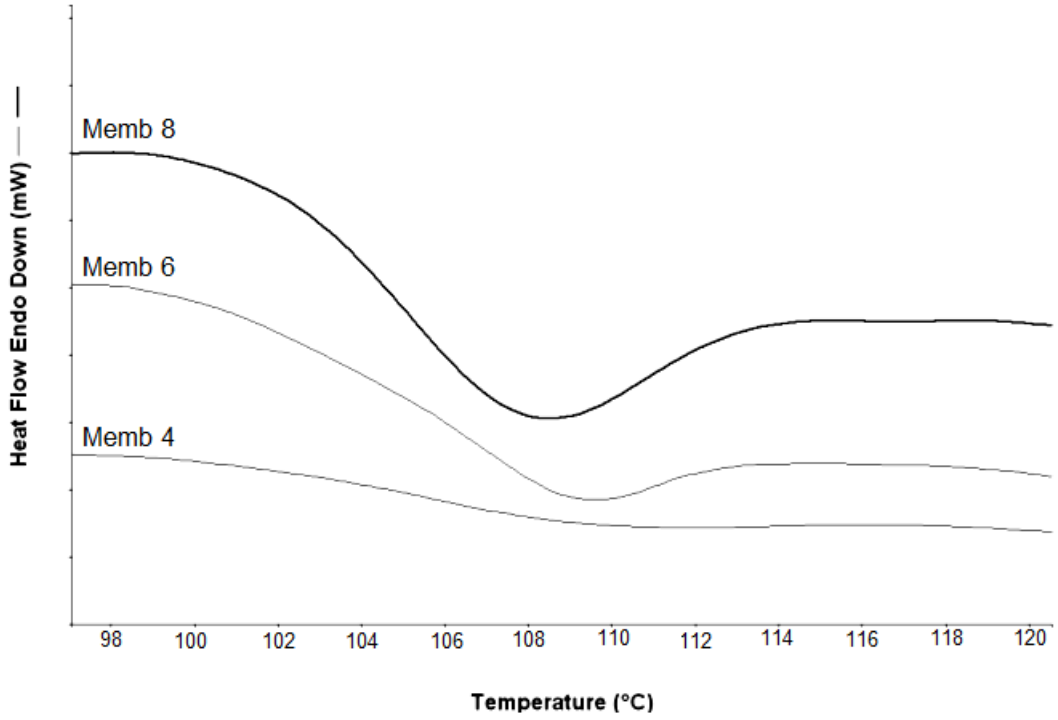

Figure 5.8 The close-up view of the DSC traces of Memb 8, Memb 6 and Memb 4.

5.1.2 Analysis of PVDF-g-PSSA / Proton Conducting Membranes

5.1.2.1 FT-IR analysis

The sulfonation was verified by FT-IR spectroscopy. Figure 5.9 shows the FT-IR spectra of the PVDF, graft membrane (Memb 8), and the proton conducting membrane PVDF-*g*-PSSA (Memb 8/SA).

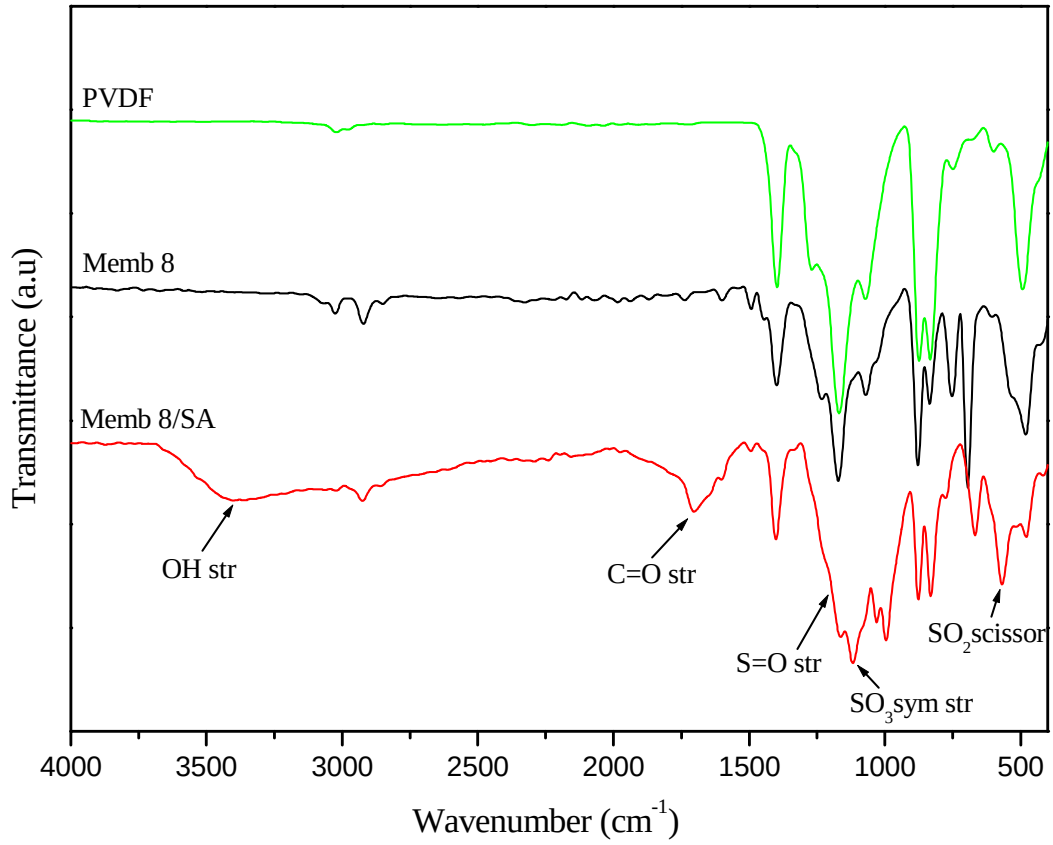

Figure 5.9 FT-IR spectra of base PVDF, styrene grafted PVDF (Memb 8) and proton conducting PVDF-*g*-PSSA membrane (Memb 8/SA).

The broad band in the range of 3000–3600 cm^{-1} was attributed to the stretching vibration of the –OH that came from the $–SO_3H$ group of sulfonic acid. The PVDF-*g*-PSSA copolymer also exhibited the strong absorption band at 1180 cm^{-1}, resulting from stretching vibration of sulfonate groups (Kim et al., 2002). The bands at 1105 and 1036 cm^{-1} can be attributed to the vibrations of phenyl rings substituted with sulfonate groups and sulfonate anions attached to phenyl rings. The vibration bands at 752 cm^{-1} and 695 cm^{-1}, associated with the monosubstitution of the benzene ring, disappeared, and the new peak, at 775 cm^{-1}, was due to the disubstitution of the benzene ring after sulfonation (Asano, 2007).

5.1.2.2 The IEC Analysis

It has been well known that the IEC values directly depend on the amount of sulfonated sites in the polymer film and thus they are indicative of the actual ion exchange sites available for proton conduction. Generally, the higher the values of the

IEC are desirable to achieve higher proton conductivities in the polymer electrolyte membranes. Figure 5.10 shows the IEC of the proton conducting PVDF membranes as a function of degree of grafting (see Table 5.2).

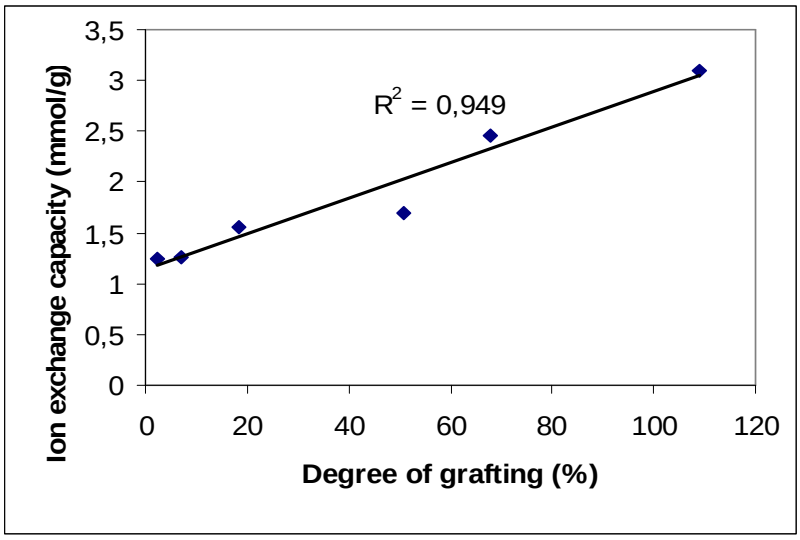

Figure 5.10 Behavior of the ion exchange capacity versus the degree of grafting for proton conducting membranes.

In this study, the IEC increased with the increase in the degree of grafting. This increasing trend can be attributed to the increase in the number of incorporated aromatic rings available for sulfonation in the membranes prepared by UV irradiation. Nasef and his co-workers (Nasef, 2010) found that the IEC value of 65 % grafted PVDF film prepared using two step radiation induced grafting method was about 2.52 mmol/g with a 90 % degree of sulfonation. Hietala et al. (Hietala et al., 1999) also reported that the IEC of the proton conducting PVDF membranes prepared by electron beam irradiation reached up to 2.55 mmol/g with a 73 % grafted membrane. In this study, the IEC of the membrane was found to be 2.46 mmol/g with a 68 % degree of grafting. The calculated degree of sulfonation was also found to be above 85%, indicating that most of the styrene units were sulfonated under the experimental conditions. It was seen that the IECs obtained in this study were in accordance with the previously reported values. The calculated IECs for PVDF-*g*-PSSA membranes were found to be higher than that of (0.91 mmol/g) commercial Nafion membrane.

5.1.2.3 The Water Uptake and Hydration Number

The water uptake of the PVDF graft copolymer membranes was evaluated at 50°C and listed in Table 5.2. Water sorption depends on the extent of sulfonation, hence higher the degree of substitution, greater the water uptake. In addition, the water uptake has a direct connection to the proton conductivity and the dimensional stability. An ideal fuel-cell membrane has higher proton conductivity with lower water uptake (Asano, 2007). Figure 5.11 shows the water uptake as a function of the degree of grafting of the PVDF based proton-conducting membranes. The higher degree of grafting was associated with a higher water uptake, indicating the presence of hydrophilic sites (sulfonated graft chains) on the hydrophobic PVDF base films. The sulfonated Memb 0 with 2.4 % degree of grafting has 6 % water uptake, whereas the sulfonated Memb 8 with 109.1 % degree of grafing has 396 % water uptake. Generally, higher IEC values give higher water uptake because both properties are strongly related to the amounts of sulfonic acid groups (Kim, 2002). PVDF-*g*-PSSA membranes exhibited 109.1 % water uptake, which are higher than that of Nafion (water uptake 30%) (Asano, 2007).

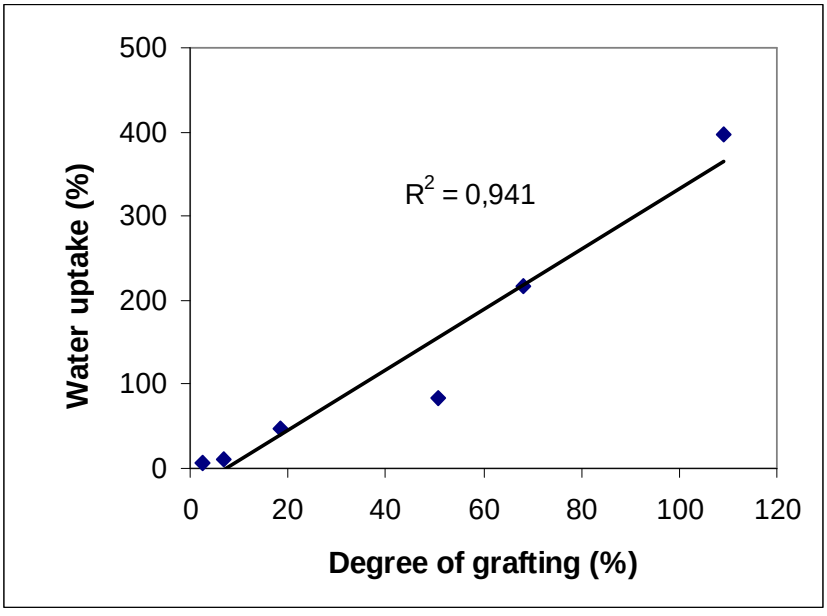

Figure 5.11 WU of the proton conducting membranes versus degree grafting.

The hydration number of the proton conducting membranes as a function of degree of grafting is shown in Figure 5.12. The hydration number is defined as the number of water molecules per sulfonic acid group (nH_2O/SO_3H). It was observed that the hydration number increased with the degree of grafting of polymers. The higher hydration number could stem from the larger ionic clusters, in which larger volumes of unbound water were contained (Asano, 2007).

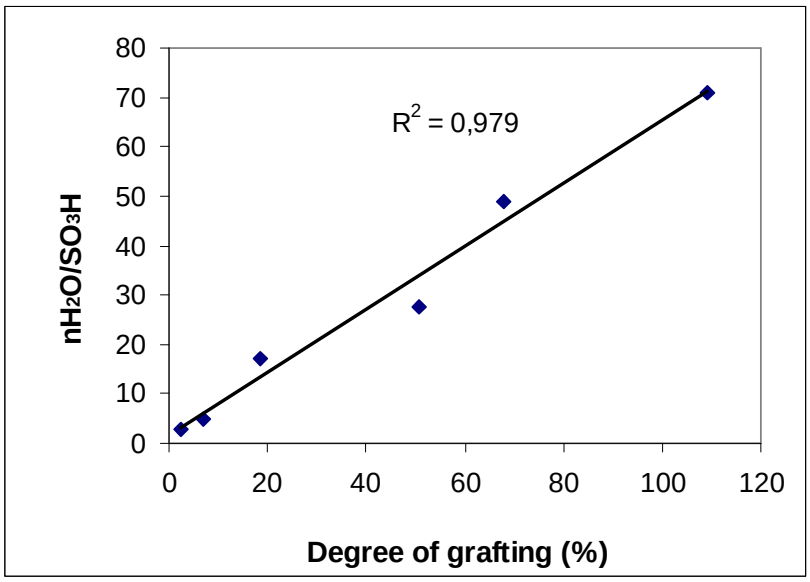

Figure 5.12 Hydration number of the proton conducting membranes versus degree of grafting

Table 5.2 Degree of sulfonation, Tm, IEC, water uptake, hydration number and conductivity of PVDF-*g*-PSSA membranes

Sample	DG (%)	Sulfonation (%)	T_m (°C)	IEC (mmol/g)	WU (%)	nH_2O/SO_3H	Conductivity at 40°C (S/cm)
Memb 0	2.4	87	155	1.25	6	2.66	a
Memb 1	6.9	91	144	1.26	11	4.85	a
Memb 2	18.4	89	160	1.55	48	17.20	a
Memb 4	50.8	84	156	1.70	84	27.45	a
Memb 6	68.0	96	156	2.46	217	49.00	1×10^{-3}
Memb 8	109.1	81	156	3.10	396	70.96	5×10^{-3}

a: Not measured

5.1.2.4 Thermogravimetric Analysis (TGA)

The thermal properties of pure PVDF, styrene grafted PVDF (Memb 6) and proton conducting membrane (sulfonated Memb 6) were investigated comparatively by TGA, as shown in Figure 5.13. Moreover, the TGA curves of proton conducting membranes are given in Figure 5.14. The first slight weight loss of proton conducting membrane was observed around 50–100°C, which is mostly attributable to the loss of adsorbed water by the hygroscopic property of the membrane.

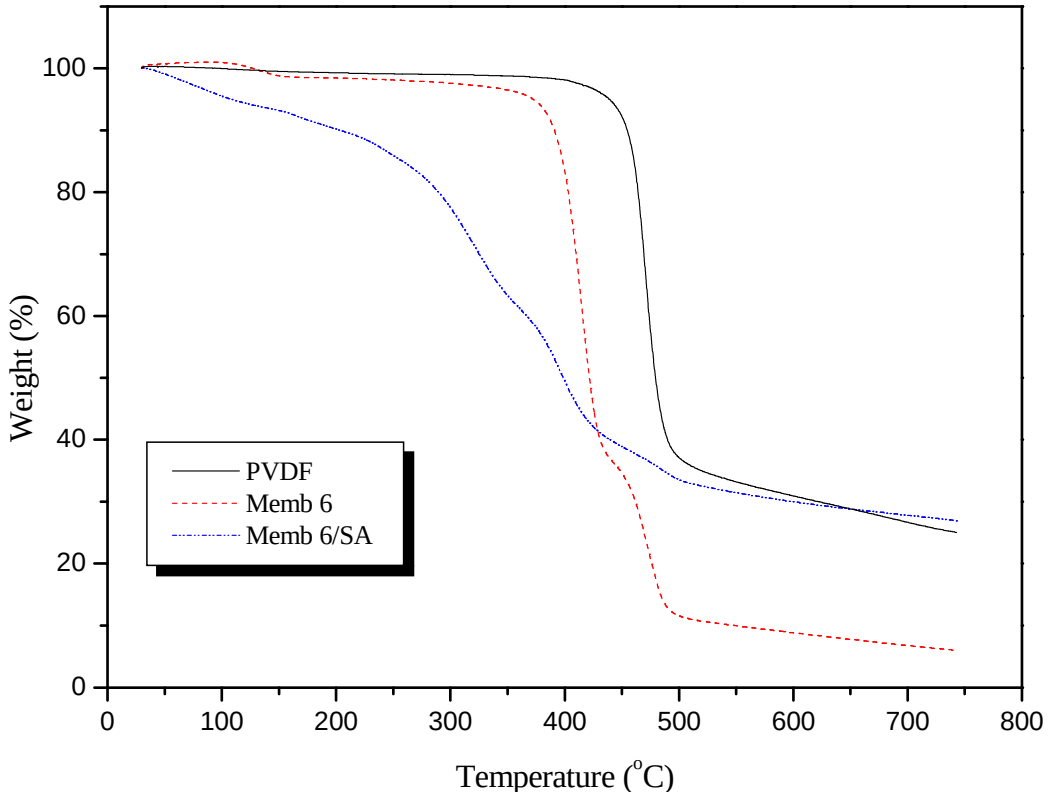

Figure 5.13 TGA data of PVDF, PVDF-g-PS (Memb 6) and PVDF-g-PSSA (sulfonated Memb 6) membranes were recorded under N_2 atmosphere at a heating rate of 10°C/min.

The second weight loss took around 100–190°C owing to the existence of poly(vinyl acetate), which was used as an adhesion agent. Then the loss of the sulfonic group from the main chain backbones was observed around 250°C. The decomposition temperatures of PVDF-*g*-PS were around 380°C. The PVDF graft membranes with

PSSA showed less thermal stability than PVDF base membrane, which is due to the decomposition of the sulfonic acid groups. However, the TGA data showed that the amphiphilic PVDF graft membranes were thermally stable up to around 250°C.

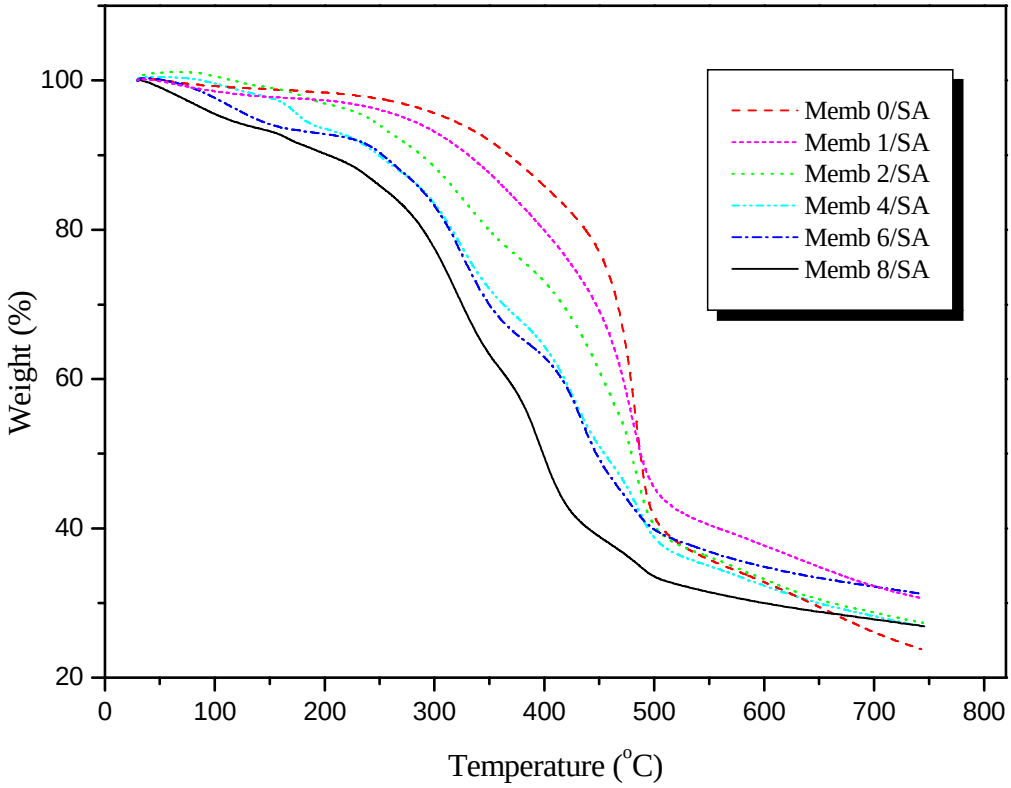

Figure 5.14 TGA data of proton conducting membranes were recorded under N_2 atmosphere at a heating rate of 10°C/min.

Most of the membranes did not undergo complete degradation and some residues of carbon-sulfur complex might be left behind at the end of the heating process (Nasef, 2010).

5.1.3 Analysis of Triazole doped PVDF-*g*-PSSA

The effect of triazole doping on anhydrous proton conductivity of the membranes at high temperatures was also studied. For this purpose, Memb 4 and Memb 6 were selected due to the fact that they possess high degree of grafting and solubility in DMF. Two different mole ratios of triazole were used, being 1:1 ratio of PVDF-*g*-PSSA: Tri

and 1:2 ratio of PVDF-*g*-PSSA: 2Tri for Memb 4 and 1:2 mole ratio of triazole was used for Memb 6.

5.1.3.1 FT-IR analysis

The FT-IR spectra of triazole doped proton conducting membranes (Memb 4) are given in Figure 5.15.

Memb 4/SA-Tri exhibited a medium absorption at 1577 cm^{-1} and 1450 cm^{-1} due to C=N and C-N stretching of the triazole ring (Krishnakumar and Xavier, 2004). Additionally, the peak which appears at 3400 cm^{-1} shows the N-H absorption.

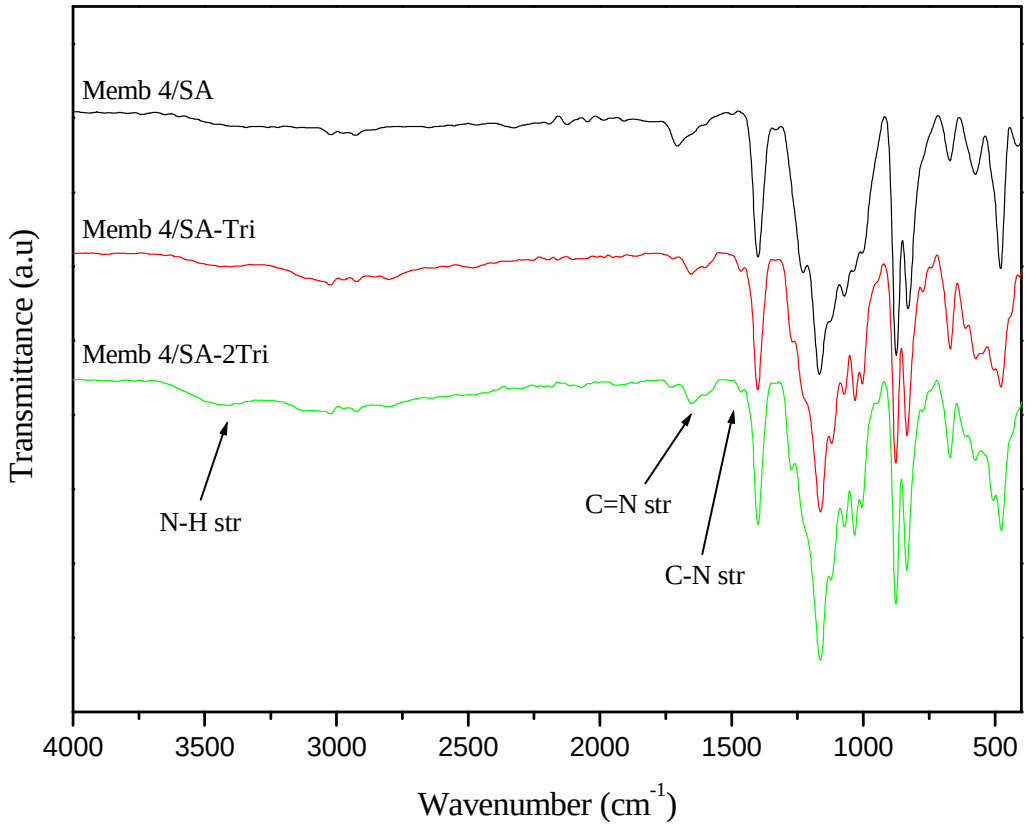

Figure 5.15 The FT-IR spectra of triazole doped proton conducting membranes

5.1.4 Proton conductivity

Proton conductivity is one of the most important properties of polymer electrolyte membranes for fuel cells. The charge density of fuel cells strongly depends on proton conductivity and thus the membranes with high proton conductivity are highly desired.

In this study, hydrous proton conductivities of hydrated membranes in the temperature range between 20°C-80°C and anhydrous proton conducting of triazole doped membranes in the temperature range between 20°C-150°C were measured by AC impedance spectroscopy. AC and DC proton conductivities of samples at high temperature were shown in Figures 5.16-5.18 and maximum proton conductivities of all samples were summarized in Table 5.3.

Table 5.3 Maximum anhydrous proton conductivities of the polymer membranes with triazole dopant at 150°C.

Sample	Triazole Doping ratio	Conductivity (mS/cm)
Memb 4/SA	1	1.0×10^{-2}
	2	5.0×10^{-2}
Memb 6/SA	1	1.0×10^{-4}
	2	2.0×10^{-4}

5.1.4.1 The Effect of Humidity on Conductivity

The proton conductivities of the PVDF-*g*-PSSA polymer membranes selected according to the amount of degree of grafting were measured by AC impedance spectroscopy. Membranes (Memb 6/SA and Memb 8/SA) were initially hydrated by immersion in water for at least 12 h at 50 °C. The proton conductivities, listed in Table 5.2, were all measured between at 20°C-80°C and at 200-400% relative humidity. Expectedly, the proton conductivities increased with increasing degree of grafting. The proton conductivities of the PVDF-*g*-PSSA membranes were in range of 1-5 $mScm^{-1}$ which are close to the reported results by Lehtinen et al., (Lehtinen, 1998). These highly proton conducting PEMs are undoubtedly promising for fuel cell applications. It is also clear that the increase in proton conductivity parallels the enhancement in the water uptake of the sulfonated polymer membranes as well as their IECs (see Table5.2).

5.1.4.2 Anhydrous Proton Conductivity

The AC and DC conductivities of triazole doped Memb 4/SA and Memb 6/SA membranes were measured (see Figures 5.16-5.18). The curves for all the samples

involve the frequency dependent and independent areas which are typical in ion conducting polymers. At lower frequencies, an increase in conductivity up to a certain level is due to electrode polarization. Then a frequency independent region over 2-3 decades was observed at higher frequencies. The direct current (DC) conductivity, σ_{dc} of the sample was derived from those plateau regions by linear fitting.

The proton conductivity of Memb 6 (D.G = 68%) is lower than Memb 4 (D.G = 50.8%). Memb 6 has higher D.G and sulfonation values than Memb 4, whereas its conductivity is lower than Memb 4. The reason for this might stem from the fact that Memb 6 could be highly crosslinked when the reaction occurs (Yu et al., 2010).

The proton conductivities increased with the increase of temperature for all the membranes. The elevation of temperature favors both the dynamics of proton transport and the structural reorganization of polymeric chains, resulting in the increased proton conductivity at high temperatures (Kim, 2007).

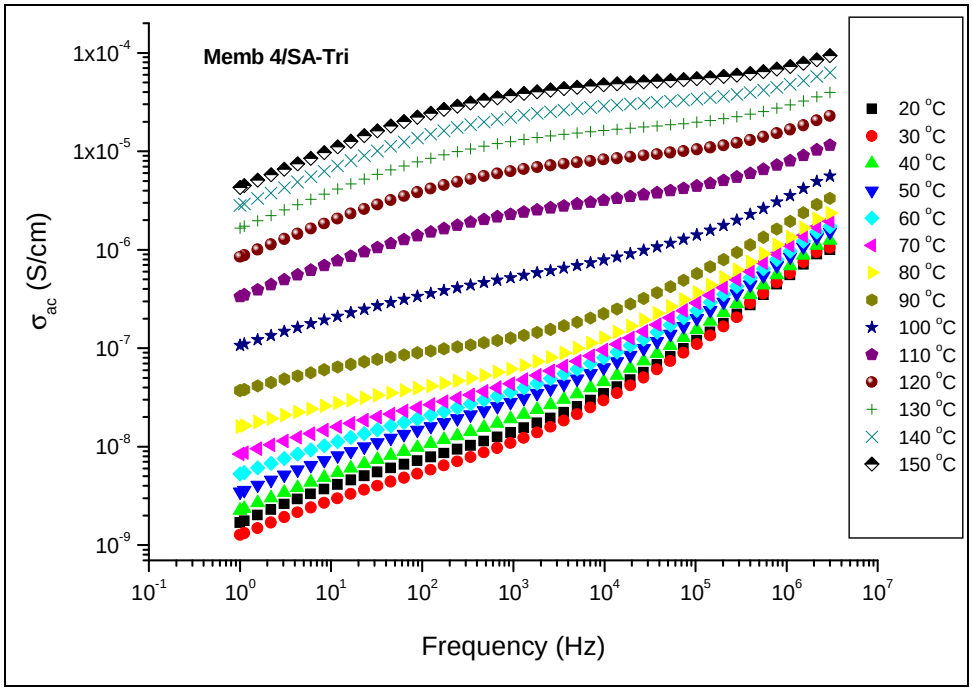

Figure 5.16 AC conductivity versus Frequency (Hz) for Memb 4/SA-Tri at various temperatures.

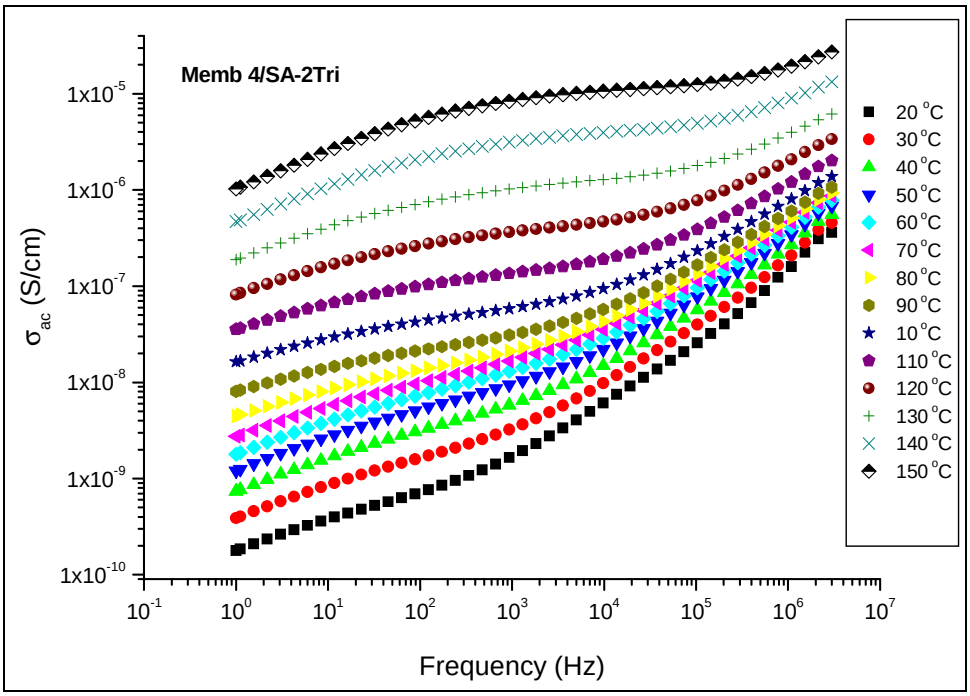

Figure 5.17 AC conductivity versus Frequency (Hz) for Memb 4/SA-2Tri at various temperatures.

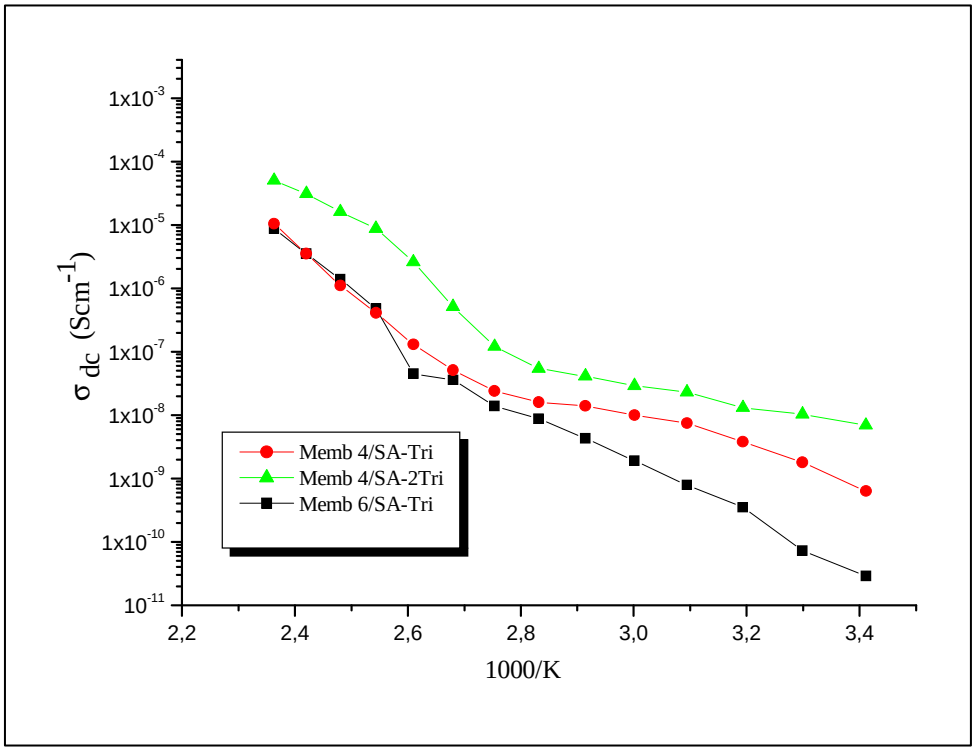

Figure 5.18 DC conductivities of Memb 4/SA-Tri, Memb 4/SA-2Tri and Memb 6/SA-Tri, as a function of reciprocal temperature.

5.2 UV-INDUCED HOMOGENEOUS PHOTOGRAFTING OF STYRENE ONTO PVDF

PVDF-*graft*-polystyrene was synthesized upon exposure to UV-light in the presence of benzophenone. Carbon centered radicals generated via H-abstraction from PVDF by the triplet benzophenone initiated the polymerization. After subsequent sulfonation, proton conducting membranes were prepared as outlined in Figure 5.19.

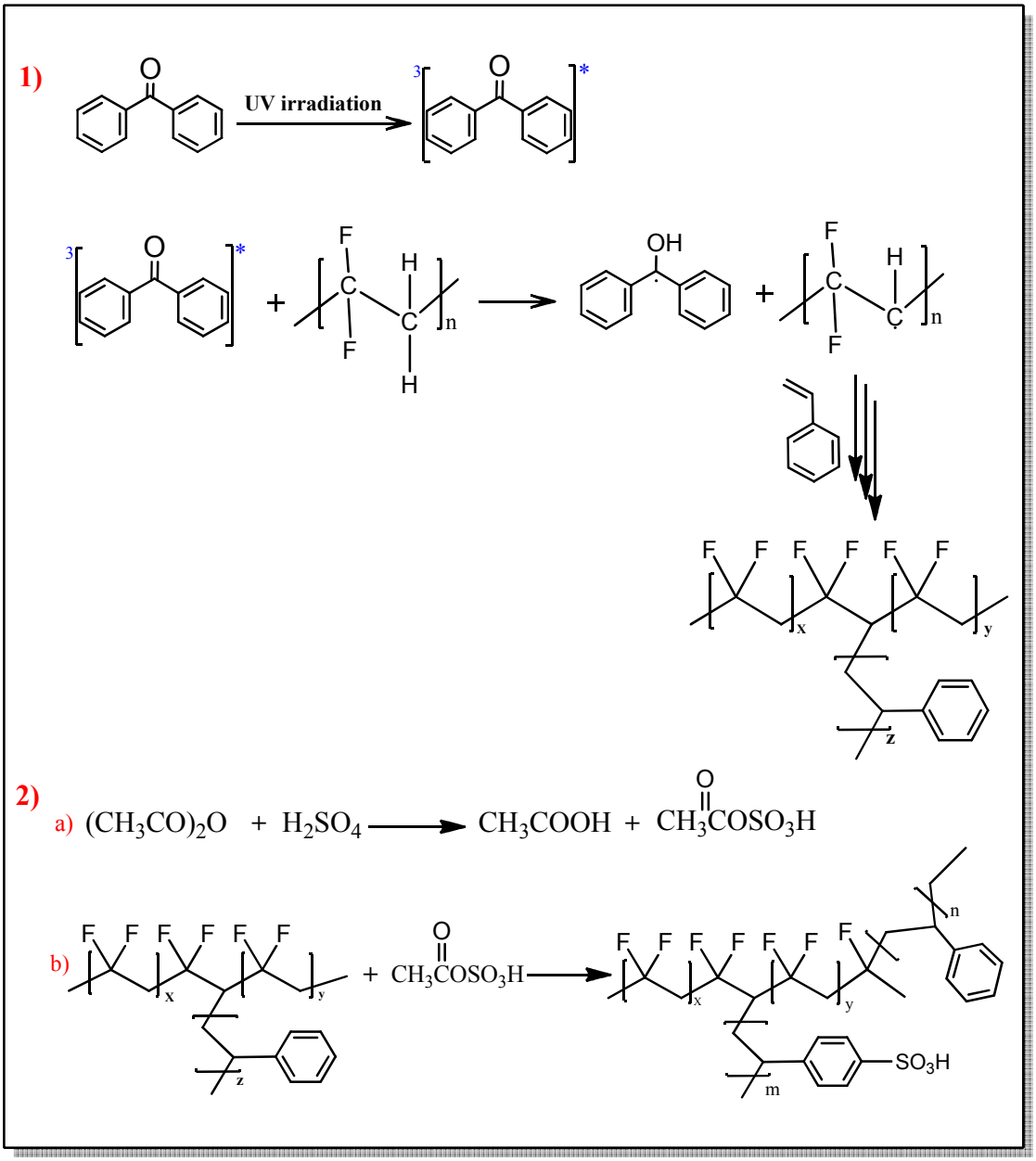

Figure 5.19 Process for synthesis of PVDF-*g*-PSSA proton conducting membranes by UV homogeneous photografting method.

Table 5.4 Synthesis conditions and results of PVDF-*g*-PS graft copolymers

PVDF (g)	Styrene (g)	Irradiation Time (h)	Product (g)	CH_2Cl_2 insoluble (%)	Yield (%)	Tg (°C)	Tm (°C)
0.8	21.8	0.5	1.005	0.198	0.8	a	158
0.8	21.8	4	1.112	0.216	12	87.3	158

a: Not detected due to low degrees of grafting.

5.2.1 Analysis of the Grafted PVDF

5.2.1.1 ^{1}H NMR Result

The successful graft copolymerization was confirmed using ^{1}H NMR spectroscopy. ^{1}H-NMR spectra for pure PVDF and styrene grafted PVDF copolymers obtained after 0.5 h and 4 h UV irradiation were presented in Figure 4.20.

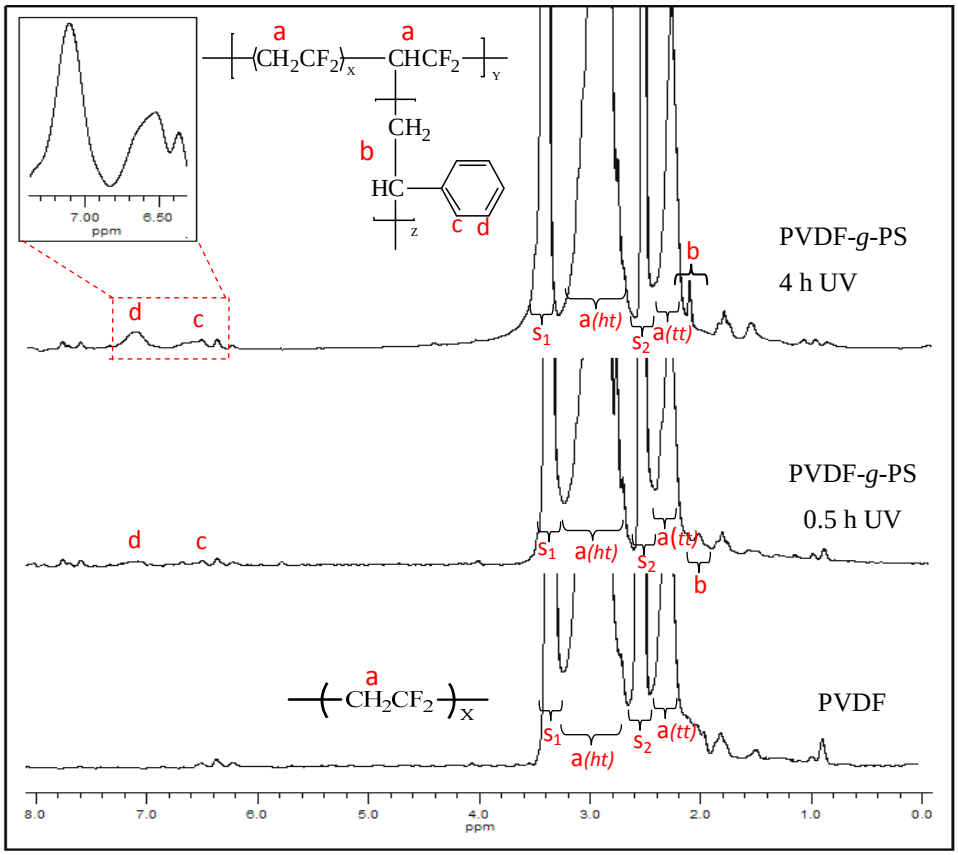

Figure 5.20 ^{1}H NMR spectra of pure PVDF and PVDF-*g*-PS graft copolymers obtained with 0.5 h and 4 h UV irradiation.

For both samples, the peaks of solvent (DMSO) and water appeared at 2.6 and 3.5 ppm, respectively. In addition, the spectrum exhibits the presences of the characteristic multiplets centered at 2.9 and 2.3 ppm assigned to the methylene groups in -CH_2-CF_2-CH_2-CF_2-CH_2-CF_2- and -CF_2-CH_2-CH_2-CF_2- sequences resulting from the normal tail-to-head and reversed tail-to-tail VDF additions. (Guiot et al. 2002, Guiot et al., 2005) The spectrum of the PVDF-*g*-PS graft copolymer exhibits additional signals located in the 1.8-2.1 ppm and 7.3-6.4 ppm ranges assigned to methylene and methyne groups of poly(styrene) and to the aromatic protons, respectively.

5.2.1.2 FT-IR Studies

Figure 5.21 shows the FT-IR spectra of the PVDF base film and styrene grafted PVDF copolymers with different UV irradiation times. The characteristic peaks of pure PVDF was observed between 1200-1000 cm^{-1} and 450 cm^{-1}, which represents fluorocarbon absorption (C–F band absorption). In addition, the strong peak appeared at 1403 cm^{-1}, corresponds to CH_2 stretching vibrations of PVDF.

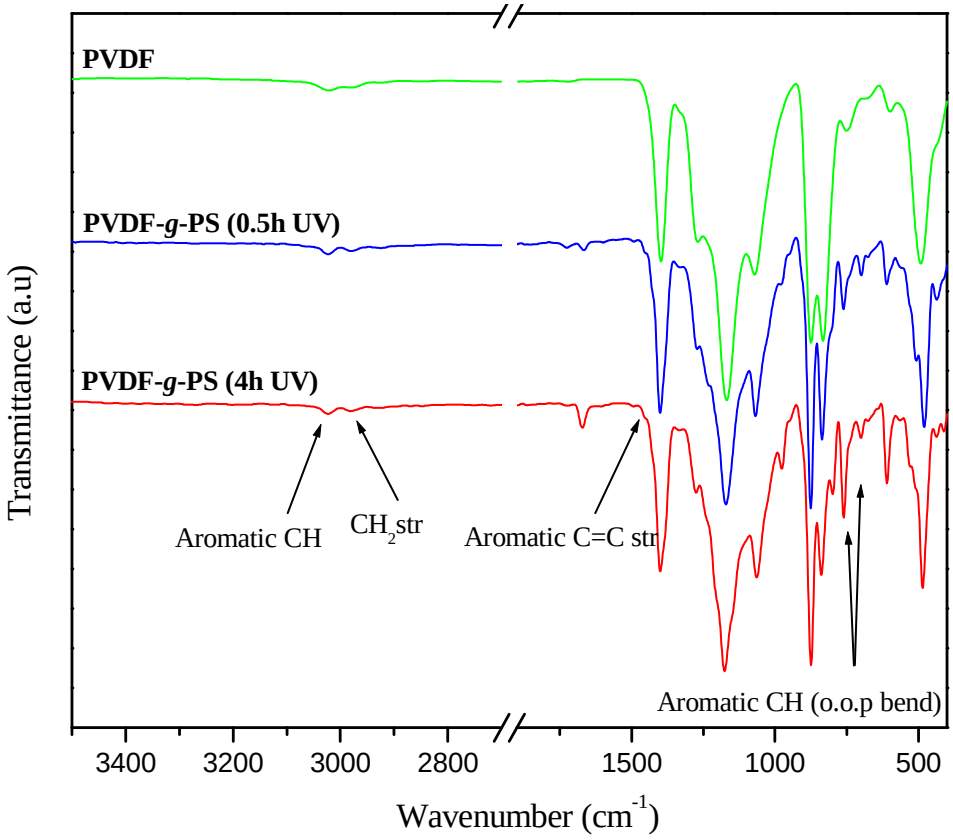

Figure 5.21 Typical FTIR spectra of pure PVDF and PVDF-*g*-PS graft copolymers obtained with 0.5 h and 4 h UV irradiation.

The existence of polystyrene in graft copolymer PVDF-*g*-PS was verified by the two bands of C–H aromatic out-of-plane deformation at 752 cm^{-1} - 695 cm^{-1} and 3026 cm^{-1}, which was due to the aromatic =C–H bonds. It is also worth noting that there was a peak at 1500 cm^{-1}, which was a result of the aromatic C=C stretching vibrations. These signs confirmed that the monomers were grafted onto the PVDF backbone, and the variation in the intensity of the polystyrene characteristic bands reflects the differences in the degrees of grafting with increasing irradiation time.

5.2.1.3 Thermogravimetric (Tg) Analysis

The thermal stabilities of pure PVDF and PVDF-*g*-polystyrene graft copolymers were investigated by TGA as shown in Figure 5.22. The base PVDF showed excellent thermal stability up to 448 °C, above which it started to decompose to about 30 wt % (Kim, 2008).

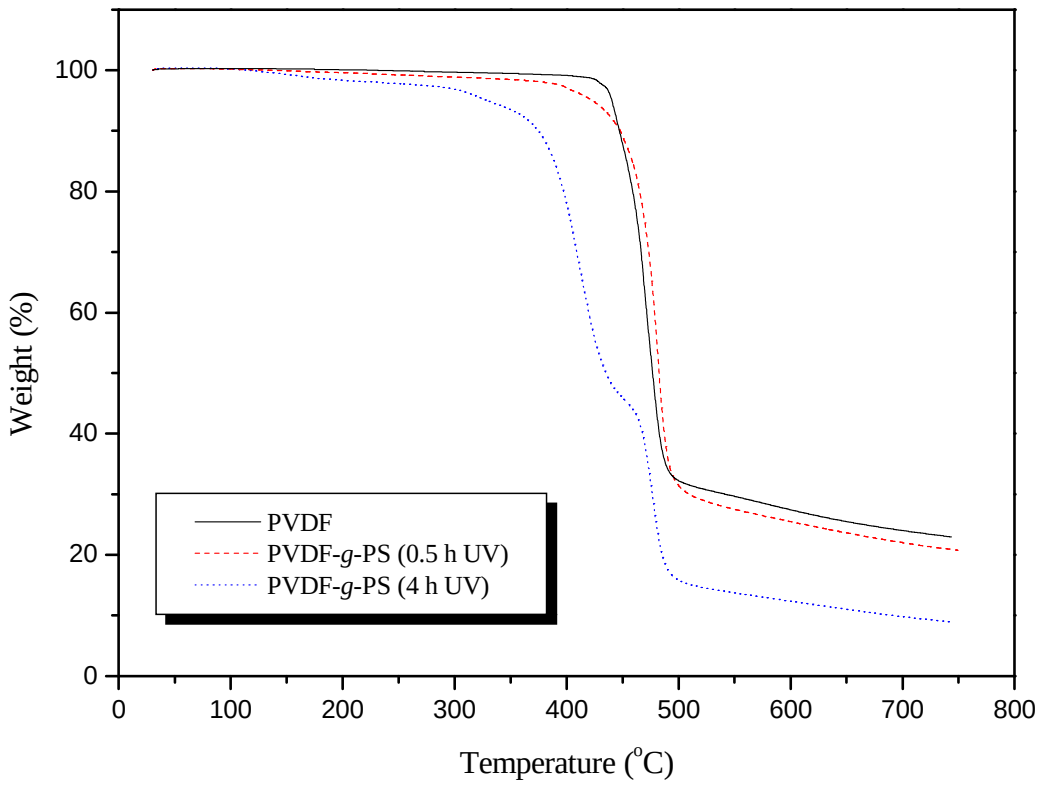

Figure 5.22 TGA data of pure PVDF and 0.5 h UV and 4 h UV graft copolymer PVDF-*g*-PS were recorded under N_2 atmosphere at a heating rate of 10°C/min.

The graft polymers showed degradation patterns owing to depolymerization and decomposition of PVDF. The initial weight loss was attributed to the loss of polystyrene (depolymerization). The weight loss in the second step was due to decomposition of PVDF by random chain scissions, reported as characteristic of the PVDF backbone degradation (Sauguet, 2006 and Nasef, 2010). Clearly, PVDF-*g*-PS showed a satisfactory thermal stability up to 380 °C. The slight weight change until 100-150 ^{o}C can be attributed to absorbed humidity.

5.2.1.4 DSC Analysis

Differential scanning calorimetry (DSC) was performed to measure the glass transition temperatures of the pure PVDF and PVDF-*g*-PS graft copolymers synthesized by 0.5 h and 4 h UV irradiation. Figure 5.23 shows the DSC curves between 54 °C - 240 °C for the membranes and their corresponding Tg values are listed in Table 5.4.

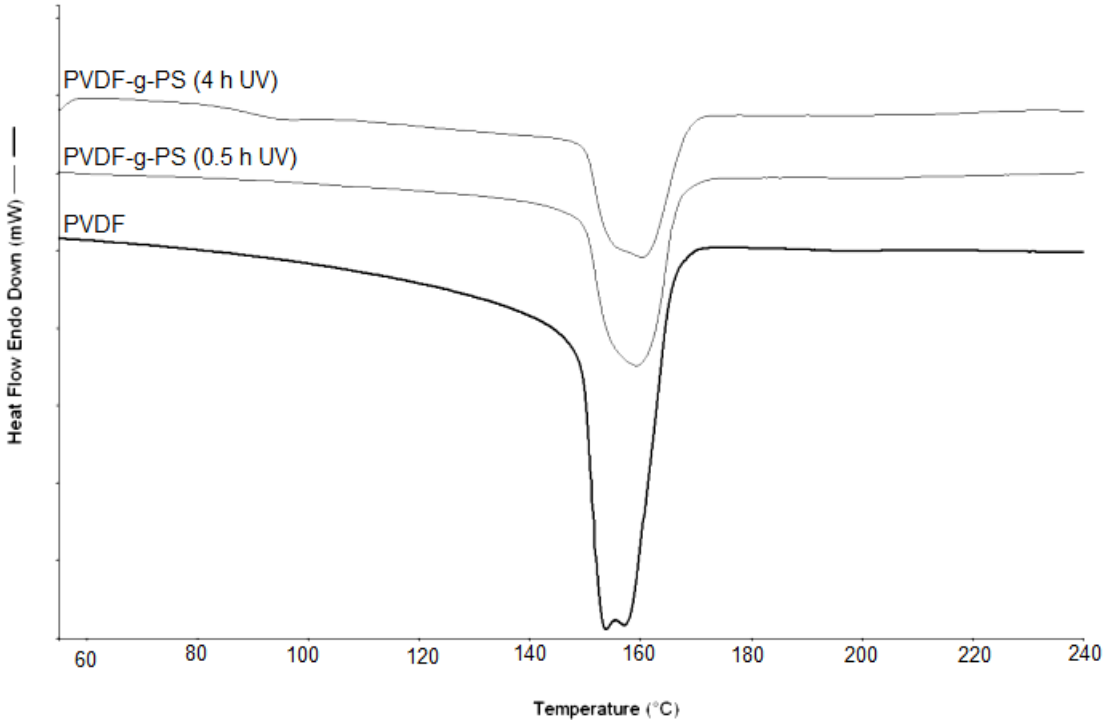

Figure 5.23 DSC traces of pure PVDF and PVDF-*g*-PS graft copolymers obtained with 0.5 h and 4 h UV irradiation were recorded under inert atmosphere at a heating rate of 10 °C/min.

Figure 5.24 illustrates a close-up view of the DSC curves between 60°C -130°C. Tg of pristine PS was nearly 108°C. PVDF-*g*-PS obtained via 4 h irradiation had definite glass transition temperature at 87.3 °C. The obtained Tg value was assigned to the presence of polystyrene grafts. However, PVDF-*g*-PS obtained via 0.5 h irradiation did not show any Tg value, which might be due to low degree of grafting. The DSC results demonstrated that as the quantity of grafting PS increased, the glass transition temperature of the sample was detected more easily.

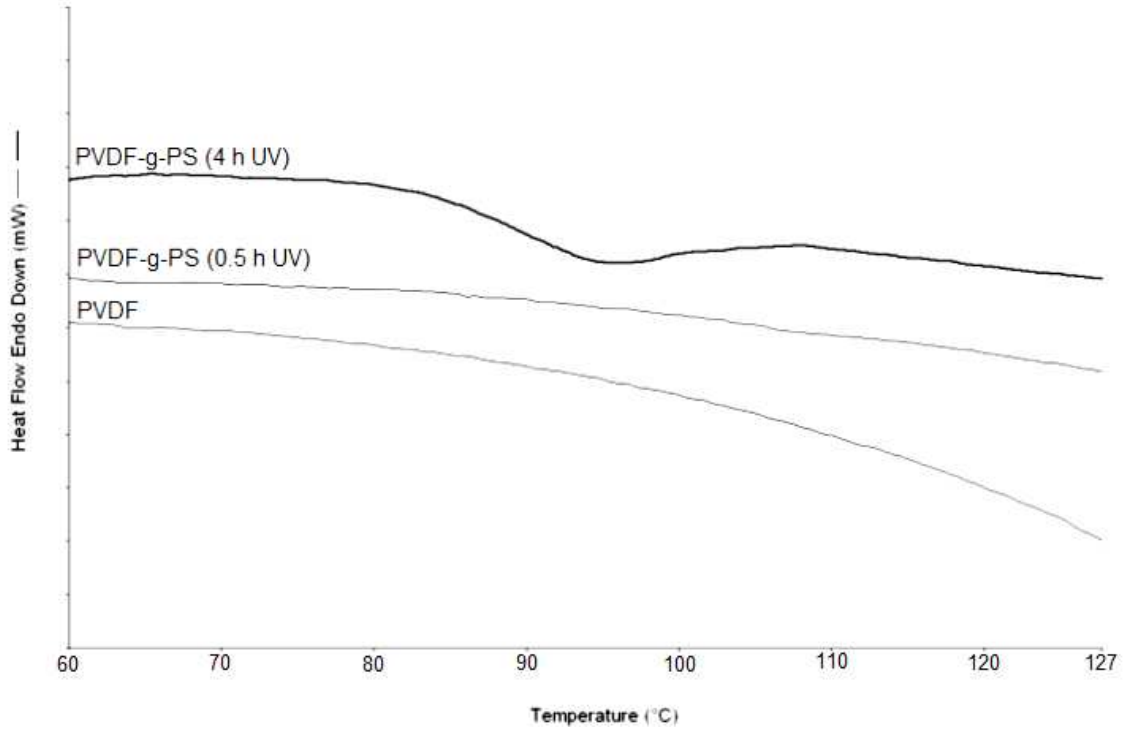

Figure 5.24 The close-up view of the DSC traces of pure PVDF and PVDF-*g*-PS graft copolymers.

5.2.2 Analysis of PVDF-g-PSSA / Proton Conducting Membranes

5.2.2.1 FT-IR analysis

The sulfonation was verified by FT-IR spectroscopy. Figure 5.25 shows the FT-IR spectra of the pure PVDF, graft copolymer, PVDF-*g*-PSSA, and proton conducting polymer PVDF-*g*-PSSA. The broad band in the range of 3000–3600 cm^{-1} was attributed to the stretching vibration of the –OH that came from the $–SO_3H$ group of sulfonic acid. The PVDF-*g*-PSSA copolymer also exhibited the strong absorption band at 1180 cm^{-1},

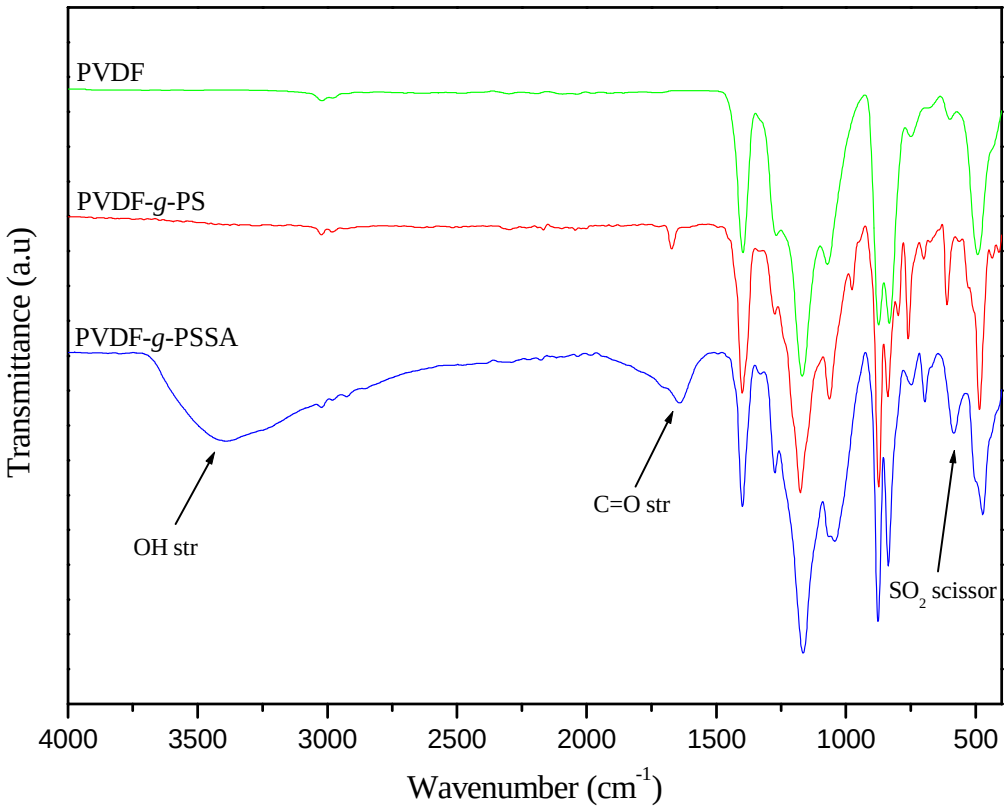

Figure 5.25 FT-IR spectra of base PVDF, styrene grafted PVDF and proton conducting PVDF-*g*-PSSA.

resulting from stretching vibration of sulfonate groups (Kim et al., 2002). The bands at 1105 and 1036 cm^{-1} can be attributed to the vibrations of phenyl rings substituted with sulfonate groups and sulfonate anions attached to phenyl ring. The vibration bands at 752 cm^{-1} and 695 cm^{-1}, associated with the monosubstitution of the benzene ring, became weaker, and the new peak, at 582 cm^{-1}, was due to the scissor vibration of the SO_2 groups (Asano, 2007 and Socrates, 2006).

Table 5.5 Degree sulfonation, Tg, Tm, IEC, water uptake, and conductivity of PVDF-*g*-PSSA

Sample	Yield (%)	Sulfonation (%)	IEC (mmol/g)	WU (%)	T_g (°C)	T_m (°C)	Conductivity at 150°C (S/cm)
PVDF-*g*-PSSA	12	22	0.24	a	98	158	1.0×10^{-7}

a: Not measured due to low degree of sulfonation.

5.2.2.2 The IEC Analysis

IEC values directly depend on the amount of sulfonated sites in the polymer and thus they are indicative of the actual ion exchange sites available for proton conduction. Generally, the higher the values of the IEC are desirable to achieve higher proton conductivities in the polymer electrolyte membranes. In this study, the IEC of the PVDF-*g*-PSSA was found to be 0.24 mmol/g with a 12% degree of grafting and 22% degree of sulfonation (see Table 5.5).

5.2.2.3 The Water Uptake

Water sorption depends on the extent of sulfonation, hence higher the degree of substitution, greater the water uptake. The higher degree of grafting was associated with a higher water uptake, indicating the presence of hydrophilic sites (sulfonated graft chains) within the hydrophobic PVDF base polymer. In this study, the water uptake of the PVDF-*g*-PSSA was evaluated at 50°C but polymer did not adsorb water due to low degree of grafting and sulfonation (see Table 5.5).

5.2.2.4 Thermogravimetric Analysis (TGA)

The thermal properties of pure PVDF, grafted PVDF and proton conducting polymer PVDF-*g*-PSSA were investigated comparatively by TGA, as shown in Figure 5.26. The first weight loss of the sulfonic group from the main chain backbones was observed around 250°C. The decomposition temperatures of PVDF-*g*-PS were around 380°C. The PVDF graft membranes with PSSA showed less thermal stability than base PVDF membrane, which are due to the decomposition of the sulfonic acid groups. However, the TGA data showed that the amphiphilic PVDF graft membranes were thermally stable up to around 250°C.

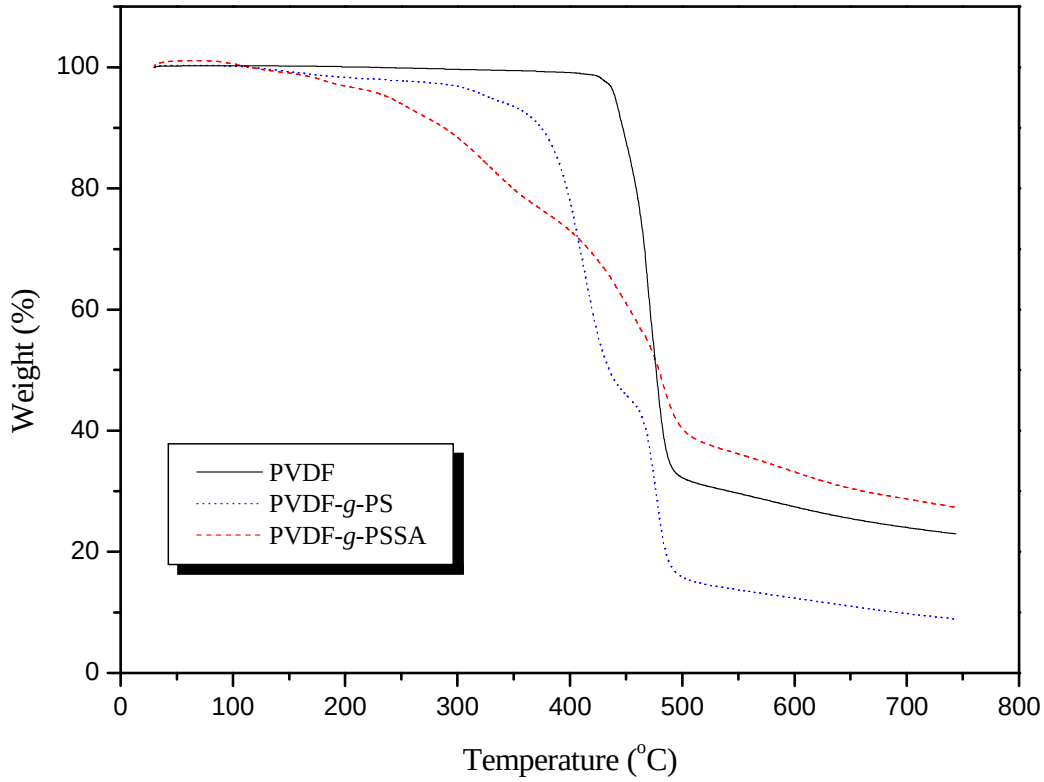

Figure 5.26 TGA data of PVDF, PVDF-*g*-PS and PVDF-*g*-PSSA were recorded under N_2 atmosphere at a heating rate of 10°C/min.

5.2.2.5 DSC Analysis

Figure 5.27 shows the DSC curves between 55°C - 240°C for the pure PVDF, PVDF-*g*-PS and PVDF-*g*-PSSA. Figure 5.28 illustrates a close-up view of the DSC curves between 75°C - 110°C. PVDF-*g*-PS and PVDF-*g*-PSSA had definite glass transition temperatures at 87.3°C and 98°C. The DSC results demonstrated that as the graft copolymer was sulfonated, the glass transition temperature of the polymer shifted to higher temperatures.

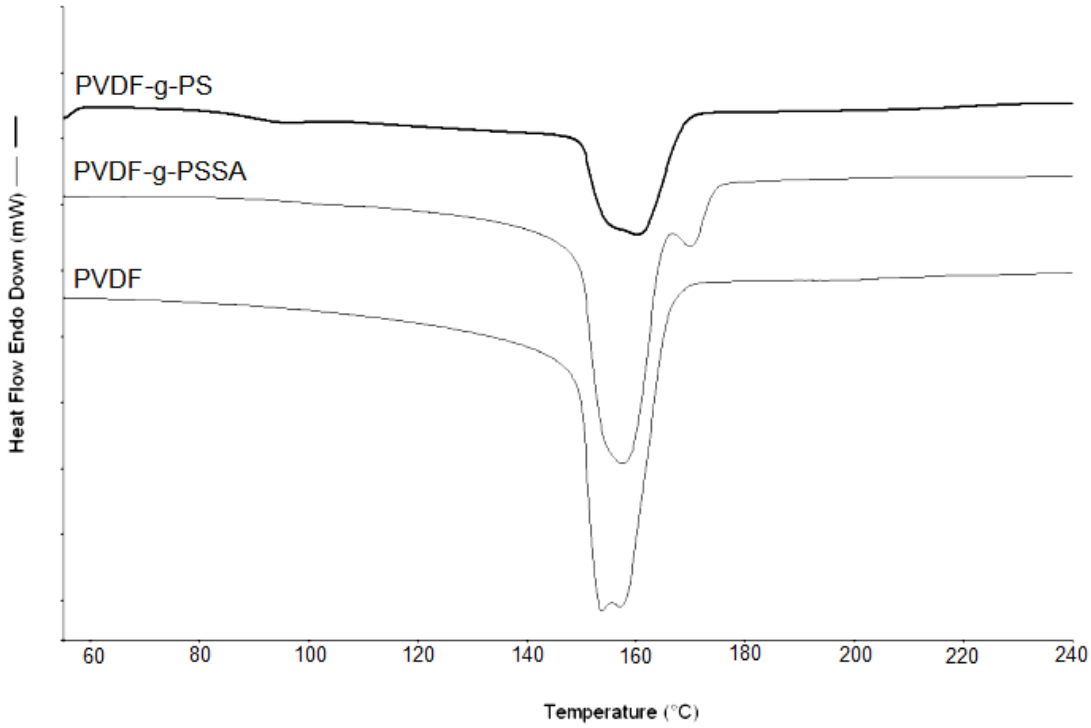

Figure 5.27 DSC traces of pure PVDF and PVDF-*g*-PS graft copolymers obtained with 0.5 h and 4 h UV irradiation were recorded under inert atmosphere at a heating rate of 10 °C/min.

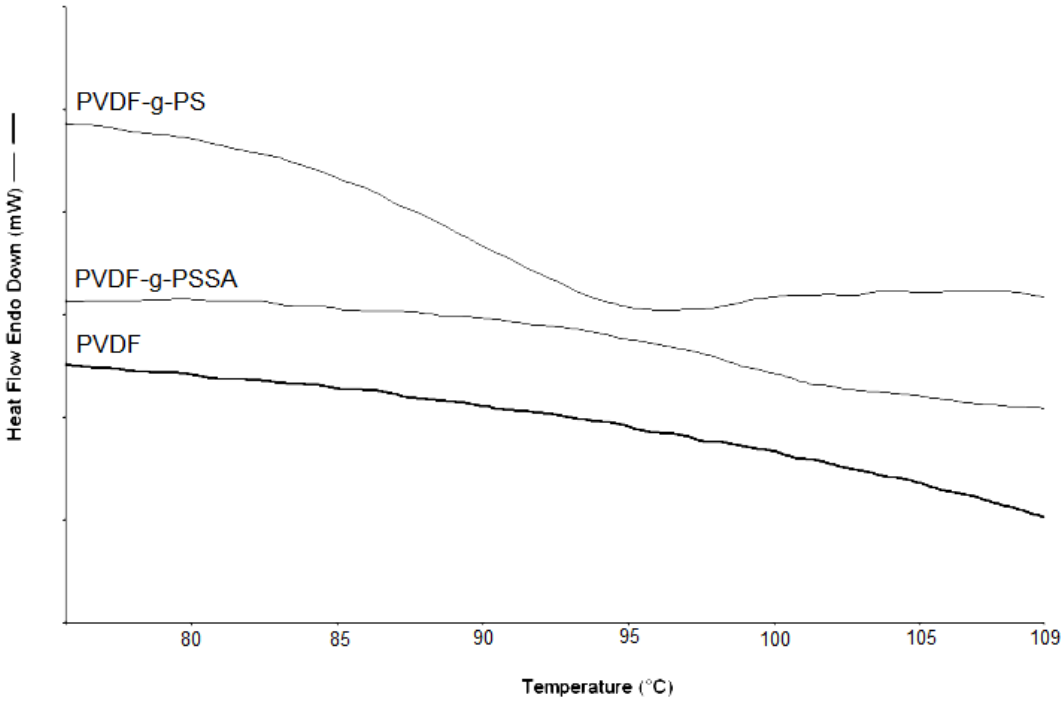

Figure 5.28 The close-up view of the DSC traces of pure PVDF, PVDF-*g*-PS and PVDF-*g*-PSSA graft copolymers.

5.2.2.6 Proton conductivity

The samples were dried under vacuum at 40 °C for 24 h. Alternating current (AC) conductivity, σ_{ac} versus frequency curves are shown in Figure 5.29 for anhydrous PVDF-*g*-PSSA. The curves for all the samples involve the frequency dependent and independent areas which are typical in ion conducting polymers. At lower frequencies, an increase in conductivity up to a certain level is due to electrode polarization. Then a frequency independent region over 2-3 decades was observed at higher frequencies. After doped PVDF-g-PSSA with triazole, the maximum proton conductivity of PVDF-*g*-PSSATri with 22% sulfonation was measured about $1x10^{-4}$ mS/cm at 150°C. The direct current (DC) conductivity, σ_{dc} of the sample was derived from those plateau regions by linear fitting as shown in Figure 5.30.

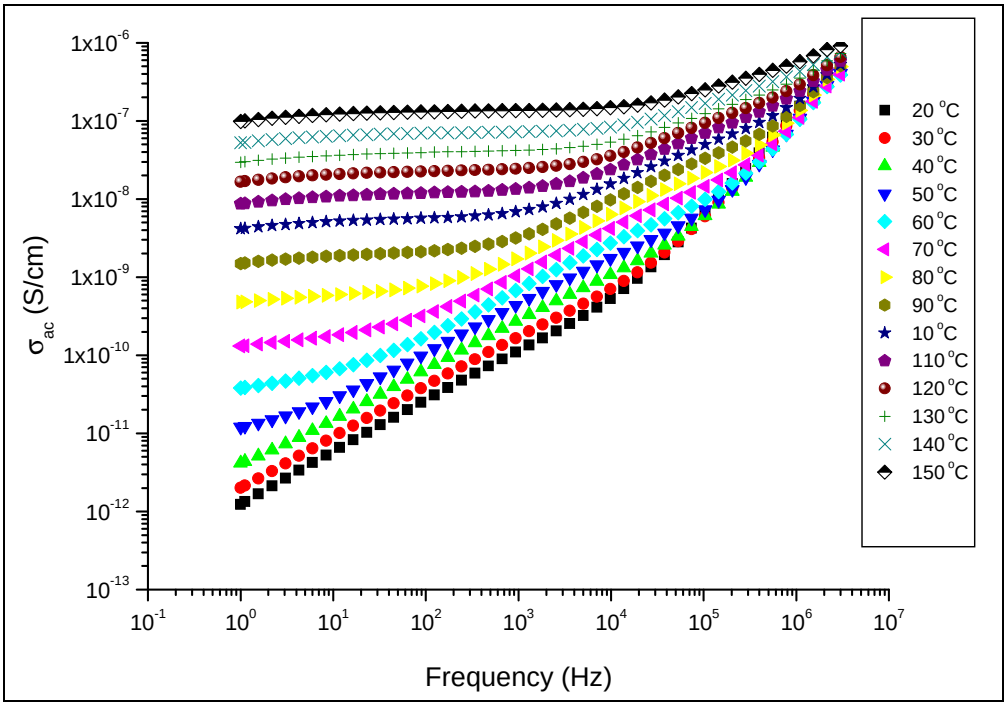

Figure 5.29 AC conductivity versus Frequency (Hz) for PVDF-*g*-PSSA at various temperatures.

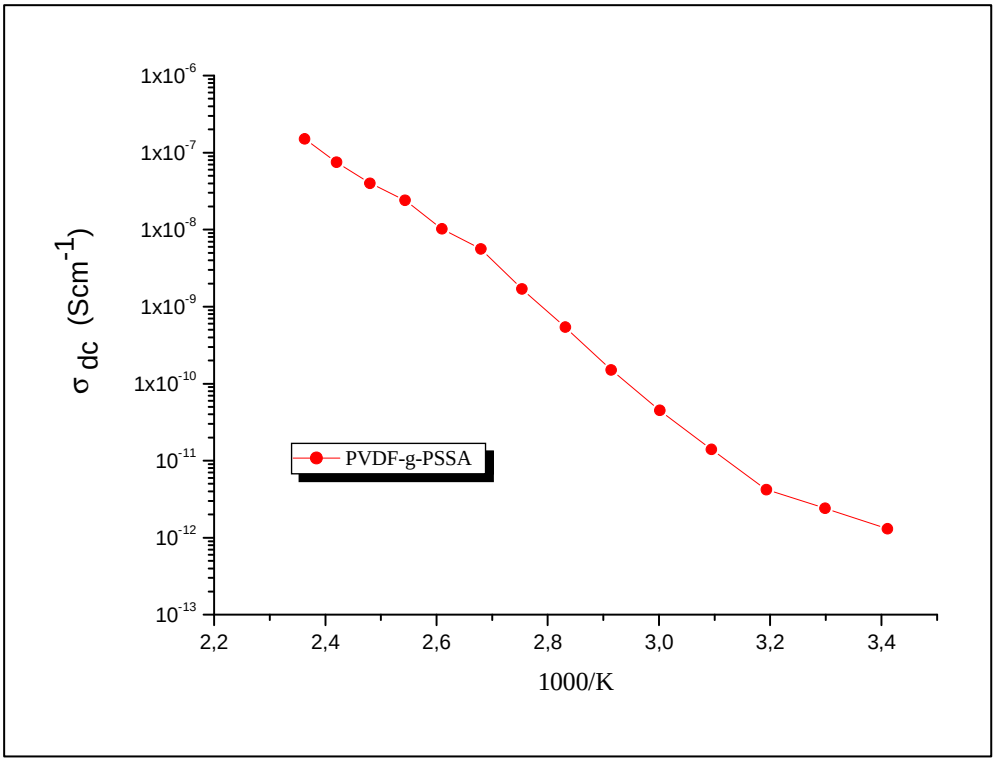

Figure 5.30 DC conductivities of PVDF-*g*-PSSA as a function of reciprocal temperature.

CHAPTER 6

CONCLUSION

Proton exchange membranes were prepared by UV photoinduced surface and homogeneous grafting of styrene onto poly(vinylidene fluoride) followed by a sulfonation reaction. The degrees of grafting in PVDF-*g*-PS films obtained by surface grafting increased with irradiation time, reaching above 100 % after 8 h. The success of graft copolymerization was confirmed using ^{1}H NMR and FT-IR. Thermal properties (melting and glass transition temperatures) and thermal stability of the membranes were also studied using DSC and TGA, respectively. The TGA curves of PVDF-*g*-PS polymers with varying degrees of grafting showed satisfactory thermal stabilities up to 381 °C. The DSC results demonstrated that as the degrees of grafting increased, the glass transition temperatures of the samples shifted to higher values.

The sulfonation was verified by FT-IR spectroscopy. The polymer electrolyte membranes were also characterized in terms of IEC, which is a direct indication of the extent of ion exchanging groups present in the membrane. The IEC increased with an increase in the degree of grafting. The IEC of the membrane with a 68 % degree of grafting was found to be 2.46 mmol/g. The degree of sulfonation was calculated to be around 85%, indicating that most of the styrene units were sulfonated under the experimental conditions. As expected, water uptake values were found to be directly proportional with degree of grafting, which was attributed to the presence of hydrophilic sites (sulfonated graft chains) on the hydrophobic PVDF base films. PVDF-*g*-PSSA with a degree of grafting of 2.4 % had 6 % water uptake, while it reached 396% for a degree of grafting of 109.1 %.

Anhydrous proton conducting properties of 1,2,4-triazole-functional PVDF-*g*-PSSA polymers were investigated. PVDF-*g*-PSSA(Tri)$_2$ with a degree of grafting of 50.8% showed a maximum water-free proton conductivity of approximately $5x10^{-2}$ mS/cm at 150°C. For the films obtained by homogeneous grafting, the anhydrous proton conductivity of PVDF-*g*-PSSA with 22% sulfonation was measured about $1x10^{-4}$ mS/cm at 150°C.

REFERENCES

Akbari, A., S. Desclaux, J. C. Remigy, P. Aptel, *Desalination*, Vol. 149, pp. 101, 2002.

Akbari, A., S. Desclaux, J. C. Rouch, P. Aptel, J. C. Remigy, *J Membr Sci*, Vol. 286, pp. 342, 2006.

Akbari, A., S. Desclaux, J. C. Rouch, J. C. Remigy, *J Membr Sci*, Vol. 297, pp. 243, 2007.

Allcock H. R. and R. M. Wood, *Journal of Polymer Science Part B Polymer Physics*, Vol. 44, pp. 2358-68, 2006.

Allcock H. R., H. A. Hofmann, C. M. Ambler, R. V. Morford., *Macromolecules*, Vol. 35, pp. 3484-9, 2002.

Allen, N. S., *Handbook of photochemistry and photophysics of polymer materials*, J. Wiley, 2010.

Allmer, K., A. Hult, B. Ranby, *J Polym Sci Pol Chem*, Vol. 26, pp. 2099, 1988.

Amornsakchai, T., H. Kubota, *J Appl Polym Sci*, Vol. 70, pp. 465, 1998.

Appleby, A. J. and F. R. Foulkes, *Fuel cell handbook*, Van Nostrand Reinhold, New York, 1989.

Asano, M., J. Chen, Y. Maekawa, T. Sakamura, H. Kubota, M. Yoshida, *J. Polym. Sci., Part A: Polym. Chem.*, Vol. 45, pp. 2624–2637, 2007.

Bai, H., W. S. W. Ho, *Polymer International*, Vol. 60, pp. 26–41, 2010.

Bequet, S., T. Abenoza, P. Aptel, J. M. Espenan, J. C. Remigy, A. Ricard, *Desalination*, Vol. 131, pp. 299, 2000.

Bequet, S., J. C. Remigy, J. C. Rouch, J. M. Espenan, M. Clifton, P. Aptel, *Desalination*, Vol. 144, pp. 9, 2002.

Bouchet, R, E. Siebert, *Solid State Ionics*, Vol. 18, pp. 287, 1991.

Bozkurt, A., M. Ise, K. D. Kreuer, W. H. Meyer, G. Wegner, *Solid State Ionics*, Vol. 125, pp. 225, 1999.

Capek, I., *Eur Polym J*, Vol. 36, pp. 255, 2000.

Celik, S. U., A. Bozkurt, *European Polymer Journal*, Vol. 44, pp. 213–218, 2008.

Chen, J. H., M. Asano, Y. Maekawa, T. Sakamura, H. Kubota, M. Yoshida, *Electrochemical and Solid State Letters*, Vol. 9, pp. G326, 2006.

Chen, J. H., M. Asano, Y. Maekawa, T. Sakamura, H. Kubota, M. Yoshida, *J Membr Sci*, Vol. 283, pp. 373, 2006.

Chen, J. H., M. Asano, Y. Maekawa, T. Sakamura, H. Kubota, M. Yoshida, Electrochem Solid State Lett 9, G184 2006.

Chen, J., M. Asano, Y. Maekawa, M. Yoshida, *J Membr Sci*, Vol. 277, pp. 249, 2006.

Chen, J., M. Asano, T. Yamaki, M. Yoshida, *J Membr Sci*, Vol. 269, pp. 194, 2006.

Chen, Y., D. Liu, Q. Deng, X. He, X. Wang, *J Polym Sci A Polym Chem*, Vol. 44, pp. 3434, 2006.

Chuy, C., J. Ding, E. Swanson, S. Holdcroft, J. Horsfall, K.V. Lovell, *J. Electrochem. Soc.*, Vol. 150, pp. E271, 2003.

Chuy, C., V. I. Basura, E. Simon, S. Holdcroft, J. Horsfall, K. V. Lovell, *J. Electrochem. Soc.*, Vol. 147, pp. 4453, 2000.

Costamagna P. and S. Srinivasan, *J. Power Sources*, Vol. 102, pp. 242-253, 2001.

Costamagna, V., D. Wunderlin, M. Larranaga, I. Mondragon, M. Strumia, *Journal of Applied Polymer Science*, Vol. 102, pp. 2254, 2006.

Cremlyn, R. J., '*Chlorosulfonic acid: a versatile reagent'*, Royal Society of Chemistry, 2002.

Curti, P. S., M. R. de Moura, W. Veiga, E. Radovanovic, A. F. Rubira, E. C. Muniz, *Applied Surface Science*, Vol. 245, pp. 223, 2005.

Degirmenci, M., O. Izgin, Y. Yagci, *J Polym Sci Pol Chem*, Vol. 42, pp. 3365, 2004.

Deluca, N. W., and Y.A. Elab, *J Polym Sci Part B Polym Phys*, Vol. 44, pp. 2201–2213, 2006.

Deng, H. P., W. T. Yang, *Eur Polym J*, Vol. 41, pp. 2685, 2005.

Deng, J. P., W. T. Yang, B. Ranby, *Macromol Rapid Comm*, Vol. 22, pp. 535, 2001.

Deng, J. P., W. T. Yang, *J Beijing Univ Chem Technol*, Vol. 27, pp. 16–9, 2000.

Deng, J. P., W. T.Yang, *J Polym Sci Pol Chem*, Vol. 39, pp. 3246, 2001.

Ding, J., C. Chuy, S. Holdcroft, *Macromolecules*, Vol. 35, pp. 1348, 2002.

Flint, S. D., R. C. Slade, *Solid State Ionics*, Vol. 97, pp. 299, 1997.

Fujimura, M., T. Hashimoto, H. Kawai, *Macromolecules*, Vol. 14, No. 5, pp. 1309-1315, 1981.

Gao, Y., G. P. Robertson, M. D. Guiver, X. G. Jian, *Journal of Polymer Science Part A-Polymer Chemistry*, Vol. 41, No. 4, pp. 497-507, 2003.

Gautier-Luneau I., A. Denoyelle, J. Y. Sanchez, C. Poinsignon, *Electrochimica Acta*, Vol. 37, pp. 1615-8, 1992.

Geismann, C., A. Yaroshchuk, M. Ulbricht, *Langmuir*, Vol. 23, pp. 76, 2007.

Gierke, T. D. and W. Y. Hsu, *ACS Symposium Series*, Vol. 180, pp. 283-307, 1982.

Gierke, T. D., G. E. Munn, F. C. Wilson, *ACS Symposium Series*, Vol. 180, pp. 195-216, 1982.

Gierke, T. D., G. E. Munn, F. C. Wilson, *Journal of Polymer Science, Part B: Polymer Physics*, Vol. 19, No. 11, pp. 1687-1704, 1981.

Goma-Bilongo, T., A. Akbari, M. J. Clifton, J. C. Remigy, *J Membr Sci*, Vol. 278, pp.308, 2006.

Grotthuss, C. J. D. v., Ann. Chim., LVIII, pp. 54, 1806.

Guan, J. J., C. Y. Gao, L. X. Feng, J. C. Shen, *J Appl Polym Sci*, Vol. 77, pp. 2505, 2000.

Gubler, L. N., Beck, S. A. Gürsel, F. Hajbolouri, D. Kramer, A. Reiner, *Chimia*, Vol. 58, pp. 826-36, 2004.

Guillet, J. E. R. G. W. Norrish, *Proc R Soc London Ser A*, Vol. 233, pp. 172, 1955.

Guiot, J., B. Ameduri, B. Boutevin, *Macromolecules*, Vol. 35, pp. 8694-8707, 2002.

Guiot, J., M. A. Neouze, L. Sauguet, B. Ameduri, B. Boutevin, *J. Polym. Sci., Part A: Polym. Chem.* Vol. 43, pp. 917-935, 2005.

Guo, Q. H., P. N. Pintauro, H. Tang, S. O'Connor, *Journal of Membrane Science*, Vol. 154, No. 2, pp. 175-181, 1999.

Hickner, M. A., H. Ghassemi, Y. S. Kim, B. R. Einsla, J. E. McGrath, *Chemical Reviews*, Vol. 104, No. 10, pp. 4587-4611, 2004.

Hietala, S., E. Skou, and F. Sundholm, *Polymer*, Vol. 40, pp. 5567–5573, 1999.

Hilal, N., L. Al-Khatib, B. P. Atkin, V. Kochkodan, N. Potapchenko, *Desalination*, Vol. 158, pp. 65, 2003

Hodgdon, R. B. *Journal of Polymer Science, Part A: Polymer Chemistry*, Vol. 6, (1PA1), pp. 711-717, 1968.

Holmberg, S., P. Holmlund, R. Nicolas, C. E. Wilen, T. Kallio, G. Sundholm, *Macromolecules*, Vol. 37, pp. 9909, 2004.

Hsu, W. Y. and T. D. Gierke, *Journal of Membrane Science*, Vol. 13, No. 3, pp. 307-326, 1983.

Hsu, W. Y. and T. D. Gierke, *Macromolecules*, Vol. 15, No. 1, pp. 101-105, 1982.

Iguerb, O., P. Bertrand, *Surf Interface Anal*, Vol. 40, pp. 386, 2008.

Irwan, G. S., S. Kuroda, H. Kubota, T. Kondo, *J Appl Polym Sci*, Vol. 93, pp. 994, 2004.

Irwan, G. S., S. Kuroda, H. Kubota, T. Kondo, *J Appl Polym Sci*, Vol.87, 458 2003.

Ivanov, V.S., *Radiation Chemistry of Polymers*, pp. 123-196, VSP, Utrecht, 1992.

Kato, K., E. Uchida, E. T. Kang, Y. Uyama, Y. Ikada, *Prog Polym Sci*, Vol. 28, pp. 209, 2003.

Kim, J., B. Kim, B. Jung, *J Membr Sci*., Vol. 207, pp. 129, 2002.

Kim Y.W., D. K. Lee, K. J. Lee, J. Kim, European Polymer Journal, Vol 44, 932–939, 2008.

Kobayashi, T., M. Rikukawa, K. Sanui, N. Ogata, *Solid State Ionics*, Vol. 106, No. 3-4, pp. 219-225, 1998.

Kobayashi, T., N. Fujii, *J Appl Polym Sci*, Vol. 45, pp.1897, 1992.

Kobayashi, T., K. Kumagai, Y. Nosaka, H. Miyama, N. Fujii, H. Tanzawa, *J Appl Polym Sci*, Vol. 43, pp. 1037, 1991.

Kopitzke, R. W., C. A. Linkous, G. L. Nelson, *Journal of Polymer Science Part A-Polymer Chemistry,* Vol. 36, No. 7, pp. 1197-1199, 1998.

Kreuer, K. D., A. Fuchs, M. Ise, M. Spaeth, *J. Electrochim Acta,* Vol. 43, pp. 1281, 1998.

Kreuer, K. D., A. Rabenau, W. Weppner, *Angew. Chem.-Int. Edit. Engl*., Vol. 21, No. 3, pp. 208, 1982.

Kreuer, K. D., *Technology and Applications*, John Wiley & Sons Ltd, Chichester, U.K., 2003.

Kreuer, K.D., T. Dippel, W. H. Meyer, J. Maier, *Mat. Res. Soc. Symp. Proc.*, Vol. 293, pp. 273-282, 1993.

Kruczek, B. and T. Matsuura, *Journal of Membrane Science,* Vol. 146, No. 2, pp. 263-275, 1998.

Kubota, H., Y. Hata, *J. Appl. Polym. Sci.*, Vol. 41, pp. 689, 1990.

Kubota, H.; Nagaoka, N.; Katakai, R.; Yoshida, M.; Omichi, H.; Hata, Y., Journal of Applied Polymer Science 51, 925 1994.

Larminie, J., *Fuel Cell System Explained*, John Wiley, 2003.

Lassegues, J. C., J. Grondin, M. Hernandez, B. Maree, *Solid State Ionics*, Vol. 145, pp. 37, 2001.

Lecolley, F., C. Waterson, A. J. Carmichael, G. Mantovani, S. Harrisson, H. Chappell, *J Journal of Materials Chemistry,* Vol. 13, pp. 2689–2695, 2003.

Lehtinen, T., Sundholm, G, et al, *Electrochimica Acta*, Vol. 43, No 12, pp. 1881-1890, 1998.

Li, S., L. Krishnan, S. Srinivasan, J. Benziger, A.B. Bocarsly, *J. Membrane Science,* Vol. 243, pp. 327, 2004.

Lin, J., *Preparetion and Characterization of Composite Proton Exchange Membranes for Fuel Cell Applications*, Ph.D. Thesis, University of Connecticut, 2000.

Londono, J. D., R. V. Davidson, S. Mazur, *Abstracts of Papers of the American Chemical Society*, Vol. 222, 14-PMSE, 2001.

Ma, H. M., R. H. Davis, C. N. Bowman, *Macromolecules*, Vol. 33, pp. 331, 2000.

Ma, H. M.; Davis, R. H.; Bowman, C. N., Polymer 42, 8333 2001.

Martwiset, S., *High temperature proton conducting materials and fluorescent-labeled polymers for sensor applications*, Ph.D. Thesis, University of Massachusetts Amherst, 2009.

Mateo, J. L., P. Bosch, F. Catalina, R. Sastre, *J Polym Sci Pol Chem*, Vol. 31, pp. 153, 1993.

Mishra, M. K., and Y. Yagci, eds., *Handbook of Vinyl Polymers: Radical Polymerization, Process, and Technology*, CRC Pres, 2009.

Moore, B. D, D. C. Sherrington, A. Zitsmanis, *J. Mater. Chem.*, Vol. 2, pp. 1231-, 1992.

Motupally, S., A. J. Becker, J. W. Weidner, *J. Electrochem. Soc.*, Vol. 147, No. 9, pp. 3171-3177, 2000.

Muaritz, K. A., R. B. Moore, *Chemical Review*, Vol. 104, pp. 4535-4585, 2004.

Muftuoglu, A. E., M. A. Tasdelen, and Y. Yagci, *Handbook of photochemistry and photophysics of polymer materials*, Chapter 13, pp. 509-541, J. Wiley, 2010.

Muftuoglu, A. E., M. A. Tasdelen, Y. Yagci, and M. K. Mishra, *Handbook of Vinyl Polymers: Radical Polymerization, Process, and Technology*, Chapter 11, pp. 307-344, 2nd ed., CRC Press Taylor & Francis, 2008.

Müftüoğlu, A. E., Y. Yagcı, K. Se, *Turkish J Chem*, Vol. 28, pp. 469, 2004.

Murthy, M (ed), *Proton conducting membrane fuel cells IV*, ECS publishing, New Jersey, 2005.

Nasef, M. M., N. A. Zubir, A. F. Ismail, M. Khayet, K. Z. M. Dahlan, H Saidi, *J Membr Sci*, Vol. 268, pp. 96, 2006.

Nasef, M., H. Saidi, K. Dahlan, *Polymer International*, Vol. 60, No. 2, pp. 186–193, 2011.

Ogiwara, Y., M. Kanda, M. Takumi, H. Kubota, *J Polym Sci Pol Lett*, Vol. 19, pp. 457, 1981.

Oster, G., *J Polym Sci*, Vol. 26, pp. 233–4, 1957.

Peng, T., and Y. L. Cheng, *Polymer*, Vol. 42, pp. 2091, 2001.

Piletsky, S. A., H. Matuschewski, U. Schedler, A. Wilpert, E. V. Piletska, T. A. Thiele, M. Ulbricht, *Macromolecules*, Vol. 33, pp. 3092, 2000.

Ranby, B., *Makromol Chem-M Symp*, Vol. 63, pp. 55, 1992.

Ranby, B., *Polym Eng Sci*, Vol. 38, pp. 1229, 1998.

Rikukawa, M, K. Sanui, *Prog. Polym Sci.,* Vol. 25, pp. 1463, 2000.

Rikukawa, M. and K. Sanui, *Prog. Polym. Sci.*, Vol. 25, pp. 1463-1502, 2000.

Rikukawa, M. and K. Sanui, *Progress in Polymer Science,* Vol. 25, No. 10, pp. 1463-1502, 2000.

Roche, E. J., M. Pineri, R. Duplessix, A. M. Levelut, *Journal of Polymer Science, Part B: Polymer Physics,* Vol. 19, No. 1, pp. 1-11, 1981.

Roche, E. J., M. Pineri, R. Duplessix, *Journal of Polymer Science, Part B:Polymer Physics,* Vol. 20, No. 1, pp. 107-116, 1982.

Rusanov, A. L., D.Y. Likhatchev, K. Mullen, *Russian Chem. Rev.* Vol. 71, No. 9, pp. 761-774, 2002.

Sauguet, L., B. Boyer, B. Ameduri, Boutevin, *Macromolecules*, Vol. 39, pp. 9087, 2006.

Savadogo, O., *Journal of New Materials for Electrochemical Systems,* Vol. 1, No. 1, pp. 47-66, 1998.

Schmidt-Rohr, K. and Q. Chen, *Nature Materials,* Vol. 7, No. 1, pp. 75-83, 2008.
Science 101, 2269 2006.

Sevil, F. and A. Bozkurt, *J Phys Chem Solids,* Vol. 65, pp. 1659, 2004.

Shen, Y., X. Qiu, J. Shen, J. Xi, W. Zhu, *J Power Sources,* Vol. 161, pp. 54, 2006.

Shim, J. K., Y. B. Lee, Y. M. Lee, *J Appl Polym Sci*, Vol. 74, pp. 75, 1999.

Smitha, B., S. Sridhar, and A.A. Khan, *Solid polymer electrolyte membranes for fuel cell applications* - a review, *J Membr Science*, Vol. 259, No. 10, pp. 26, 2005.

Socrates, G., *Infrared and Raman characteristic group frequencies: tables and charts*, J. Wiley, 3rd ed, 2006.

Steele, B. C. H. and A. Heinzel, *Nature,* Vol. 414, No. 6861, pp. 345-352, 2001.

Sui, A. R., I*nfluence of Water and Membrane Microstructure on the Transport Properties of Proton Exchange Membrane Fuel Cell,* Ph.D Thesis, Simon Fraser University, 2000.

Susanto, H., M. Balakrishnan, M. Ulbricht, *J Membrane Sci*, Vol. 288, pp. 157, 2007.

Susanto, H. and M. Ulbricht, *Langmuir,* Vol. 23, pp. 7818, 2007.

Uchida, E., Y. Uyama, Y. Ikada, J *Polym Sci Pol Chem*, Vol. 27, pp. 527, 1989.

Ulbricht, M., *Polymer*, Vol. 47, pp. 2217, 2006.

Unugur, S. C., S*ynthesis and Proton Conductivity Studies of Azole-modified Poly(glycidylmethacrylate),* M.S. Thesis, Fatih University, 2008.

Uyama, Y., K. Kato, Y. Ikada, *Adv Polym Sci*, Vol. 137, pp. 1, 1998.
Van der Heijden, P. C., L. Rubatat, O. Diat, *Macromolecules,* Vol. 37, No. 14, pp. 5327-5336, 2004.

Veriss, R. A., A. Sen, C. L. Willis, L. A. Pottick, *Polymer*, Vol. 32, pp. 1867, 1991.

Wang, H. L. and H. R. Brown, *Macromol Rapid Comm*, Vol. 25, pp. 1095, 2004.

Wang, H. L. and H. R. Brown, *Macromol Rapid Comm*, Vol. 25, pp. 1257, 2004.

Wang, H. L., H. R. Brown, *J Polym Sci Pol Chem*, Vol. 42, pp. 253, 2004.

Wang, H. Y., T. Kobayashi, N. Fujii, *J Chem Technol Biotechnol*, Vol. 70, pp. 355, 1997.

Wang, S. and J. E. McGrath, *Synthesis of Poly(arylene ether) Synthetic Methods in Step-Growth Polymers*, pp. 327, Wiley, New York, 2003.

Wirsen, A., H. Sun, A. C. Albertsson, *Biomacromolecules*, Vol. 6, pp. 2697, 2005.

Wu, G. G., Y. P. Li, M. Han, X. X. Liu, *J Membr Sci*, Vol. 283, pp. 13, 2006.

Wycisk, R. and P. N. Pintauro, *Journal of Membrane Science,* Vol. 119, No. 1, pp. 155-160, 1996.

Xianguo L., *Principles of fuel cells*, 1st ed. Taylor & Francis Group, New York, 2006.

Xing, C. M., J. P. Deng, W. T. Yang, *Macromol Chem Phys*, Vol. 206, pp. 1106, 2005.

Xing, C. M., J. P. Deng, W. T. Yang, *Polym J,* Vol. 35, pp. 613, 2003.

Yamada, K., T. Ebihara, T. Gondo, K. Sakasegawa, M. Hirata, *J Appl Polym Sci*, Vol. 61, pp. 1899, 1996.

Yamada, K., T. Gondo, M. Hirata, *J Appl Polym Sci*, Vol. 81, pp. 1595, 2001.

Yamada, K., Y. Iizawa, J. Yamada, M. Hirata, *Journal of Applied Polymer Science,* Vol. 102, pp. 4886, 2006.

Yamada, K., J. Kimura, M. Hirata, *Journal of Applied Polymer Science,* Vol. 87, pp. 2244, 2003.

Yamada, K., R. Nagano, M. Hirata, *J Appl Polym Sci*, Vol. 99, pp. 1895, 2006.

Yamada, K., Y. Saitoh, Y. Haga, K. Matsuda, M. Hirata, *J Appl Polym Sci*, Vol. 102, pp. 5965, 2006.

Yamada, K., T. Taki, K. Sato, M. Hirata, *J Appl Polym Sci*, Vol. 89, pp. 2535, 2003.

Yamada, M, I. Honma, *Electrochim Acta*, Vol. 48, pp. 2411, 2003.

Yang, B., W. T. Yang, *J Macromol Sci Part A Pure Appl Chem*, Vol. A40, pp. 309, 2003.

Yang, B., W. T. Yang, *J Membr Sci*, Vol. 218, pp. 247, 2003.

Yang, B., W. T. Yang, *J Membr Sci*, Vol. 258, pp. 133, 2005.

Yang, C., P. Costamagna, S. Srinivasan, J. Benziger, A. B. Bocarsly, *J Power Sources*, Vol. 103, pp. 1, 2001.

Yang, J. M., C. P. C. Chian, K. Y. Hsu, *J Membr Sci*, Vol. 153, pp. 175, 1999.

Yang, J. M.; Lin, H. T., J Membr Sci 243, 1 2004.

Yang, Y., and S. Holdcroft, *Fuel Cell*, Vol. 5, pp. 171-186, 2005.

Yu, J et al., *Journal of Materials Science*, Vol. 45, No.4, pp.1017-1024, 2010.

Zhang, Z. D., L. B. Kong, J. P. Deng, P. Yang, W. T. Yang, Journal *of Applied Polymer Science*, Vol**.** 101, pp. 2269, 2006.